Effects of Frother Type on Single Bubble Rise Velocity

Amir Arash Rafiei Mehrabadi

Department of Mining, Metals and Materials Engineering
McGill University
Montreal, Canada

June 2009

A thesis submitted to McGill University in partial fulfillment of the requirements for the degree of Master of Engineering

Abstract

The addition of frother in flotation has two main functions, to help reduce bubble size and help produce a stable froth. A role of frother on bubble behavior in pulp zone is usually not considered. A previous study showed that as frother type was changed the same gas holdup was given by different size bubbles. This implies that bubble rise velocity depends on the nature of the surfactant (frother type). A study using bubble swarms appears to support the frother type effect but bubble interactions are a possible confounding factor.

This study resolved the question by measuring terminal rise velocity profile of single bubbles (ca. 1 to 2 mm) as a function of frother type. It is shown that at the concentrations of interest in flotation, 1-pentanol hardly alters the velocity compared to water alone while F150 (a polyglycol) reduces the velocity by up to 50%. The results become in 1-pentanol bubble did not reach terminal velocity. For high concentration of 1-pentanol (>130ppm) the rise velocity is reduced comparable to F150.

To investigate, experiments were performed using aliphatic alcohols from 1-butanol (C_4) to 1-octanol (C_8). It was found there is a minimum concentration for the frother to give terminal velocity close to the Clift et al. contaminated eater result. The concentration decreases as molecular weight (chain length) of alcohol increases. Larger bubbles (1.8 vs. 1.5mm) require higher minimum concentration.

To study the influence of molecular structure, three 6-C alcohols, 1-hexanol, MIBC and 2-hexanol, were used. The results show that molecular structure influences rise velocity through the position of OH group, and whether the alcohol is straight chained or branched. The observation can make a useful link frother to chemistry for understanding frother influence on bubble rise and possibly its function in flotation.

The influence of three industrial frother, MIBC, F150 and DF250, was studied and it was observed that over the practical concentration range all reduce rise velocity similar to contaminated water and their critical concentration are very low compared to the aliphatic alcohols. In addition, the influence of a salt, NaCl, on bubble rise velocity was compared to MIBC and confirms a previous observation that reported the similar capability of NaCl to act like MIBC.

Résumé

Deux raisons principales commandent à l´ajout de la mousse dans le processus de flottation, à savoir, la réduction de la bulle et la production d´une mousse stable. L´effet de la mousse sur le comportement de la bulle en zone pulpaire n´est pas pris en compte. Un travail antérieur a démontré que pour la même fraction d´air transporté par les bulles, le type de mousse a de l´influence sur la taille des bulles. Cela implique que la vélocité de la bulle dépend de la nature du surfactant (type de mousse). Une étude basée sur l´usage de plusieurs bulles semble s´accorder avec l´hypothèse relative au type de mousse, néanmoins les interactions des bulles rendent le problème complexe.

La présente étude a résolu cette question en mesurant la vélocité d´une bulle dont les dimensions sont presque égales à 1 ou 2 mm, suivant le type de mousse. Il en est résulté que dans l´intervalle des concentrations d´importance en flottation, le pentanol peine à influencer la vélocité, alors que l´eau toute seule en serait capable. En revanche, le F150 (un polyglycol) réduit la vélocité de 50%. Pour les concentrations élevées de pentanol (>100 ppm), la vélocité décroit et devient comparable à celle engendrée par la présence du F150. Il va de soi que l´observation antérieure est confirmée dans l´intervalle pratique des concentrations.

En guise d´investigations, des expériences au cours desquelles les alcools aliphatiques allant du butanol (C4) à l´octanol (C8), ont été réalisées. Il a été démontré que l´effet du type de mousse sur la vélocité dépend de la concentration. Il existe une concentration minimale de la mousse en dessous de laquelle, la bulle monte comme dans le modèle de l´eau contaminée de Clift et al. La concentration minimale critique dépend de la dimension de la bulle et du déplacement mesuré à partir du point terminal du tube capillaire. L´on rapporte que les bulles les plus larges et les mousses de petite masse moléculaire nécessitent une concentration élevée pour épouser le comportement de l´eau contaminée. Au dessus de cette concentration, la vélocité de la bulle est indépendante du type de mousse et de la concentration.

Afin d´étudier la possible influence de la structure moléculaire, trois alcools (C6) dont 1-hexanol, MIBC et 2-hexanol ont été utilisés. Les résultats ont montré que la structure moléculaire influence la vélocité via la position du groupe OH, selon qu´elle est linéaire ou ramifiée. Cette observation fait clairement un lien avec la chimie et permet de mieux comprendre la relation entre la mousse et la vélocité de la bulle et possiblement sa fonction. L´influence de 3 mousses industrielles dont le MIBC, le F150 et le DF250, a été étudiée. L´on a observé qu´au - delà de l´intervalle pratique de concentrations, ces mousses réduisent la vélocité de la même manière que l´eau contaminée. Leurs concentrations critiques sont de beaucoup inferieures à celles des alcools aliphatiques. En plus, l´influence du sel (NaCl) sur la vélocité a été comparée à celle du MIBC. Cette expérience a confirmé que le NaCl peut se comporter comme le MIBC.

Acknowledgements

I wish to express my sincerest appreciation and utmost gratitude to my supervisor, Professor James A. Finch, for his guidance, support, patience, continuous encouragement, trust, discussions, valuable technical assistance, very high teaching skills and especially his brilliant vision about the current research. During all precious days of my work at McGill his integrity, discipline, well-organized planning, timing and attitude gave me very important experiences and ideas to be more successful in my future life. Briefly, as a very important key of success that I have learned, he is one of the people who really enjoys from his work life.

I would like to thank Dr. Ram Rao who helped me to understand some problems in organic chemistry. Also I want to thank Dr Cesar O. Gomez for all his efforts in preparing the column for running experiments and his brilliant engineering ideas in re-designing the column for providing better performance.

Thanks must go to my colleagues for providing support and very good collaboration, especially Dr. Mitra Mirnezami for her advice and help.
I would like to gratitude the organizations and companies that provided sufficient financial support for doing my work.

The last but the most gratitude must go to my family and especially my mother who means every thing to me.

Table of Contents

List of Figures

List of Tables

Nomenclature

A	Area, m^2 or cm^2
B_O	Bond number
c	Concentration of surfactant, mol/m^3 or ppm
C_D	Drag coefficient
d_e	Equivalent diameter of the bubble, mm or cm
E	Aspect ratio
E_O	Eotvos number
F_B	Buoyant force
F_D	Drag force
F_r	Froude number
g	Acceleration constant, m/s^2
H	Bubble distance over the capillary, mm
H_l	Liquid height
J_{ad}	Adsorption flux to the interface, $mol/(m^2.s)$
J_{des}	Desprption flux from the interface, $mol/(m^2.s)$
M_O	Morton number
mol	Mole
P_{atm}	Atmospheric pressure
P_0	Absolute pressure
R	Gas constant, 8.314 N.m/(mol.K)
Re	Reynolds number
t	Time, s
T	Absolute temperature, K
T_a	Tadaki number
U_b	Local velocity of bubble, cm/s
W_e	Webber number
α	Desorption rate constant, 1/s
β	Adsorption rate constant, $m^3/(s.mol)$
γ	Surface tension of surfactant solution, N/m
γ_0	Surface tension of water, N/m
Γ	Surfactant concentration on bubble surface, mol/m^2
Γ_∞	Maximum surfactant concentration on bubble surface, mol/m^2
μ_l	Viscosity of liquid, $N.s/m^2$
ρ	Denssity, kg/m^3 or g/cm^3
ρ_l	Liquid denssity, kg/m^3 or g/cm^3

CHAPTER ONE: INTRODUCTION

Particulate systems can be categorized on the basis of the phases involved: solid particle, liquid and gas bubble. There are many wide industrial processes based on two or three phase systems. It is important to understand the interactions to optimize these processes. The complex nature of water requires special attention to understand water-based two and three phase systems.

Bubble rise in liquids under different conditions is one of the oldest of scientific investigations. It is of interest as the characteristics of a rising bubble (e.g. size, shape, velocity and trajectory) give insight into the dynamics of a system. Rise velocity is one of the most important characteristics of a rising bubble.

1.1. Single bubble rise velocity

Numerous studies have been performed on the motion of single bubbles. Clift et al. (1978) reviewed the research prior to 1978. Kulkarani and Joshi (2005) provide the most recent review on bubble formation and bubble rise velocity in gas-liquid systems. There remain problems with some of the previous works because of restrictions imposed by the experimental set-up and differences in understanding the nature of bubble velocity especially in surfactant solutions.

The measurement of terminal velocity is a case in point: it is important to clarify what velocity is being determined experimentally. Most studies report the terminal velocity as an average velocity of a bubble over a given distance. Others use the velocity at a fixed distance above the point of bubble release. Both measures overlook a possible time-dependence of the velocity. This has led to confusion over interpreting the impact of surfactant type and concentration.

Sam (1995) was one of the pioneers who applied an adjustable speed moving video camera system to measure the velocity of a rising bubble as a function of time or height, referring to this as the “velocity profile” (Sam et al., 1996). This setup has opened a new approach to the fundamental study of the bubble motion

mechanism, as recognized by Dewsburry et al. (1999) and Kulkarani and Joshi (2005).

In the presence of surfactant, depending on type and concentration, the velocity profile (time-history) revealed three stages: acceleration, deceleration and constant (terminal) velocity.

The common interpretation is that surfactants adsorb on the bubble and retard the mobility of surface resulting in increased drag (Frumkin and Levich, 1947). As the bubble rise and surfactant accumulates the corresponding increase in drag can account for the three stages (Sam et al., 1996). Theoretically, the velocity of a single bubble rising in surfactant solution can be solved by a combination of the Navier-Stokes equation, mass transfer and the Marangoni effect. These govern the fluid flow around the bubble, the amount of surfactant on the bubble, and the extent of surface retardation and distribution of surfactant on the surface, respectively. The surface retardation can be simulated by uniform and stagnant cap models that determine rise velocity according to rate and extent of accumulation of surfactant molecules on the bubble surface (Zhang et al.., 2001; Zhang and Finch, 2002).

1.2. Velocity profile and terminal velocity of a single bubble

Sam et al. (1996) characterized the single bubble velocity profile by suggesting three stages (Figure 1.1): first, a rapid increase to a maximum value (acceleration); second, a decrease (deceleration); and third, a constant (terminal) velocity stage. They observed the profile was strongly dependent on surfactant type and concentration.

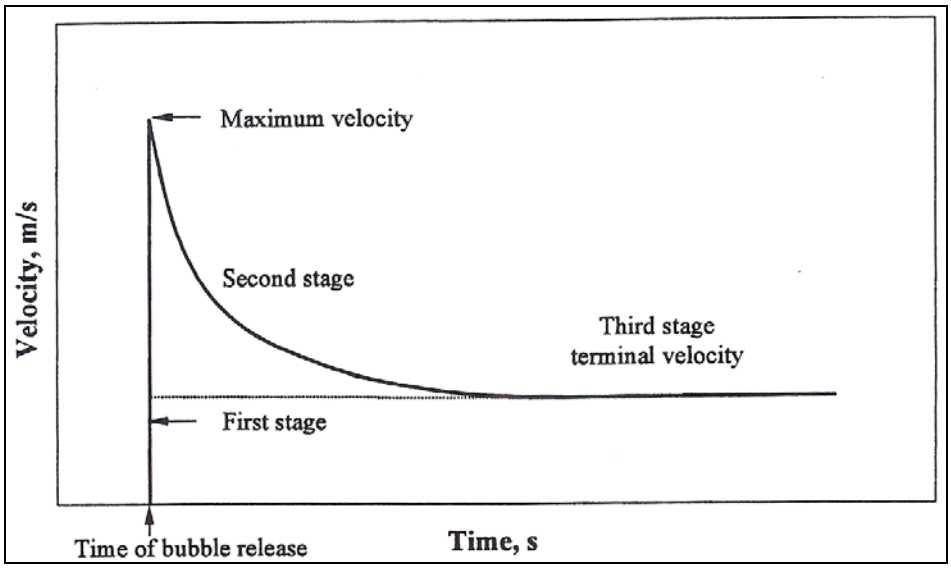

Figure1.1: The stages of a typical velocity profile.

The different stages in the profile reflect different amount of adsorbed surfactant. Initially the bubble surface is almost free of surfactant and the bubble accelerates towards the velocity in a surfactant-free system. As surfactant molecules accumulate drag increases and the bubble slows and eventually decelerates. When adsorption reaches equilibrium (a steady state between adsorption at the forward part of the bubble from where surfactant is swept by the flowing liquid and desorption from the rear of the bubble to where the surfactants are swept) the velocity of the bubble becomes constant considered as the terminal velocity.

According to Newton's second law the terminal velocity of a body is the velocity at which the body moves under a zero-acceleration condition. In the case of terminal velocity of a bubble this indicates a balance between upward buoyancy and downward drag forces.

Sam et al. (1996) reported that terminal velocity of a single bubble appeared to depend on surfactant type but not surfactant concentration, only the time to reach terminal velocity is affected. According to that conclusion, analysis of single bubble terminal velocity vs. bubble size should reveal the influence of surfactant

type. Figure 1.2 presents the terminal velocity extremes, the trend for “clean” and “contaminated” water (Clift et al., 2005).

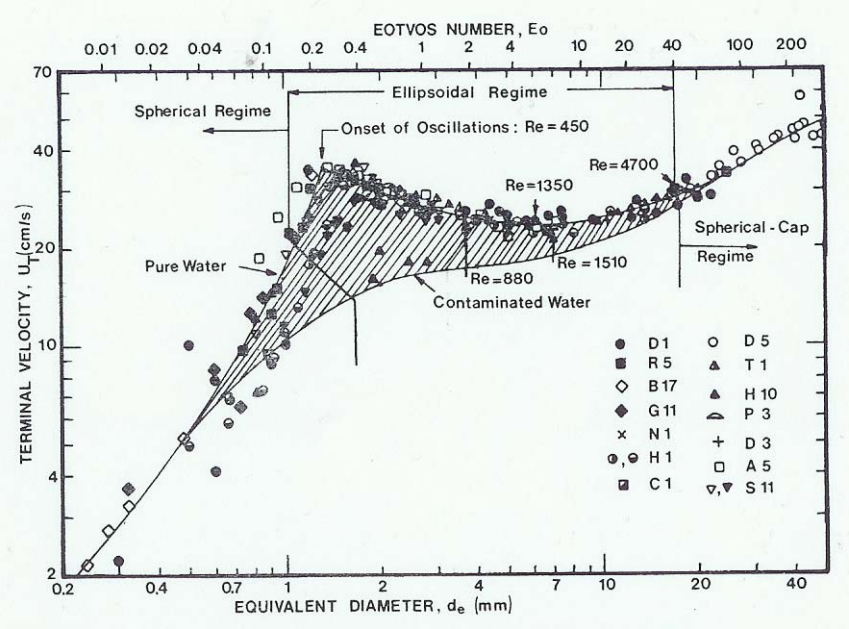

Figure 1.2: Typical trend for terminal rise velocity in clean and contaminated water (reproduced with permission from Clift et al. 2005).

While terminal velocity is an important property, the velocity profile can provide further insight into surfactant action on bubble motion. This thesis will examine velocity profile and terminal velocity of single bubbles in systems of interest in mineral flotation.

1.3. Objectives of the study

The general objective is to use local rise velocity vs. distance (time) of single bubbles (i.e., the velocity profile) to characterize systems of interest in flotation. Some specific objectives include:

- Measure the velocity profile of some selected frothers, alcohols and salts over a range of concentration and bubble size of interest to flotation (0.5-2.5mm);
- Compare velocity vs. bubble size in 1-Pentanol (as a simple alcohol) and F150 (as a polyglycol) to test the claim of frother type effect on velocity presented by Azgomi et al. (2006);

- Compare velocity vs. bubble size between MIBC (as a weak frother) and NaCl (as a salt) to verify their common effect, according to the observation of Quinn et al. (2007);
- Compare velocity vs. bubble size among some alcohols (C_4-C_8) to track the effect of chain length;
- Compare single bubble results with recent swarms results (Acuna and Finch, 2008).

1.4. Structure of the thesis

Chapter 1. Introduction: The gas/liquid system and parameters of bubble rise in water are introduced followed by introduction to concept of velocity profile and terminal rise velocity. The chapter ends by introducing objectives of the study and structure of the thesis.

Chapter 2. Background and Literature Review: Required background concerning forces acting and surfactant properties are presented. The literature review begins with an introduction to bubble behavior and ends with more detailed discussion on the impact of contaminants on bubble rise velocity.

Chapter 3. Experimental Setup: Here the experimental setup, methods, measurement techniques and software are described.

Chapter 4. Results and Discussion: The results achieved toward each objective are presented. Data are analyzed and compared with published works.

Chapter 5. Conclusions and Recommendations: The conclusions are summarized and recommendations for future work entertained.

CHAPTER TWO: BACKGROUND

2.1. Bubble formation in gas-liquid systems

Some of the earliest studies on the formation of single bubbles were by Tate (1864) and Bashforth and Adams (1883). A significant body of work on bubble formation over a wide range of design and operational parameters has appeared in the literature over the last few decades (Davidson and Schuler (1960), Tsuge and co-workers, (1983, 1986, 1992, 1993, 1997, and 1999), Kumar et al.(1969), Marmur et al. (1973, 1976), Vogelophl and co-workers (1982, 1986), Tan and co-workers (2000, 2003).

A model of bubble formation from submerged orifice was proposed by Kumar et al. (1969). Tsuge (1986) reviewed the hydrodynamics of bubble formation and discussed various models. Rabiger and Vogelpohl (1986) discussed the various factors affecting bubble formation. There have been several recent developments in both numerical and experimental methods (Kulkarani and Joshi, 2005).

Bubble formation at a single submerged orifice can be classified according to the following modes: low frequency bubbling, chain bubbling, wobbling and jetting. These modes are dependent on the orifice configuration, the gas velocity, and gas/liquid system properties.

2.2. Theoretical aspects

2.2.1. Forces

Particle (defined generally to include solid, liquid (droplet) or gas (bubble)) motion in a liquid is controlled by forces that act on the particle. The fundamental aspects are based on Newton's second law illustrated by the momentum "Navier-Stokes" equation.

The motion of a bubble in a liquid is subjected to buoyancy and drag forces and, because there is a different cohesive force between water and air molecules, an interfacial force also appears, surface tension. The forces are briefly described.

2.2.1.1. Surface tension

The Navier-Stokes equation can be considered as a general force balance for a fluid in motion. When an interface is involved (e.g., bubble/water interface), an interfacial (or surface) tension force is present. The interface behaves like a thin stressed membrane under tension (Eskinazi, 1968).

Surfactant and salts affect the surface tension of the air/water interface, the former reducing surface tension the later often increasing surface tension. The surface tension may be a function of time called dynamic surface tension (Defay and Prigozine, 1960). That feature is recognized to have a role in some flotation systems (Defay and Prigozine, 1960; Finch and Smith, 1972; Kulkarani and Somasundaran, 1975; Leja, 1982; Comley et al. 2002). The equilibrium surface tension of an air/water interface depends on the quantity of adsorbed molecules of surfactant. Above a certain concentration of surfactant, the surface tension becomes constant and any surfactant forms colloidal aggregates within the bulk solution known as micelles where CMC stands for critical micelle concentration.

2.2.1.2. Buoyancy

According to Archimedes' principle a particle whose average density is less than that of the liquid floats on that liquid. The direction of the buoyancy force for both falling (object has higher density than water) and rising (object has lower density than water) motion in water is upward. For a sphere the buoyancy force F_B, is determined by:

$$F_B = \frac{\pi d_e^3 \rho_l g}{6} \qquad (2\text{-}1)$$

where, d_e and ρ_l, are particle equivalent diameter and liquid density, respectively.

In bubble motion analysis, it is usually assumed that because the density of air is very small the gravitational force is negligible.

2.2.1.3. Drag

Drag force is defined as the resultant of the forces acting to resist motion of a particle in a liquid; on a bubble rising through a liquid the direction of this force is downward. For a bubble in motion relative to liquid, a skin (viscous or shear) drag will exist between the bubble surface and the fluid. The drag comes from the friction of the fluid on the bubble surface and demonstrates itself as the viscous force in the Navier-Stokes equation even if viscosity is very low (Binder, 1973).

During motion of a bubble the liquid passes over the bubble and the flow separates at some point on the rear half of the bubble. Thus a pressure difference occurs between the separated and non-separated flow regions. By considering a pressure difference on a projected area of a bubble, a drag force called pressure or shape drag is derived.

The drag coefficient (C_D) is a dimensionless quantity which is used to describe the drag force. The total drag force can then be expressed as:

$$F_D = C_D \frac{\rho_l U_b^2}{2} A \qquad (2\text{-}2)$$

where, ρ_l, U_b and A are liquid density, bubble local rise velocity and area, respectively.

According to the dependency of the drag force on the bubble shape and Reynolds number, it is normally presented as a plot of Reynolds number vs. particle shape (Massey, 1983).

2.2.2. Force ratio

Dimensionless analysis is a tool for checking equations and units, determining a convenient arrangement of physical variables and planning systematic experiments (Binder, 1973). Since physical laws express natural phenomena,

they are independent of the units of the dimensions used; thus it is possible to express the laws in dimensionless form.

Dimensionless groups arise from dynamic similarity (Massey, 1983). If two systems are dynamically similar then the magnitude of forces at similarly located points in each system are in a fixed ratio. Consequently, when the ratio of forces acting on a fluid particle in one case is the same as the ratio of those forces at a corresponding point in another case, then mechanical similarity is realized (Binder, 1973). In general, the similarity of flow depends not only on one ratio of forces, but on two or possibly three ratios.

The dimensionless groups which have usually been considered in bubble motion analysis are[1]:

$$\text{Re (Reynolds No.)} = \frac{inertia\ force}{viscous\ force} = \frac{\rho_l U_b^2 d_e}{\mu_l} \tag{2-3}$$

$$\text{We (Webber No.)} = \frac{inertia\ force}{surface\,tension\ force} = \frac{\rho_l U_b^2 d_e}{\sigma} \tag{2-4}$$

$$\text{Eo (Eotvos No.)} = \frac{gravity\ force}{surface\,tension\ force} = \frac{g\rho_l d_e^2}{\sigma} \tag{2-5}$$

$$\text{Fr (Froude No.)} = \frac{inertia\ force}{gravity\ force} = \frac{U_b^2}{d_e g} \tag{2-6}$$

$$\text{Bo (Bond No.)} = Eo^{1/2} = d_e\left[\frac{g\rho_l}{\sigma}\right]^{1/2} \tag{2-7}$$

$$\text{Mo (Morton No.)} = \frac{g\mu_l^4}{\rho_l \sigma^3} \tag{2-8}$$

$$\text{Ta (Tadaki No.)} = g^{1/4}\left(\frac{\rho_l}{\sigma}\right)^{3/4} d_e U_b \tag{2-9}$$

[1] See nomenclature for definition of symbols

2.2.3. Wake phenomenon

It is known that the rise characteristics of bubbles in liquid, such as shape, rise velocity and oscillations are closely related to the bubble wake behavior (Tsuchiya and Fan, 1988). The wake structure is dependent upon several factors including: particle geometry, size and nature of the particle surface; relative motion between the particle and surrounding medium; and the physical properties of particle and liquid.

Vannard and Street (1975) characterized wake phenomenon as a function of Reynolds number (Figure 2.1). At Re<1 there is no wake. As Re increases at a certain Re (about Re ≈ 20), the flow starts to separate from the particle surface. This critical Re is dependent on particle shape, particle surface nature and the turbulence intensity in the surrounding media. As the Reynolds number increases from the critical value, the separated streamlines branch off from the particle contour. This creates a closed region behind the particle called the “wake or circulation region” (Figure 2.1).

The wake structure for bubbles is known to differ from that for solid particles, due to bubble oscillation or rocking under the influence of asymmetric vortex shedding at least for bubbles ≥1.5mm. Bhaga (1976), Clift et al. (1978), Bhaga and Weber (1980, 81), Weber and Bhaga (1982), Tsuchiya and Fan (1988), Kreischer et al. (1990) and Fan and Tsuchiya (1990) among others have investigated bubble wake phenomena. They discussed the bubble wake structure and geometry, circulation flow pattern in the bubble wake and bubble wake instability for different bubble sizes and shapes or, generally, for different Reynolds numbers.

The wake volume is a function of Reynolds number and the ratio of the wake volume to the bubble volume increases with increasing Reynolds number (Bhaga and Weber, 1981). George et al. (2006) report an empirical correlation for volume.

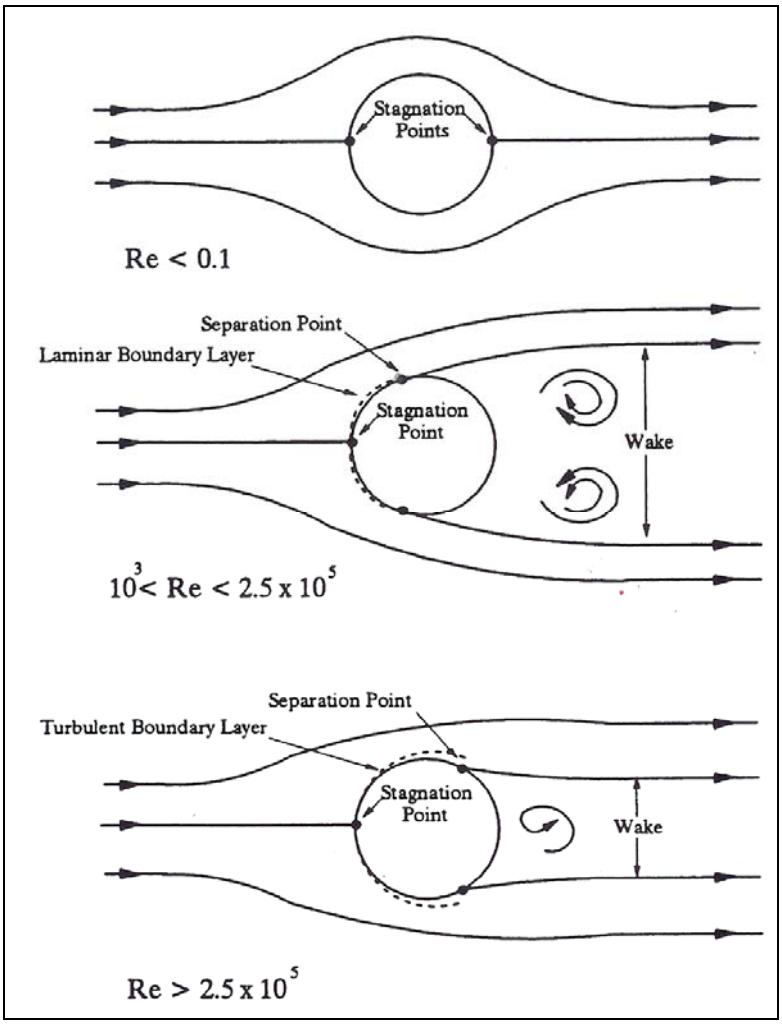

Figure 2.1: Circulation region (wake) behind a sphere at various Reynolds numbers (Vennard and Street, 1975).

2.3. Surfactants and their influence at air/water interface

2.3.1. Surfactant and frother

A surface active agent or surfactant is a compound that in very small quantities is able to change the properties of a surface, often with little to no influence on any other properties. A surfactant's surface activity is most widely encountered in the lowering of surface tension of water (Tsujii, 1997).

Surfactant structure consists of a polar group with a hydrocarbon chain, i.e., they belong to the mixed hydrophilic/hydrophobic structural class. By residing at the

interface with the polar part in the water and the hydrocarbon chain in air both the hydrophilic and hydrophobic properties are satisfied simultaneously. Consequently, surfactant accumulates at the interface.

Frothers, the reagents added in most flotation systems to control bubble related properties, are surfactants. Most frothers are based on alcohols and polyglycols. Their main tasks are to reduce bubble size and promote froth stability

2.3.2. Surfactant adsorption mechanism

The exchange rate of surfactant between the bulk solution and interface is a function of surfactant concentration and surface activity. Two mechanisms, diffusional transport and non-diffusional adsorption, govern the exchange rate. For highly surface active (or strong) surfactants, i.e., those for which rate of surface tension decrease with concentration is high, the exchange rate is controlled by diffusional transport if the concentration is low. For weak surfactants and comparatively high concentrations of strong surfactants, non-diffusional adsorption kinetics govern (Bleys and Loos, 1985; Fainerman, 1985).

The Langmuir adsorption model is one of the first and most important models. Here, the adsorption rate is described as a balance of surfactant adsorption flux to the interface (J_{ad}) and desorption flux from the interface (J_{des}):

$$\frac{d\Gamma}{dt} = J_{ad} - J_{des} \qquad (2\text{-}10)$$

The Langmuir model can be presented as:

$$\frac{d\Gamma}{dt} = \beta c(0,t)\left(\Gamma_{\infty} - \Gamma\right) - \alpha\Gamma \qquad (2\text{-}11)$$

For most surfactants non-diffusional adsorption kinetics can be expected if the Langmuir-Von Szyskowski constant ($a = \alpha/\beta$) is larger than 1 $mol.m^{-3}$ (Fainerman et al., 1998).

When equilibrium is reached the Gibbs adsorption isotherm relates the surfactant excess concentration on the interface to the surface tension:

$$\Gamma = -\frac{1}{RT}\frac{d\gamma}{d\ln c} \qquad (2\text{-}12)$$

Combining with the Langmuir adsorption isotherm gives:

$$\gamma_0 - \gamma = -RT\Gamma_\infty \ln(1 - \frac{\Gamma}{\Gamma_\infty}) \qquad (2\text{-}13)$$

where γ_0 is the surface tension of water. If the surfactant concentration is very low, $\frac{\Gamma}{\Gamma_\infty}$ would be close to zero and the Langmuir isotherm can be simplified to:

$$\gamma_0 - \gamma = RT\Gamma \qquad (2\text{-}14)$$

In the other words in this situation there is a linear dependency between surface tension and surface concentration (or adsorption density). Frumkin (1925) introduced additional interaction forces between adsorbed molecules into the Langmuir adsorption isotherm.

2.3.3. Surfactant distribution

Dukhin et al. (1995) reviewed developments in the theory, and experimental aspects of surfactant adsorption at a liquid interface. One of the models of surfactant distribution between interface and bulk solution is shown schematically in Figure 2.2.

According to Figure 2.2 the air/water interface is divided into three regions: the interface, where the surfactant molecules accumulate; the sublayer that is adjacent to the interface and is in equilibrium with the interface at all times; and the bulk solution that has a uniform concentration of surfactant. Here the transport of surfactant from bulk solution to the interface occurs by migration of surfactant from the bulk to the sublayer, followed by its adsorption at the interface.

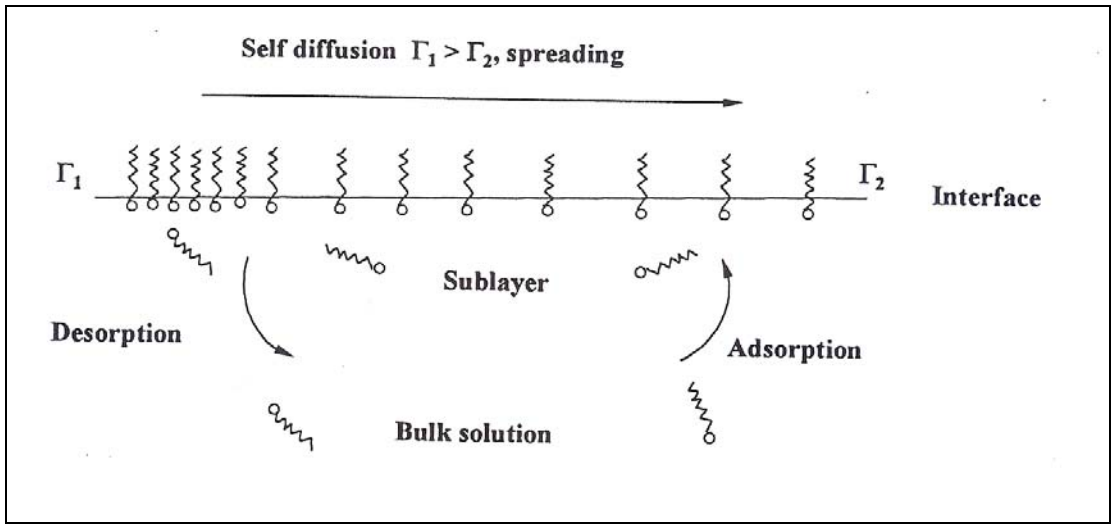

Figure 2.2: Accumulation of surfactant at air/water interface (after Dukhin et al., 1995).

The distribution of surfactant over the bubble surface is governed by the adsorption kinetics and transport properties of the surfactant. The nature of the adsorbed layer at the interface can be characterized by two extremes: soluble and non-soluble. If the surfactant flux from the bulk is extremely slow compared to surface convection, the adsorbed surfactant behaves as an insoluble monolayer. At this extreme the interface can be divided into two zones, the leading zone, which is mobile and swept free of surfactant, and the trailing zone which has a high surfactant concentration and is considered stagnated (Cuenot et al., 1997). The size of this stagnant region is specified by a cap angle (θ) measured from the trailing pole to the edge of the stagnated zone. At the opposite extreme, when the surfactant flux from the bulk is only slightly less than the surface convective flux, a smoothly changing concentration gradient develops over the entire surface. The bubble surface can then be classified into four cases according to the surface velocity: the unretarded surface; the uniformly retarded surface; the partly stagnated surface; and the completely stagnant interface. Figure 2.3 shows the distribution of surfactant and surface velocity (U_S) on the bubble for the two extremes of the adsorption layer.

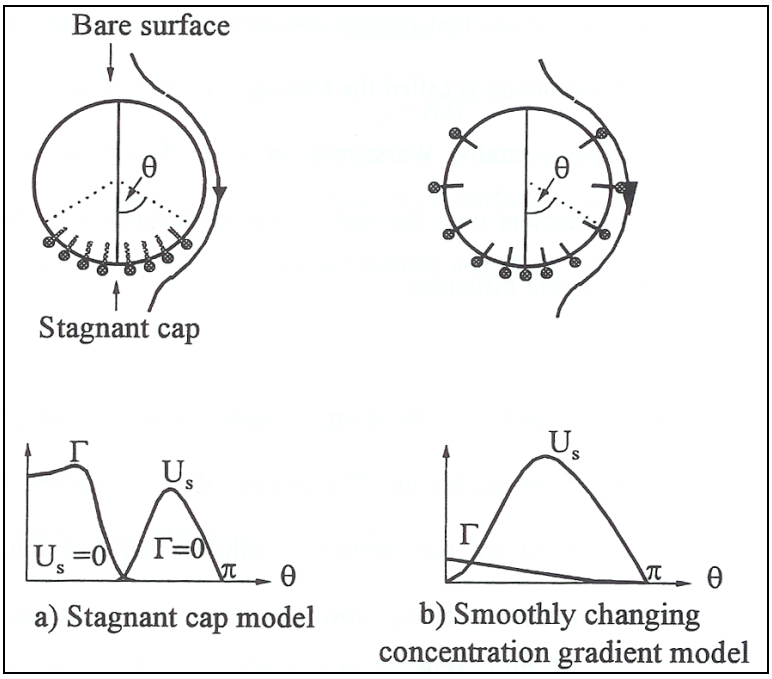

Figure 2.3: Surfactant and velocity distribution on bubble surface for the two extremes (Cuenot et al., 1997).

The uniformly retarded surface model has been considered by many researchers (Levich, 1962; Schechter and Fairley, 1963; Newman, 1967; Harper, 1972; He et al., 1991). However, stagnant cap model is considered appropriate in most cases (Savic, 1953; Garner and Skelland, 1955; Elzinga and Banchero, 1961; Griffith, 1962; Horton el al., 1965; Huang and Kintner, 1969; Beitel and Heidegger, 1971; Yamamoto and Ishii, 1987).

2.3.4. Some consequences of presence of surfactant at air/water interface

2.3.4.1. Marangoni effect

Natural convection due to density differences and Marangoni convection due to an interfacial tension gradient at the free interface of the fluid (Marangoni effect) can occur spontaneously (Okano et al., 1989; Bergman and Webb, 1990; Gaskell, 1992; Lan and Kou, 1992).

In an isothermal system the Marangoni effect can be explained as follows. After releasing a bubble into water that contains surfactant, the surfactant adsorbs at

the air/water interface. But the motion of the bubble sweeps the adsorbed surfactant molecules from the front of the bubble to the rear; i.e., provides a non-uniform distribution of surfactant (Figure 2.4). Therefore, the concentration of surfactant at the rear is larger than that at the front. This non-uniformity induces a surface tension gradient toward the front of the bubble which subsequently generates a tangential shear stress that retards the surface velocity and increases the drag coefficient. This phenomenon is called the Marangoni effect (Frumkin and Levich, 1947; Levich 1962).

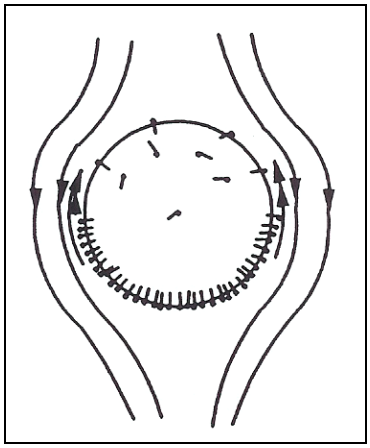

Figure 2.4: The distribution of adsorbed surface active solute on the surface of a rising bubble (Linton, 1957).

One consequence is a reduced bubble rise velocity because of the increase in drag coefficient. Another consequence is the bubble attains a more spherical shape, the shear stress opposing the force resulting from the pressure drop across the bubble which causes it to flatten. The bubble is said to become more “rigid”.

In a non isothermal system the convection direction is from the hot to the cold region. Density and surface tension are lower on the hot side and, consequently Marangoni convection again occurs.

2.3.4.2. Interaction between surfactant and water molecules

In addition to surface tension gradient driven phenomena the interaction between the polar group and water molecules via H-bonding can also be a factor controlling bubble motion. Water molecules can be seen as traveling with the bubble and retarding the bubble rise through an increase in surface viscosity. It is the combination of interaction with water molecules and the surface tension gradient effect that increases the drag on the bubble according to some (Fuerstenau and Wayman, 1958; Leja, 1982; King, 1982; Crozier, 1992; Urry, 1995). In a similar vein Malysa et al. (1988) reported that long chain polymers could reduce the settling velocity of colloidal particles significantly, which was attributed to interaction with water molecules.

By introducing this chemical aspect an effect of surfactant type as well as concentration is anticipated which is not so readily associated with the physical properties due to surface tension phenomena.

2.3.4.3. Effect on bubble internal circulation

There are a few studies on bubble internal circulation (Hadamard and Rybczynski, 1911; Garner and Hammerton, 1954; Linton and Sutherland, 1957; Griffith, 1962; Lochiel, 1965; Clift et al., 1978). As the internal circulation depends on the mobility of the surface, the properties of the interface and the effect of surfactants play a significant role.

For a moving bubble any part of the surface experiences a tangential force proportional to the viscosity of the external medium. The circulation pattern is dependent on the fluid properties, and size and shape of the bubble (Linton and Sutherland, 1957).

Schechter and Farley (1963) considered the circulation as resulting from the air inside the bubble near the interface being swept from the leading end to the rear by the action of the flowing liquid inducing stress on the interface. At the rear of

the bubble air flowing along the interface is then forced into the interior of the bubble and the circulation pattern is established.

If due to presence of surfactant the surface becomes sufficiently rigid the internal circulation decreases. In the other words, an opposing force to circulation is introduced if the interfacial tension varies over the surface. If the adsorption-desorption process of surfactant is fast the surface tension will be almost constant over the surface and the resultant surface tension gradient would be small. Oppositely, if the adsorption-desorption process is slow higher surface tension gradients would be produced. The modes of internal circulation are: complete circulation, part circulation, and stagnant (Figure 2.5).

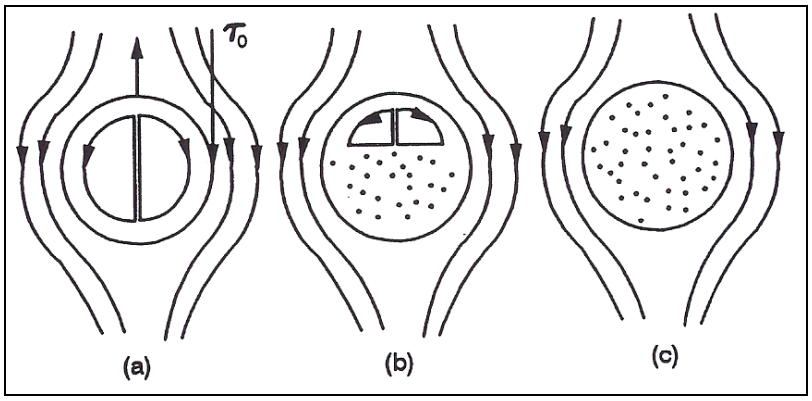

Figure 2.5: The internal circulation of moving fluid showing the direction of relative flow: (a) complete circulation, (b) part circulation, (c) stagnant (Linton, 1957).

According to Figure 2.5 complete circulation occurs in pure liquids and fully stagnant mode can be achieved as a result of a large enough surface tension gradient. In general, the internal circulation is governed by the velocity, pressure drop across the bubble and time dependent surface tension gradient in the bubble surface. One consequence is that larger bubbles experience more internal circulation.

2.3. Bubble behavior

Bubble rise in liquids has been investigated over many decades. In the early work it was assumed that the fluid surrounding the bubble has zero viscosity, and there is no slip at the boundary (Lamb, 1954). But for real fluids the situation is more complex because the gas bubble does experience slip and viscous and inertial forces are present.

The regimes of bubble motion in liquid can be classified as Stokes regime, Hadamard regime, Levich regime, and Taylor regime (Astarita and Apuzzo, 1965). The characteristics of a rising bubble (i.e., its size, rise velocity, trajectory, etc.), differ from system to system, making it difficult to develop generalized correlations. To understand bubble behavior fundamental analyses have been performed from different points of view (Auton, 1987; Eames & Hunt, 1997; Magnaudet & Eames, 2000; Mei and Klausner, 1992). However, the most usual approach is through the force balance.

Many investigators (Astarita, 1996; Davis and Acrivos, 1996; Haque et al., 1987; Clift et al., 1978; Abou-ElHassan, 1983; Chhabra, 1993; Gummalam, 1987; Rodrigue, 2001, 2002) have worked extensively in various gas-liquid systems and developed correlations for a specific range of conditions. It seems the recent attempts by Nguyen (1998) and Rodrigue and co-workers (1996, 2001, 2002, 2004) to develop a generalized correlation can be considered applicable over a wide range; still, important deviations remain to be incorporated.

Single bubble rise characteristics depend on the bubble generation system and the force acting. Figure 2.6 describes the connections among various factors. Examination of these parameters can provide an indirect understanding of the forces acting and their consequences.

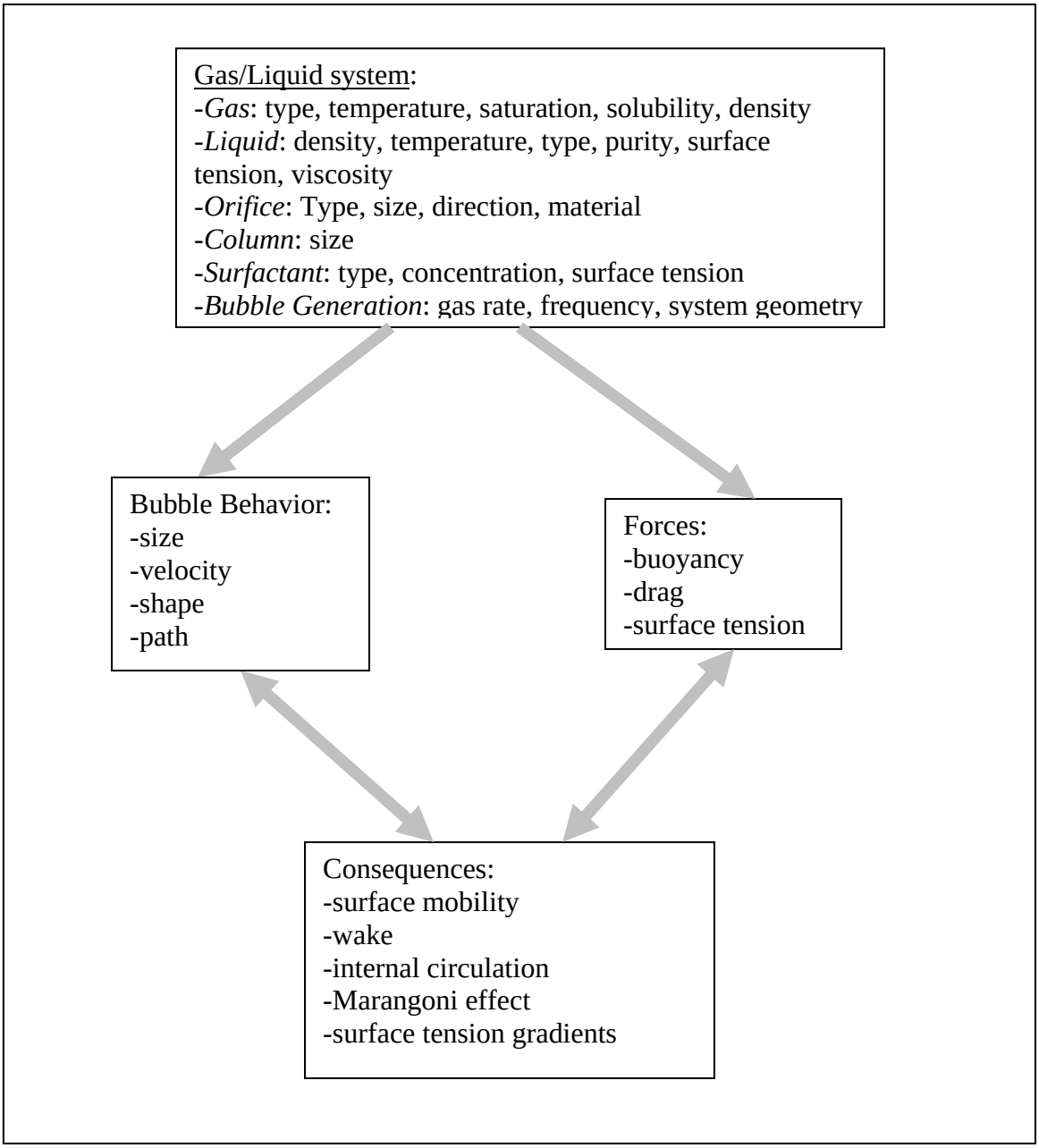

Figure 2.6: The relationships between identified factors that affect bubble behavior.

2.31. Bubble size

The surface mobility of a bubble provides for variable shape during its rise in a liquid. It is then convenient to define an equivalent diameter (d_e), namely:

$$d_e = (x.y.z)^{1/3} \qquad (2\text{-}15)$$

where, x, y and z are diameters in the X, Y, Z directions.

For a spherical bubble these diameters will be similar and for a flattened bubble (oblate spheroid), Δy, for instance, will be less than Δx. Aspect ratio (E) is the ratio of minor to major axis. If aspect ratio is close to 1 (0.9>E>1) the object can considered as spherical (Clift et al., 1978).

Bubble size is changed by hydrostatic pressure. In a static fluid, shear and tensile forces are absent, and the only force involved is a compressive one. According to Pascal's law the pressure in a static fluid is the same in all directions. The absolute pressure (P_0) is given by equation:

$$P_0 = P_{atm} + \rho g h_l \qquad (2\text{-}16)$$

where P_{atm} is atmospheric pressure and h_l is the height of liquid over the bubble.

As a bubble rises through a column the height of liquid above and therefore pressure on the bubble decreases. Assuming the ideal gas law and an isothermal system the bubble size increase during rise in a liquid can be calculated.

2.3.2. Bubble shape

The interaction between a rising bubble and the surrounding liquid medium determines the bubble shape and the extent of the disturbance in the surrounding flow field (Fan and Tsuchiya, 1990). Bubbles in motion can be classified by shape as spherical, ellipsoidal and spherical/ellipsoidal cap. De Vries (2001) summarized the results of previous work for shape of bubble and onset of shape oscillations.

For single small bubbles (e.g., d_e<1mm), bubble shape is approximately spherical. When bubble size increases dynamic, viscous and inertial forces come into play. The dynamic pressure due to the flow decreases along the bubble surface from the bubble front to the sides. Thus with increasing bubble size (or

Re), the dynamic pressure between the bubble front and bubble side increases which explains why the bubble flattens (ellipsoid oblate shape) in the direction of the bubble motion. Addition of surfactant by introducing surface viscosity and surface tension effects can reduce the effect of dynamic pressure difference on flattening; i.e., increases the aspect ratio of the bubble (Figure 2.7).

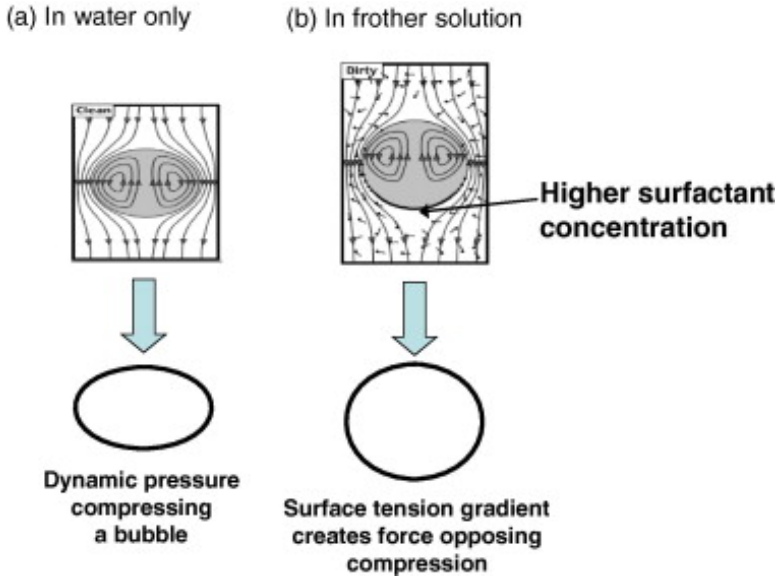

Figure 2.7: Illustration of dynamic pressure causing bubble deformation in water only case (a), and the force created by surface tension gradient that occurs in presence of surfactant that resists deformation (b) (Finch et al., 2008).

For large bubbles (d_e>18mm) (Clift et al., 1978) the effect of surface tension and viscosity are negligible and inertial or buoyancy forces are dominant and the bubble shape is ellipsoidal/spherical cap. The induced pressure difference between the front and the side of the bubble explains the transition of bubble shape from spherical to ellipsoidal but it is not enough to describe the transition of ellipsoidal to spherical/ellipsoidal cap.

Haberman and Morton (1953) suggested that a dimensional analysis for prediction of bubble shape can be based on the acceleration due to gravity, the terminal velocity of bubble rise, the diameter of volume equivalent sphere, the liquid density and viscosity and finally the interfacial tension. These variables appear in three dimensionless numbers: Reynolds, Morton and Eotvos. Figure

2.8 shows the shape regimes and bubble shape transition boundaries for bubbles in motion through liquids (Clift et al., 1978).

Generally, for a given size of bubble it becomes less flattened when the liquid surface tension is large (low We or Eo) and the liquid viscosity is large (low Re). But when the system is contaminated, by surfactant molecules that collect at the liquid-bubble interface the bubble shape cannot be determined by liquid properties alone. In other words, the bubble shape is strongly influenced by the conditions at the gas/liquid interface (Griffith, 1962; Grace et al., 1976). By adsorption of surfactant at the interface, the viscous drag increases (Boussinesq, 1913; Sciven, 1959; Agrawal and Wasa, 1979; Fan and Tsuchiya, 1990).

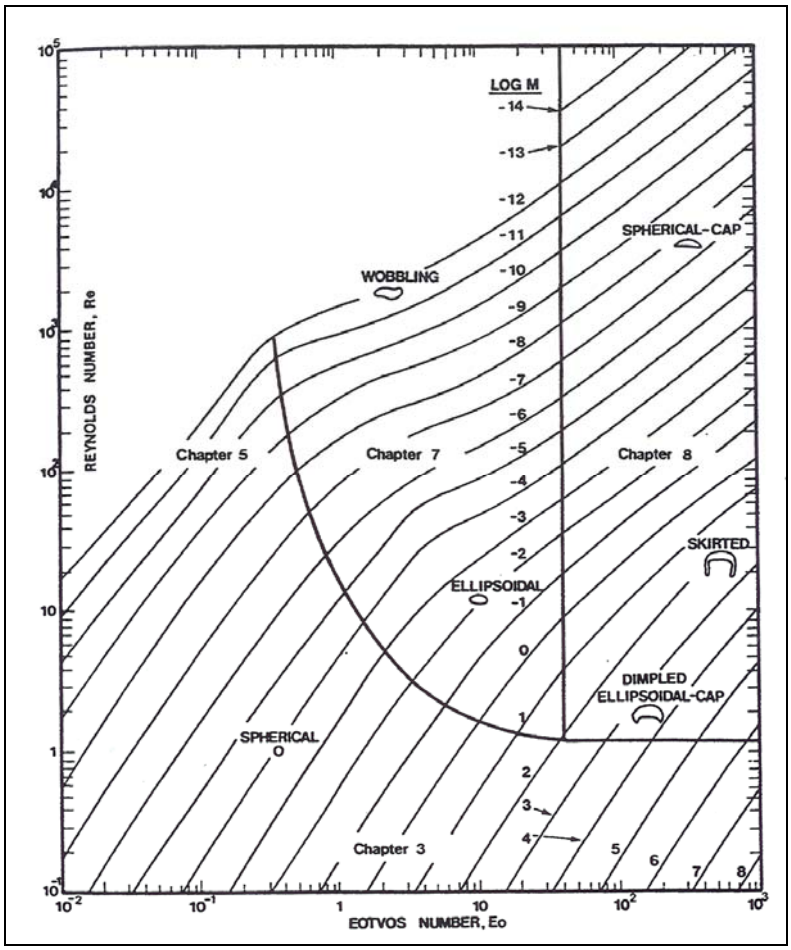

Figure 2.8: Bubble shape regime (reproduced with permission from Clift et al., 1978).

2.3.3. Bubble rise path

The bubble rise path can be defined by the trajectory of the bubble centre. Fan and Tsuchiya (1990) note that the bubble rise path and change in orientation (defined as the angle between the bubble major axis and the vertical axis of the system) are strongly dependent on the bubble shape. De Vries (2001) summarized the path instability modes and the regimes observed.

Single bubbles rise in a straight line (rectilinear) when they are spherical. On increasing bubble size the bubble starts to deform into an ellipsoidal shape and the bubble starts to exhibit zigzag or spiral motion. Bubble orientation is also affected by shape deformation (Tsuge and Hibino, 1977; Fan and Tsuchiya, 1990). As the bubble changes from ellipsoidal to spherical/ellipsoidal cap (at Re ≈ 5000 (Miyahara, 1988)), the radius of the spiral or the amplitude of the zigzag decreases and the motion becomes rectilinear, but with rocking.

The bubble rise path and fluctuations in the orientation of the bubble can be characterized by the frequency or period of cycle of the motion according to Tsuge and Hibino (1971). In general, both the amplitude and frequency of bubble oscillation are related to the bubble size, shape and presence/absence of surfactants.

Detailed experiments were discussed by De Vries et al. (2002), who investigated the motion of gas bubbles in highly purified water. For bubble size <2mm, the bubbles rise axisymmetrically. Shape oscillation for bubble size >2mm was observed at a certain height depending on the conditions and especially bubble size. In this situation bubbles establish an approximately ellipsoidal shape.

Typically, the dynamics of bubble rise is nonlinear and the extent of nonlinearity increases with bubbles size. Observations have shown that bubble trajectories have a primary and secondary structure (Yoshida and Manasseh, 1997). For high viscosity Newtonian and non-Newtonian liquids, irrespective of the size of

the bubble the trajectories are rectilinear, mainly because of the large viscous drag.

Lunde and Perkins (1997) clarified the relationship between the wake structure and trajectory of clean bubbles (helical or zigzag). They suggested that there may be a correspondence between the wake structure and the bubble trajectory.

2.3.4. Bubble rise velocity

After the detachment of a bubble from an orifice under a liquid, the buoyant force causes it to rise. The dynamics associated with the rise are mainly due to temporal variation in bubble characteristics.

Measurement of bubble rise velocity is important in order to understand, for example bubble dispersion in a liquid and the adsorption mechanism at a gas/liquid interface. Rise velocity is fundamental to the performance of bubble reactors.

To discuss rise velocity of a bubble two terms are introduced: local and terminal velocity. Local velocity is the velocity of a rising bubble at a certain time or distance after release. Terminal velocity is the velocity of a bubble when according to the Newton's second law acceleration is zero. In other words, it represents the constant velocity of the rising bubble when time no longer influences local velocity significantly. Figure 1.1 showed the terminal velocity as the third stage of the velocity profile (Sam et al., 1996). (In reality the bubble will increase in size as it rises due to decreasing hydrostatic pressure and velocity will change in a predictable manner (e.g. see Zhang et al. (2003)).

The rise of a bubble in a liquid can be considered as a function of several parameters including: bubble characteristics (size and shape); properties of the gas-liquid system (density, viscosity, surface tension, concentration of solute, density difference between gas and liquid); liquid motion (direction); and

operating conditions (temperature and pressure). Some of these will be described with regard to their importance as established in many studies.

2.3.4.1. Factors affecting the rise velocity

a- Type and purity of liquid

The rise velocity in each pure liquid would be different. However, the same trend may be observed. Kulkarani and Joshi (2005) presented bubble rise velocity for some pure and contaminated liquids.

In Figure 2.9, bubble terminal rise velocity vs. size is shown for an inviscid water. Here the upper bound of the terminal velocity data is considered to correspond to bubbles in pure water while in the presence of surfactant, the drag force increases and consequently causes a reduction in velocity leading to the scatter in the data (Clift et al., 1978; Fan and Tsuchiya, 1990). The influence of surfactants on bubble rise velocity will form a large part of this review. The results for fully contaminated water give the lower part of the data envelope.

b- Liquid viscosity

The modes of bubble rise show distinct behavior in viscous Newtonian fluids compared to inviscid and non-Newtonian liquids (Gonzaleztello et al., 1992). Rodrigue et al. (1996) reported an almost linear relationship between rise velocity and the bubble volume dependent on the liquid viscosity.

For the case of different non-Newtonian liquids, viscosity influences the relationship between the bubble size and rise velocity. For instance, terminal rise velocity may exhibit a discontinuity at a certain critical bubble size in some liquids, while no discontinuity is observed for some others. Leal et al. (1971), Astarita and Apuzzo (1965), Acharya et al. (1978), and Rodrigue (1998) have investigated this phenomenon in detail.

c-Temperature

According to the ideal gas law, at constant pressure the bubble volume increases with increasing temperature and as a consequence bubble rise velocity may change (depending on the initial size).

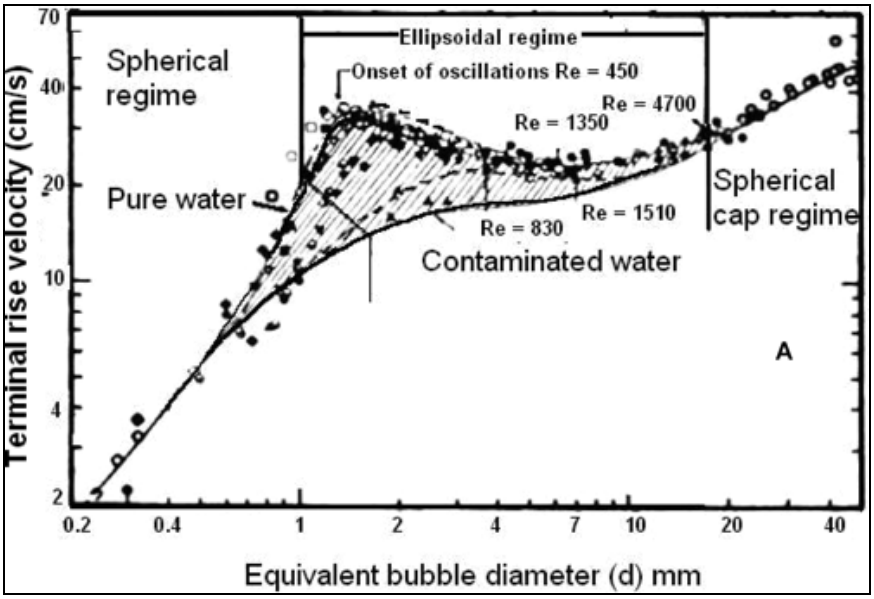

Figure 2.9: Typical trends in rise velocity with bubble size for pure and contaminated liquids (Kulkarani and Joshi, 2005).

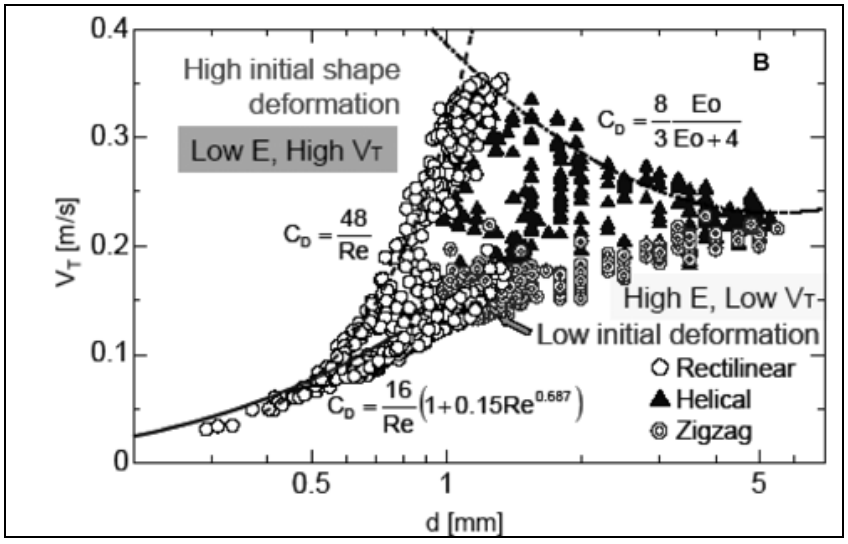

Figure 2.10: Effect of initial bubble deformation on terminal velocity in distilled water (Kulkarani and Joshi, 2005).

\

In addition liquid density is inversely proportional to the temperature variation, which influences buoyancy and thus rise velocity. However, this effect is not significant when compared to other physical properties of the liquid that affect the bubble rise velocity.

There are few studies on the effect of temperature on rise velocity of a bubble. At ambient conditions, the rise velocity follows a certain trend with bubble size. Here two different cases may be considered: rise of a gas bubble that is insoluble in the liquid and rise of vapor bubble in liquid at relatively low temperature. Both cases are common, while only the second case has been studied systematically. In the first case the heat transfer across the interface causes an increase in bubble volume. Also, at higher temperature the density difference between the two fluids decreases. Hence the buoyancy decreases and this reduces the rise velocity. The counteracting effects are dominant in different ranges of temperature and in a certain temperature range rise velocity is a strong function of size.

Zhang (2000) and Zhang et al. (2003) reported a temperature effect on single bubble velocity profile in water and surfactant solution. The profiles indicated that the time to reach constant velocity tended to decrease as temperature increased.

d- External pressure

Although most laboratory scale investigations of bubble dynamics are carried out at ambient conditions, the operating conditions in industrial systems are often significantly different (e.g. at elevated pressure). As a result of the outside pressure, bubbles are formed only after a minimum gas velocity is reached (which is higher than under ambient conditions), while the bubble sizes are smaller (subsequently reducing rise velocity). Letzel (1998) systematically analyzed the effect of gas density on the rise velocity of large bubbles. In a similar attempt, under the assumption of homogeneous nature of the suspension, Luo et al. (1997) studied the effect of external pressure on bubble rise velocity in a gas-liquid-solid fluidized bed (Newtonian viscous system). Increased pressure

was found to have less effect at higher temperatures, mainly because the difference between the vapor pressure of liquid and external pressure is decreased.

e- Initial bubble detachment condition

According to Figure 2.9 and the accompanying discussion concerning purity, the scatter has been related to the concentration of contaminants. But according to Tomiyama et al. (2001, 2002) and Wu and Gharib (2002) another reason for this scatter is the way the bubble is released from the orifice; i.e., the initial condition at detachment.

According to their analysis, for low initial shape deformation, bubble rise is at a lower velocity with a trajectory following either a rectilinear or zigzag path. For large initial shape deformation terminal velocity is high and produces wide scatter depending on the different possible release conditions and deformations. This scatter is depicted in Figure 2.10.

Tomiyama (2004) has shown that Figure 2.9 is comprised of data points that can be bounded with three drag curves. For a bubble having constant equivalent diameter an increase in aspect ratio, i.e., shape approaches a sphere, is shown to reduce terminal velocity. Kracht (2008), reported the same observation.

f-Gas type

There are few studies into the influence of gas type on rise velocity. Parkinson et al. (2008) studied the influence of some gasses on the terminal rise velocity of 1-100μm diameter bubbles in water. For N_2, He and air bubbles, excellent agreement with the Hadamard-Rybczynski equation was observed, indicating that slip was occurring at the liquid/vapor interface. For CO_2 bubbles terminal rise velocity was higher than other gasses examined, attributed to its higher solubility compared to the other gasses (Parkinson et al., 2008).

Zhang (2000) examined the influence of gas saturation (humidity) on terminal velocity. In general, air (as a gas) is able to absorb a certain amount of moisture. In that study the air was first fed through a water container to become saturated by water. The saturated air was fed to a column to generate bubbles. The results indicated that there was no significant difference between fresh and moisture saturated air bubbles.

2.3.5. Formulation for rise velocity correlation

Several investigators have developed empirical, semi-empirical and theoretical simulations for bubble rise velocity. Most apply only for a narrow range of governing parameters. In the review by Kulkarani and Joshi (2005) some rise velocity models were based on the following: force balance, dimensional analysis, and wave analogy. They listed many formulae for rise velocity in Newtonian and non-Newtonian liquids.

2.4. Contaminants and rise velocity

As the main purpose of this research is focused on the effect of frother (surfactant) on single bubble rise velocity, this will naturally occupy a significant part of the review. In addition to the effects of frother, the role of salts is included as, for some functions, frother and some salts are interchangeable.

2.4.1. Surfactant

According to Figure 2.9 at ambient conditions the velocity increases with size and passes through a maximum at ca 1.3mm (diameter) followed by a decrease in velocity over a restricted size range after which it attains a weakly positive dependence on bubble size. Depending upon the type and concentration of contaminant, the rise velocity characteristics of a bubble change significantly. The impact of surfactants on bubble rise velocity is reviewed according to liquid rheological class.

2.4.1.1. Newtonian liquids

In a Newtonian liquid the non-uniformly distributed adsorbed surfactant generates a surface tension gradient. Since the surface tension gradient must be balanced by a jump in the shear stress across the interface (Marangoni effect), a shear-free boundary condition can no longer be imposed on the liquid at the gas-liquid interface. So this leads to an increase in the drag force (stagnant cap hypothesis). As a result of formation of a rigid interface and enhancement in drag, internal circulation is reduced and the rise velocity is lower than in the clean (surfactant-free) liquid. The stagnant cap hypothesis has been used successfully for the estimation of bubble rise velocity and has also been used for the prediction of drag coefficient with respect to extent of surface contamination.

Frumkin & Levich (1947) and Levich (1962) developed a so-called adsorption theory to explain the reduction in rise velocity. Savic (1953) reported the existence of a cap (surface immobilization) on the rear part of a moving liquid drop, while the rest was tangentially stress free (mobile). Griffith (1962) studied the effect of surfactant on the terminal velocity of drops and bubbles. Kopf-Sill and Homsey (1988) applied the Hele-Shaw cell model to analyze the effect of surfactants. Fdilha and Duineveld (1995) investigated the effect of surfactant on the rise of a spherical bubble at high Reynolds and Peclet numbers. They found that the rapid slowdown of the bubble occurs when nearly half of the bubble surface is covered by the surfactant layer. De Kee et al. (1990) reported that a reduction in surface tension resulted in a decrease of bubble rise velocity of small bubbles without any discontinuity. However Rodrigue et al.(1996) reporting the same phenomenon, found no influence on bubble rise velocity over a certain concentration of surfactant. Cuenot et al. (1997) discussed how retardation of the bubble surface fluidity is dependent on the amount of adsorbed surfactant. Sam et al. (1996) studied axial velocity profiles of single bubbles in water/frother solutions and among other findings concluded there was no concentration effect on terminal velocity only on the time to reach terminal velocity. Zhang and Finch (2000) confirmed that terminal rise velocity was independent of concentration on

concentration for the surfactants tested. Krzan et al. (2004) studied the influence of the surfactant polar group on the local and terminal velocities of bubbles. Here the minimum adsorption coverage required to immobilize the bubble surface was estimated for some surfactants. They concluded that mainly surfactant adsorption kinetics governed the mobility of rising bubble interfaces. Recently, Acuna et al. (2008) reported that the frother type could affect the terminal velocities of same size bubbles in swarms, even for diameters below 1mm.

2.4.1.2. Non-Newtonian liquids

Rheological behavior of non-Newtonian liquids is complex and the motion of bubbles in these liquids has different characteristics to those observed in Newtonian liquids. For the case of power-law non-Newtonian liquids, Tzounakos et al. (2004) studied the effects of surfactants based on analysis of the drag curve. Ybert and Di Meglio (1998) measured bubble rise velocity as a function of distance traveled. After the initial stage of acceleration from rest, the instantaneous rise velocity of a given bubble depended only on the total amount of surfactant adsorbed on the bubble surface. It was also shown that the surfactants are not only absorbed onto the bubble surface, but may also desorb, which increases the bubble rise velocity.

2.4.1.3. High viscosity liquids

The few studies (Barnett et al.,1966; Haque et al., 1988; Margaritis et al.,1999; Miyahara and Yamanaka, 1993 and De Kee et al., 1986) have shown that for high viscosity Newtonian liquids, the rise velocity is a weak function of the bubble volume, while for non-Newtonian liquids, it has a linear dependence but the velocities in the former case are much higher than in the latter.

2.4.1.4. Simulation and numerical analysis

There are several published simulations and numerical analyses of bubble rise velocity in the presence of surfactant. Some that directly discuss terminal velocity are: Harper (1973 and 1987), Fdhila and Duineveld (1995), McLaughlin (1996), Nguyen (1998), Rodrigue et al. (1999), Liao and McLaughilin (2000), Bozzano

and Dente (2001), Zhang et al. (2001), Alves et al. (2005), Liao et al. (2004) and Takemura (2005).

2.4.2. Frothers

In the present context the action of frother is to retard bubble rise velocity. There have been few studies on single bubble rise velocity in the presence of frothers. Sam et al. (1996) added trace amounts of MIBC, pine oil and Dowfroth 250 to water and studying the velocity profile over some 400cm found that the profile was sensitive to frother type and concentration, but while the terminal velocity appeared dependent on frother type, it was not dependent on frother concentration. The time-dependent velocity was attributed to time dependent adsorption of surfactant causing increased bubble rigidity and surface viscosity. Figure 2.11 shows the velocity profiles for 2.2mm bubbles in MIBC (a) and terminal velocity vs. bubble size for some frothers (b).

Zhang (2000) and Zhang and Finch (2000) studied the impact of MIBC, pine oil, Dowfroth 250 and Dowfroth 1263 on the rise velocity of single bubbles. These results confirmed the previous study by Sam (1995). It was noted that the distance to reach terminal velocity in surfactant solution was dependent on bubble size, surfactant type and surfactant concentration. A good agreement was achieved between measured terminal velocity in these solutions and Karamanev's model for Re>130 (Karamanev, 1994). For Re<130 it was shown that when a bubble reaches terminal velocity, the bubble surface can be reasonably set as a no-slip boundary condition.

Krzan and co-workers report velocity profiles for 1-butanol and 1-hexanol (Krzan and Malysa, 2002), and 1-pentanol and 1-octanol (Krzan et al., 2007) at 40 and 350mm distance over a capillary tip. It was reported that at low concentrations of the alcohols, the rise velocity reached maximum at 5-50mm distance from the orifice. But, for distilled water and high concentration of alcohols no maximum velocities were observed. Finally, the local bubble velocity was analyzed as a

function of the adsorption coverage of surfactant on the bubble surface.

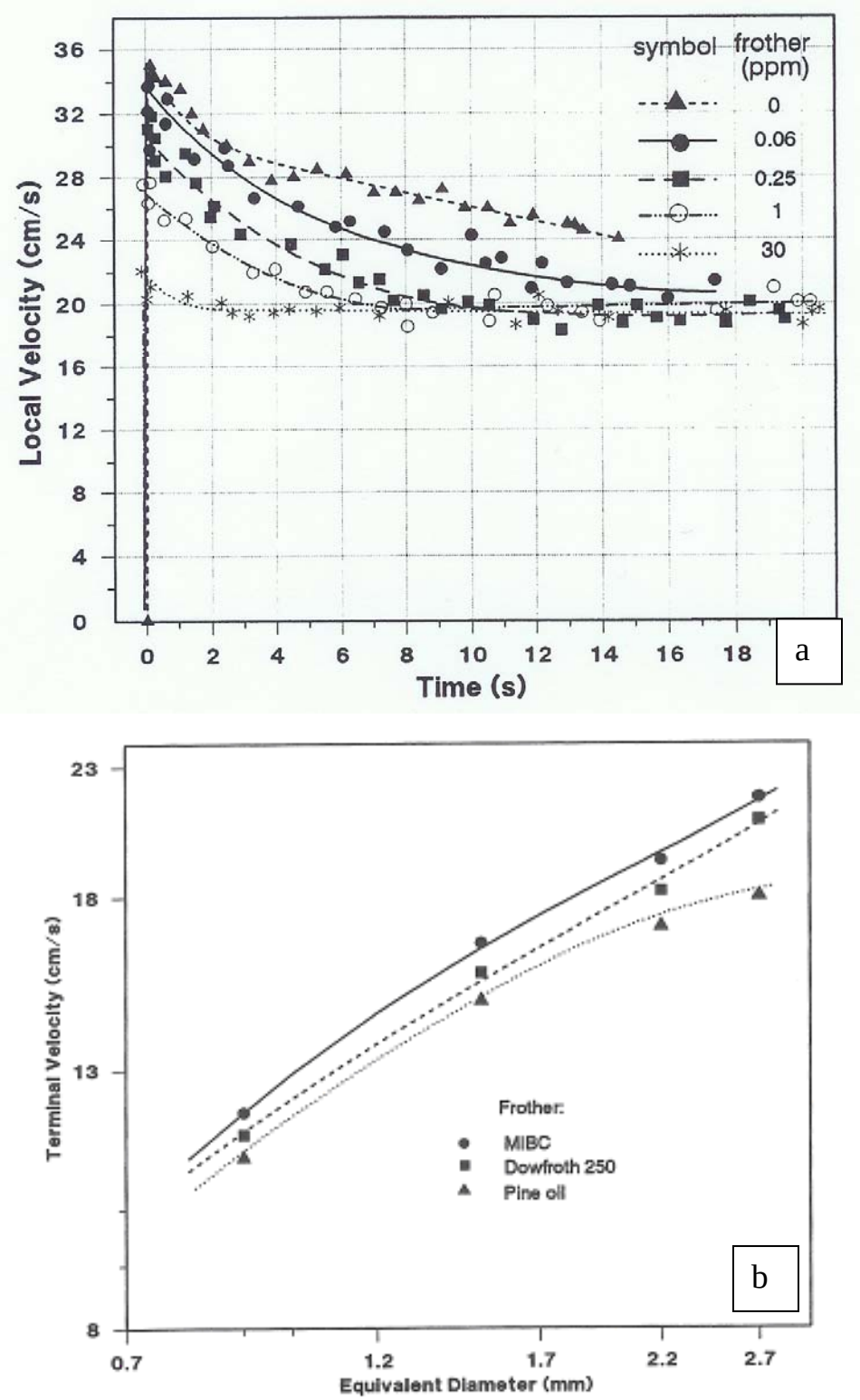

Figure 2 11: a. Velocity profiles for 2.2mm bubbles in MIBC, b. Terminal velocity vs. bubble size in the presence of some frothers (Sam, 1995).

Azgomi et al. (2007), trying to characterize frothers, reported that for the same gas holdup and gas rate, the bubble size depended markedly on frother type (Figure 2.12). This observation gave rise to the hypothesis explored in this thesis namely that frother type can affect bubble rise velocity.

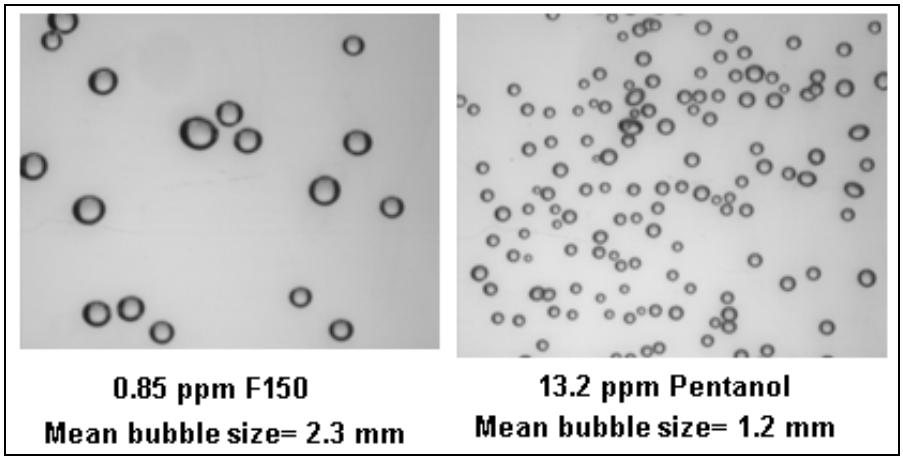

Figure 2.12: Bubble size measurement at same gas holdup (8%) for F150 and Pentanol (Azgomi et al., 2007).

As a first investigation of the hypothesis Acuna (2008) studied the impact of frother type on the rise velocity in a multi-bubble system. The results proved that frother type can have a significant effect on bubble rise velocity. Figure 2.13 shows the effect of F150 and pentanol on the velocity of bubbles in the swarm. According to Figure 2.13 F150 significantly reduced the velocity compared to pentanol, which acted similar to clean water. This result agrees with the conclusion of Azgomi et al. (2007).

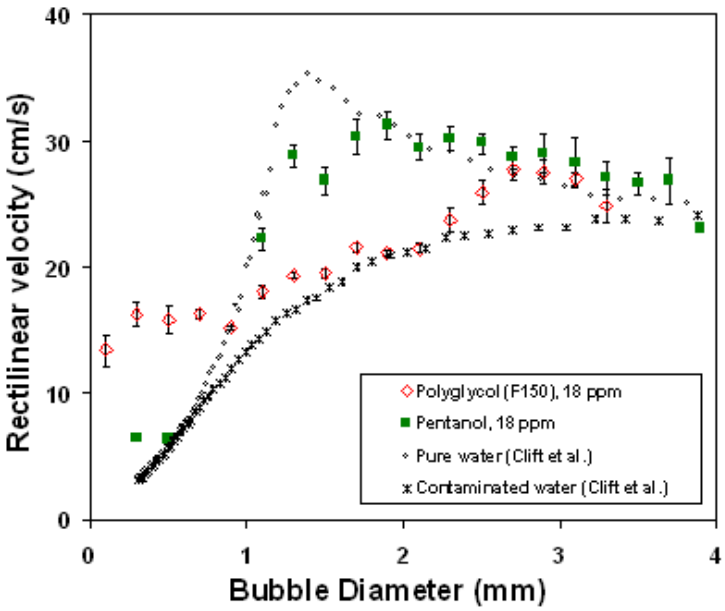

Figure 2.13: Comparison between influences of F150 and Pentanol on terminal rise velocity of bubbles in swarms (Acuna, 2008).

2.4.3. Salts

Some salts produce small bubbles and in that sense act like frothers (Quinn et al., 2007). Like surfactant salts can create surface tension gradients and set up Marangoni effect stresses. As a consequence mobility of the interface is altered and an effect on bubble rise velocity can be expected. But, the electrolyte effect is much smaller (i.e., high concentrations are required (Quinn et al., 2007)) than is the case for surfactant (Henry et al., 2008).

The effect of electrolyte remains unclear. Craig et al. (1993), Rebeiro and Mewes (2007), and Henry et al. (2008) reported that some salts inhibit coalescence and others do not. Lee and Hodgson (1968) suggested that electrolytes give rise to dynamic increases in interfacial tension and thus retard the surface flow of thin liquid films, leading to an immobile or a partially mobile interface.

Finch et al. (2008) suggested a possible explanation for the action of salts in forming small bubbles that was based on two assumptions: i) a high concentration of salt is needed; ii) salt should increase surface tension. Figure

2.14 describes the air/water interface under these conditions. Here the water molecules provide the low surface tension site (compared to salt molecules) and force is generated away from this point. Therefore an opposing force is generated like in the action of surfactant. Here water molecules have taken on the role of surfactant.

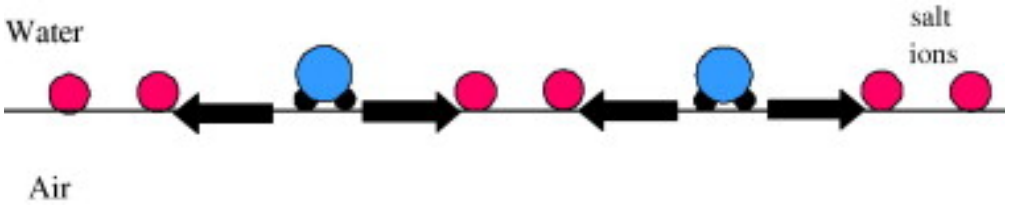

Figure 2.14: Suggested explanation for action of high concentration salts which act like frother (Finch et al. 2008).

Detsch and Harris (1989) studied the dissolution and rise velocity of small air bubbles in water and salt water. The results indicated that the bubble velocity in the presence of salt was lower than in pure water.

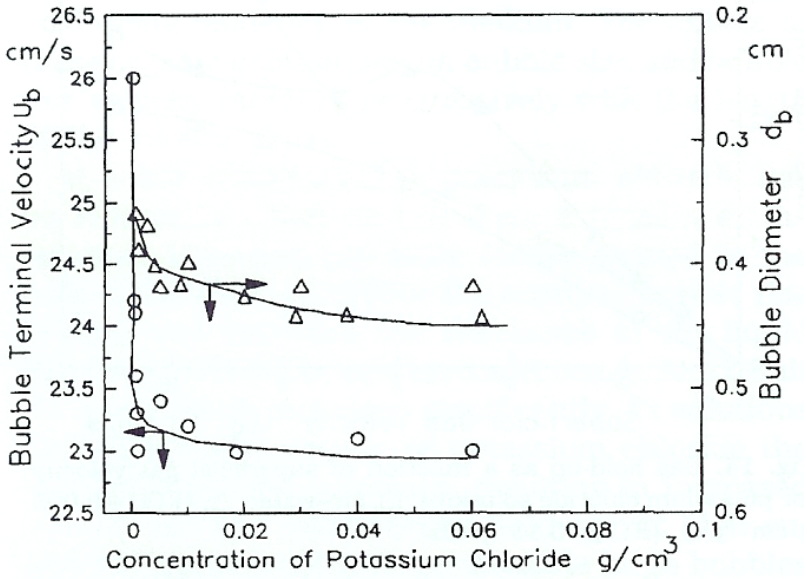

Figure 2.15: Influence of potassium chloride concentration on terminal rise velocity (Jamialahmadi and Muller-Steinhagen,1992).

Jamialahmadi and Muller-Steinhagen (1992) studied the effect of ethanol and potassium chloride concentration on bubble rise velocity in swarms. Figure 2.15

shows the dependency of bubble size and rise velocity on reagent concentration. Adding of trace amount of potassium chloride reduced the terminal rise velocity compared to pure water. However, after increasing salt concentration no frother significant reduction was achieved. The authors suggested that the ionic forces formed in the bulk of the solution reduced the terminal rise velocity and reinforce the resistance of the liquid film on the bubbles against coalescence. As a consequence the bubble size increase seems to be in contradiction.
Kugou et al. (2003) studied the motion of air bubbles in seawater. They reported that for small bubble size (<3mm) the rise velocity was almost the same as in artificial seawater and lower than that in distilled water. However, for larger bubbles (>3mm) the velocity in seawater was almost the same as in distilled water.

Quinn et al. (2007) compared the influence of some salts with MIBC (as an example frother). The results indicated that there was a correlation between gas holdup and ionic strength of salts. Gas hold up for a salt solution with ionic strength of 0.4-0.5, was similar to that of 7-10ppm MIBC, which is a typical industrial dosage for this common frother.

Henry et al. (2008) measured the terminal rise velocity of small bubbles (d_e<100μm, Re<1) in some electrolyte solutions. The results indicated that terminal rise velocity was in good agreement with the Hadamard-Rybczynski model (mobile surface as in pure water). In addition, there was no significant difference in the velocity between electrolytes that inhibit bubble coalescence, and others that have no influence.

In summary, all observations confirm the influence of high concentration of some salts on preventing coalescence and producing small bubbles. But in the case of an influence of salts on bubble rise velocity, there is no uniformity among investigators.

CHAPTER THREE: EXPERIMENTAL SETUP

The methods for measurement of bubble rise velocity can be classified as either intrusive or non-intrusive. A non-intrusive measurement method is desirable and photography is considered the most practical (Kulkarani and Joshi, 2005). Chapter three describes the photographic technique used.

3.1. Equipment

3.1.1. Column setup

A circular Plexiglas column 6.35cm diameter by 350cm high was used surrounded by a square Plexiglas water jacket (8 x 8 x 330 cm) (Figure 3.1). A measuring tape was placed along the central axis of the column to measure the size and local velocity of the bubbles. The column diameter was large enough to avoid wall effects for bubbles < 3 mm (Grace, 1973; Narayanan et al., 1974; Bhaga, 1976; Clift et al., 1978). To control a uniform temperature along the column water was circulated through the jacket; the square column also avoided optical distortion associated with a curved surface.

3.1.2. Air line

Air was provided from a controllable compressed air system with flow rate adjusted by an online monitoring system. Plastic tubes and connectors were used to transfer air from the source to the glass capillary at the bottom of the column. The air was from the university compressor and was dry.

3.1.3. Camera moving device

A mobile digital video camera was used to track a single bubble during its rise. To follow the bubble it is necessary to have a variable speed motor, in this case driving a chain belt over a pulley (Figure 3.1). Limit switches were placed at the bottom and top of the column to arrest the movement. The movement of the camera was controlled manually through the variable speed controller over a range from zero to 50 cm/s, the experimenter adjusting the speed to keep the bubble in view (on a monitor) during its rise.

A high resolution CCD digital video camera recorder (Canon GL2), a monitor (Sony PVM-1340) and a signal sender set (Radio Shack 15-2572) were used. The video camera recorded 30 frames per second. When used to obtain the shape and size of the bubble, a shutter speed 1/1000 of a second was set.

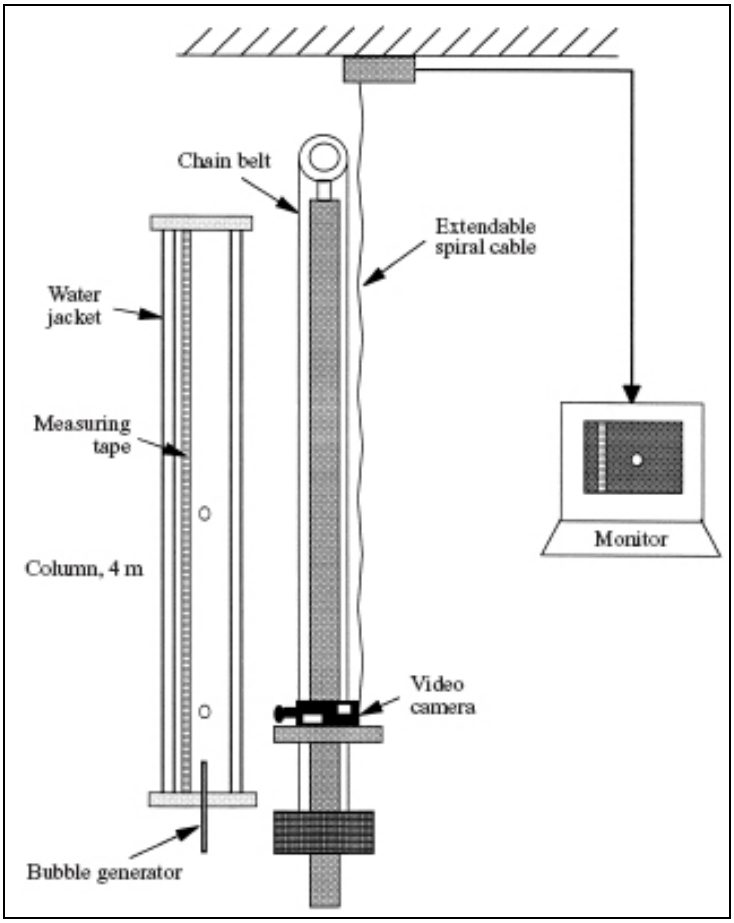

Figure 3.1: The experimental column setup.

3.1.4. Capillaries

In this work three glass capillaries were used with 25, 51 and 75mm inside diameter, manufactured by Friedrich & Dimmock.

3.2. Requirements

3.2.1. Temperature control

Any temperature variation along the column would affect bubble motion; consequently the temperature was kept uniform at room temperature by circulating water. To achieve room temperature, Montreal tap water was held in a large container (55 L, sufficient for both preparation of test solution as well as circulating water) for over 10 hours prior to a test. The temperature remained in the range 24 to 26°C.

3.2.2. Bubbling frequency

Bubble frequency up to 80 bubbles per minute has been shown to have no effect on velocity (Sam et al., 1996). As a consequence, bubble frequency was adjusted to less than 80 per minute for all current tests.

3.2.3. Water saturation

It was suspected that the humidity of the air might affect the bubble rise velocity. Zhang (2000) reported no obvious difference between “dry” and “water-saturated” bubbles in either tap water or contaminated water. Based on this no special precautions regarding humidity were taken.

3.3. Procedures

3.3.1. Bubble velocity profile

To set up, the column was filled with tap water and appropriate concentration of reagent. Tap water was circulated inside the water-jacket layer to keep the temperature uniform at room temperature. Single bubbles were generated at a stable frequency regime (less than 80 bubbles per minute). The experiment was initiated by activating the mobile video camera at the moment a bubble was released from the orifice. The images captured by the tracking camera were displayed on a monitor and the experimenter adjusted the speed to maintain the single bubble at approximately the center of the field of view. Images were

recorded on digital tape and were later transferred to a computer for data processing.

3.3.2. Data Processing

To process the data several steps were executed (Figure 3.2). The captured images contained the data required to determine velocity profile and bubble size (and to check frequency). The information was transferred from digital tape to a computer using Windows Movie Maker software and was converted to a video file. The video file was cut into parts using the software and put in different folders according to the type of information sought. The video files were processed to measure bubble size and obtain velocity profile and terminal velocity.

All results were entered into a database. The results were checked and if errors (such as low level of reliability, abnormal data, etc.) were detected the measurement was repeated. The database was developed using Microsoft Excel and consisted of four layers: data entry, data summary, calculations and results.

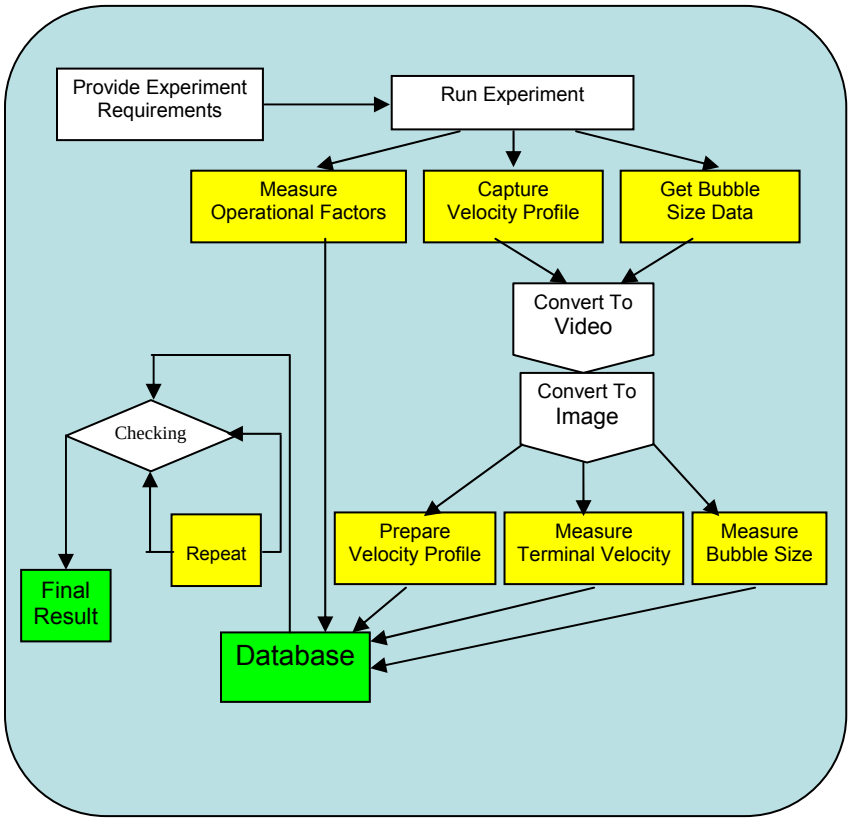

Figure 3.2: The data processing flowchart.

3.4. Reagents

Ten reagents were tested consisting of a homologous series of aliphatic alcohols, three isomers of hexanol, including MIBC, two polyglycols and salt (NaCl). Table 3.1 gives some properties of the reagents.

Table 3.1: Summary of reagents types and properties.

Reagent	Structure	Formula	Molecular Weight g/gmol	Supplier
1-Butanol	Aliphatic alcohol	$CH_3CH_2CH_2CH_2OH$	74	Sigma Aldrich
1-Pentanol	Aliphatic alcohol	$CH_3CH_2CH_2CH_2CH_2OH$	88.15	Sigma Aldrich
MIBC (Methyl Iso Butyl Carbonil)	Aliphatic alcohol	$CH_3CH(CH_3)CH_2CH(OH)CH_3$	102.18	Sigma Aldrich
1-Hexanol	Aliphatic alcohol	$CH_3CH_2CH_2CH_2CH_2CH_2OH$	102.18	Sigma Aldrich
2-Hexanol	Aliphatic alcohol	$CH_3CH_2CH_2\ CH_2\ CH_2CH_2$ OH	102.18	Sigma Aldrich
1-Heptanol	Aliphatic alcohol	$CH_3CH_2CH_2CH_2CH_2CH_2CH_2OH$	116.20	Sigma Aldrich
1-Octanol	Aliphatic alcohol	$CH_3CH_2CH_2CH_2CH_2CH_2CH_2CH_2OH$	130.22	Sigma Aldrich
Dowfroth 250	Polyglycol ether	$CH_3(C_3H_6O)_4OH$	264.35	Dow chemical company, USA
Sodium Chloride	Salt	NaCl	206.29	Flottec, USA
F150	Polyglycol	$H(C_3H_6O)_7OH$	425	Flottec, USA

3.5. Measurement techniques

3.5.1. Bubble position

To measure bubble rise distance (from zero, the capillary tip) the technique illustrated in Figure 3.3 was used. The position of the bubble centre, the height of the lower line and the distance between upper and lower lines were measured in pixels using Adobe Photoshop software. Since the distance between the upper and lower lines is 4 mm, the height of bubble center was calculated from the following equation:

$$H_B(mm) = H_L(mm) + 4 \times ((H_B(Pix) - H_L(Pix)) / ((H_U(Pix) - H_L(Pix))) \quad (3.1)$$

where H_B, H_L and H_U are height of bubble, upper line and lower line, respectively.

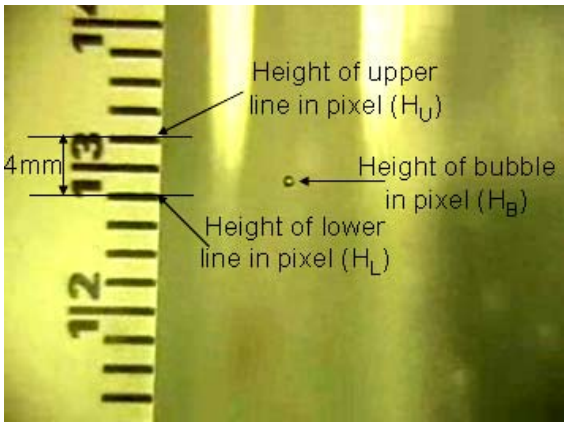

Figure 3.3: The required information for measuring bubble height during rise on one image.

3.5.2. Local velocity

Figure 3.4 shows the technique for measuring local rise velocity (U_b). Here the local velocity was considered as the average velocity of a bubble over time interval of t_1 to t_2. By measuring the corresponding distance traveled by the bubble (from H_1 to H_2) the local velocity was calculated using the following equation:

$$U_b = \frac{H_2 - H_1}{t_2 - t_1} \qquad (3.2)$$

As change in velocity is initially rapid as bubbles accelerate from zero velocity, over the first second, the $\Delta t = t_2 - t_1$ was short, 66ms; for times>1s Δt was larger, 1000ms. The velocity profile was plotted against the mid point of the interval, i.e., in space at $H = (H_1+H_2)/2$ or in time at $t = (t_1+t_2)/2$.

3.5.3. Bubble size

To measure bubble size the technique shown in Figure 3.5 was applied. A camera was put at "front" and "side" positions relative to the column. High resolution images were taken in each position recorded on digital tape. The images were extracted from the video files using Frame Shot software. The size of bubble in each image was measured using Adobe Photoshop or Able Image Analysis software.

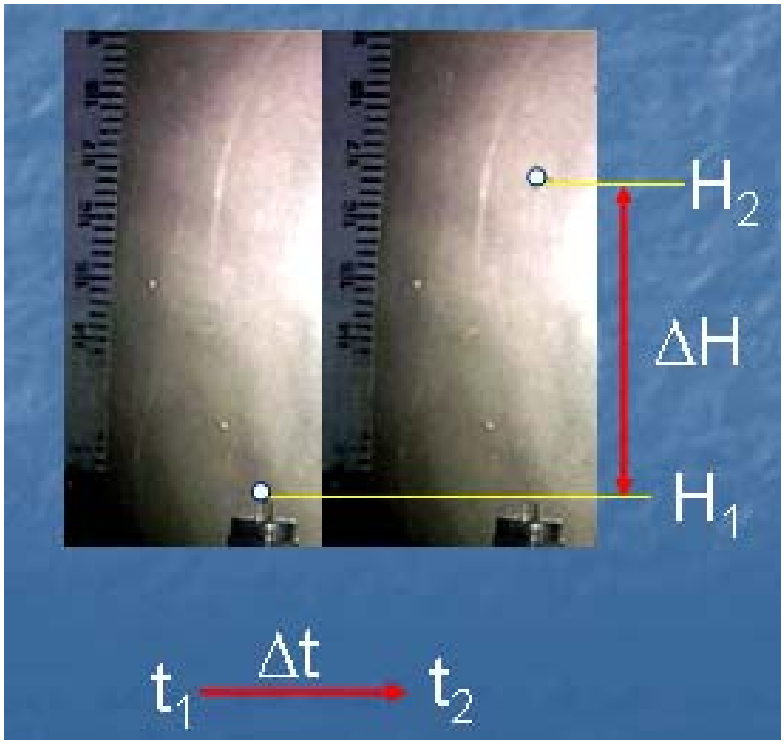

Figure 3.4: The applied technique for measuring local velocity.

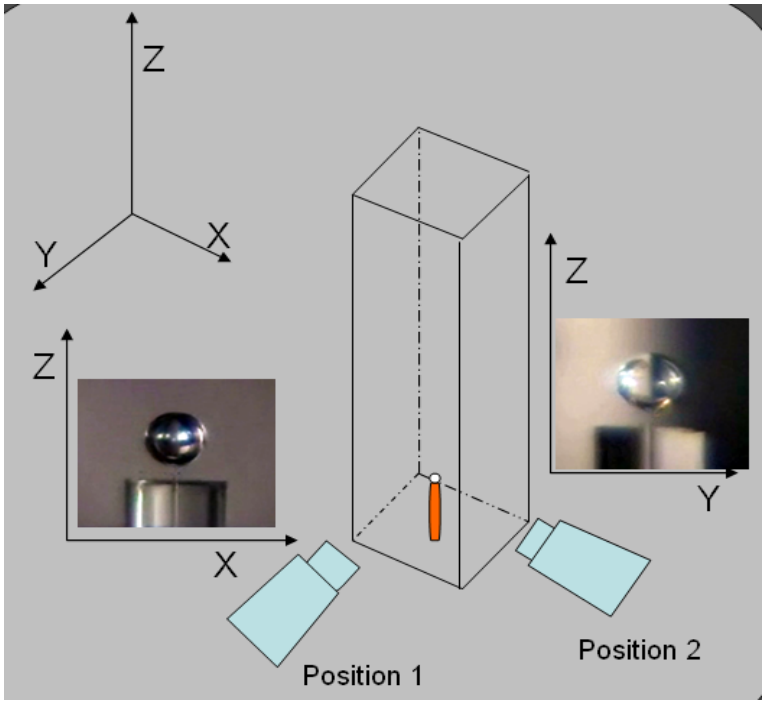

Figure 3.5: The technique applied for measuring bubble size.

3.5.4. Reagents and choice of reagent concentration

To compare the influence of reagent type on bubble rise velocity, a choice of concentration range is required. Given a prime use of frother is control of bubble size, the choice of reagent concentration was based on that criterion.

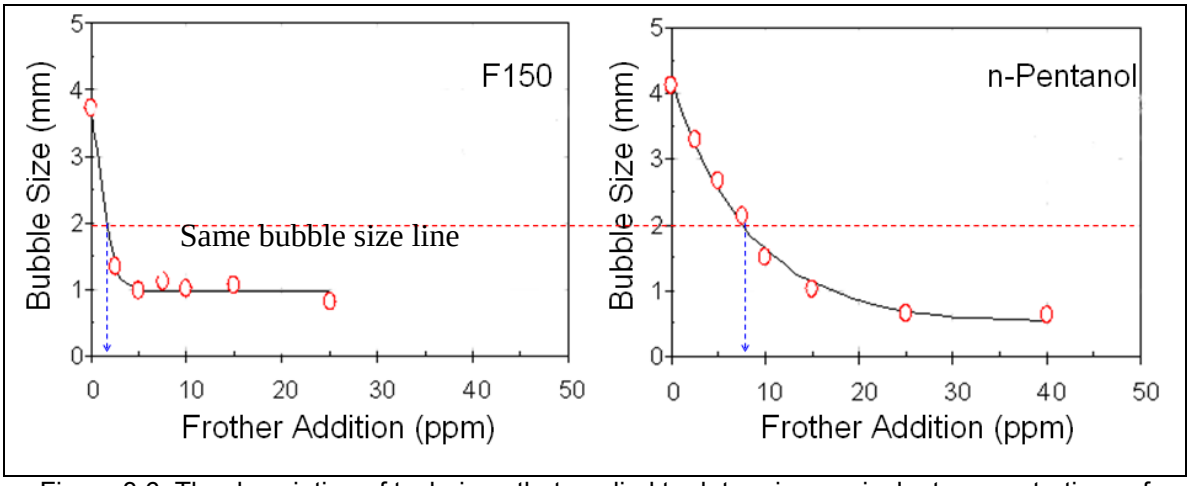

Figure 3.6: The description of technique that applied to determine equivalent concentrations of F150 and 1-Pentanol (adapted from Finch et al. 2008).

An example will serve to show the approach. Finch et al.(2008) reported the influence of type and concentration of some frothers on bubble size. Figure 3.6 presents the influence of concentration on bubble size for F150 and pentanol. A horizontal line is shown at 2mm bubble size which links the concentration for the two frothers. From this result, 2ppm of F150 is equivalent to 9ppm 1-pentanol. Table 3.2 presents the equivalent concentrations (listed 1-6) for the reagents based on this approach and applied in this work.

Table 3.2: The equivalent concentrations of applied reagents.

Reagent	type	Equivalent Concentration					
		1	2	3	4	5	6
1-Butanol (ppm)	Alcohol	11.5	25	41	58	82	246
1-Pentanol (ppm)		7	15	25	35	50	150
1-Hexanol (ppm)		5.25	11.3	18.5	26.2	37.5	112.5
2-Hexanol		5.25	11.3	18.5	26.2	37.5	112.5
1-Heptanol (ppm)		4.5	9.6	16.5	22.5	32	96
1-Octanol (ppm)		4.5	9.5	16	22.3	32	96
MIBC (ppm)		2.5	5	7.5	10	20	60
Dowfroth 250 (ppm)	Polyglycol	3	6	10	15	25	75
F150 (ppm)		1	2	3	5	10	30
Sodium Chloride (mol/L)	Salt	0.1	0.2	0.3	0.4	1	3

Six equivalent concentrations (1-6) were selected to compare reagents. Equivalent concentration 6 represents three times equivalent concentration 5 to include a “very high” concentration.

CHAPTER FOUR: RESULTS AND DISCUSSION

4.1. Reliability

4.1.1. Bubble generation

The three glass capillaries generated bubbles in three size classes. Table 4.1 shows the range of bubble frequency achieved for each capillary. The frequency of generated bubbles depends on inside diameter and length of capillary. The frequency is a function of the minimum gas rate required for generating a bubble, the water level in the column and air chamber volume. Generally, smaller inside diameter and longer capillaries help the system to work stably at low frequency.

Table 4.1: The range of bubble size and frequency.

Bubble Size (mm)	Bubble Frequency (bubble/min)
0.70-0.97	14-26
1.50-1.60	47-55
1.91-2.00	70-80

All experiments for a given capillary were executed at the same gas flow rate. Figure 4.1 presents the variation of single bubble size vs. frequency produced with the 25μm capillary.

According to Figure 4.1 bubble size was reduced by an increase in frequency, as expected, for a given flowrate. The trend appears independent of reagent type. Figure 4.2 shows the same trend is observed for all three capillaries. The two larger two capillaries gave tighter control over the bubble size. Figure 4.3 presents bubble diameter vs. equivalent concentration for some of the reagents. There is a slight but persistent difference in bubble size between frother types.

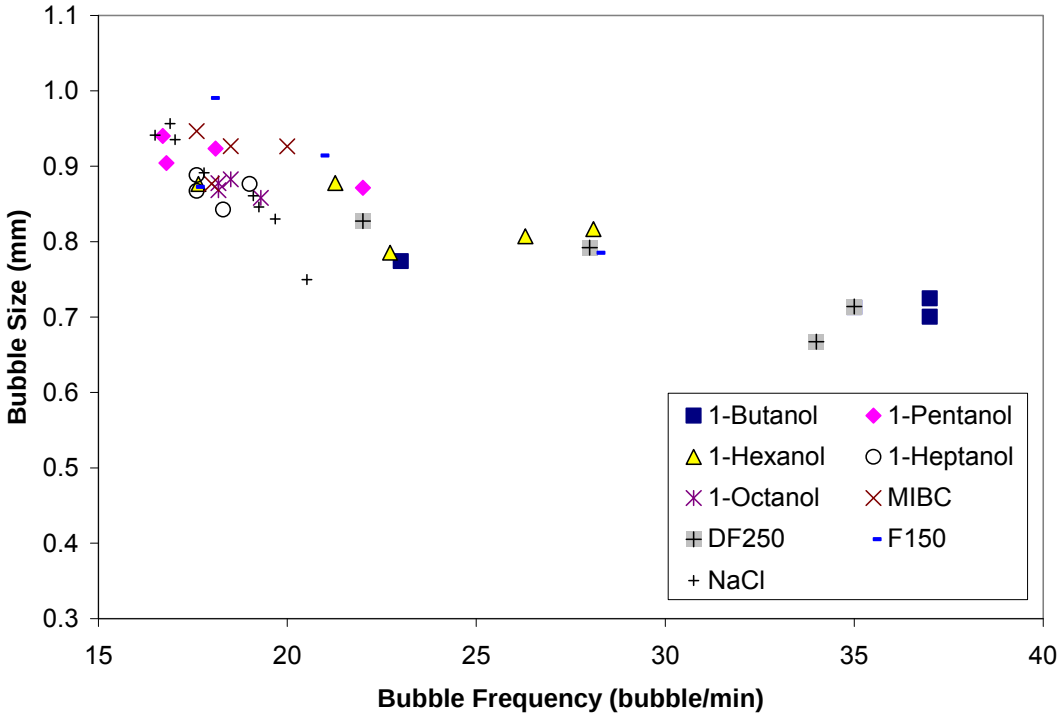

Figure 4.1: Variation of single bubble size vs. bubble frequency for reagents using 25µm capillary.

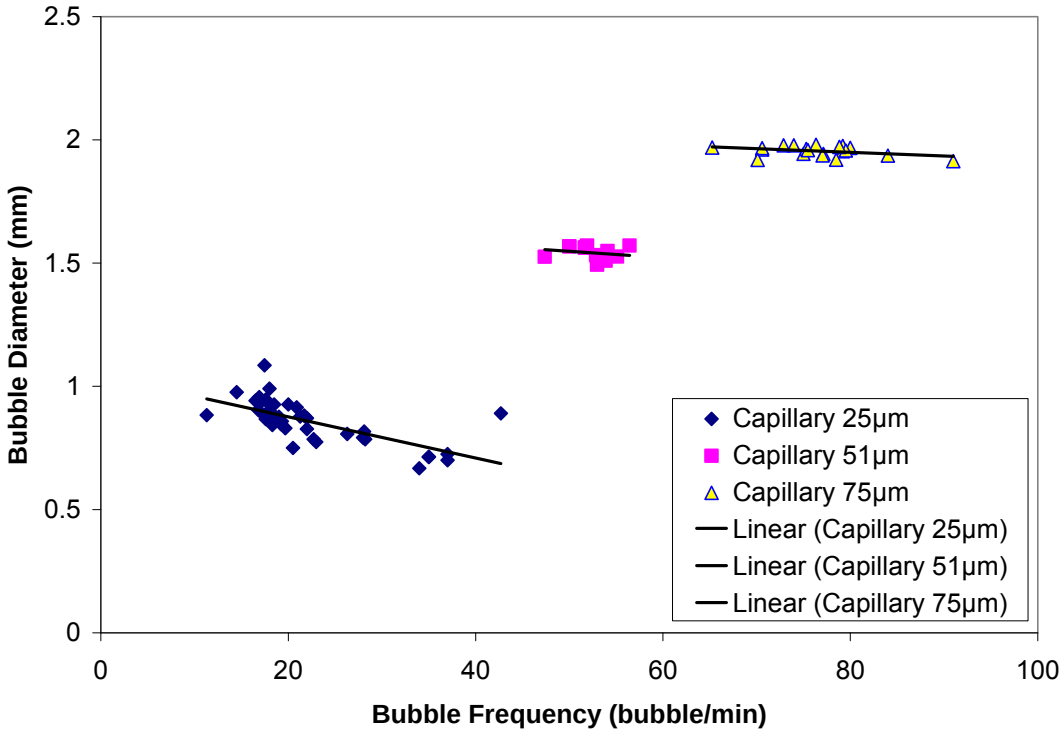

Figure 4.2: The variation of single bubble size vs. bubble frequency for the three applied capillaries.

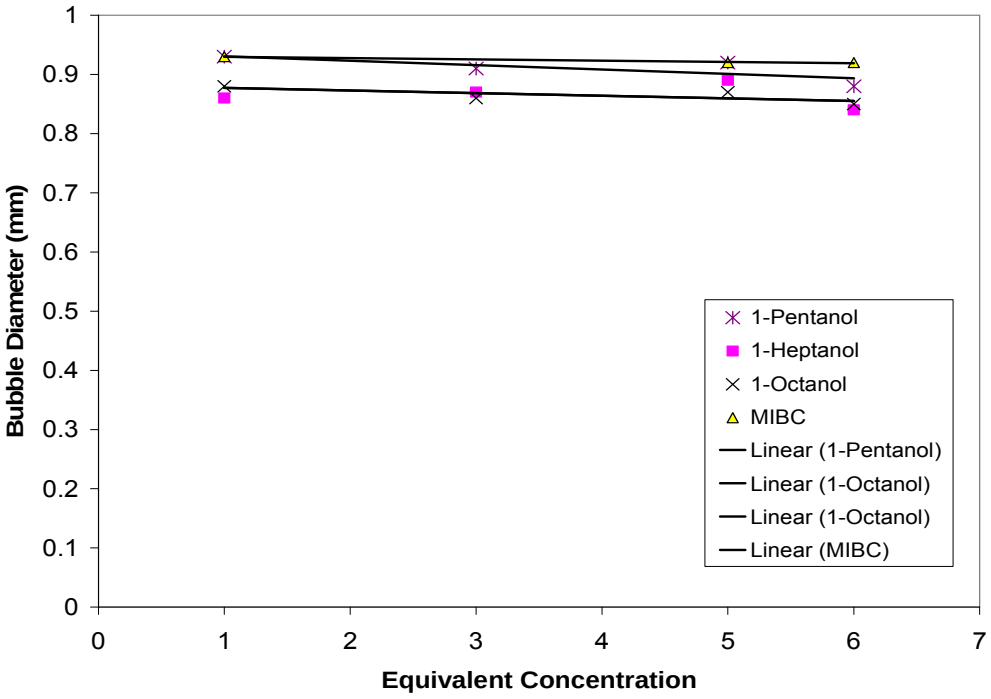

Figure 4.3: Bubble size as a function of equivalent concentration for 25μm capillary.

4.1.2. Terminal velocity

To measure terminal velocity first it is necessary to construct the velocity profile to be sure that the bubble reaches the constant terminal velocity stage (according to Figure 1.1). Figure 4.4 shows a velocity profile of a single bubble (1.45mm) rising in F150 solution, which exhibits the characteristic profile and shows that the bubble does reach terminal velocity in this case. In the Figure the main clue that terminal velocity is reached is the gradual increase in the "constant" velocity due to gradual increase in bubble size during rise. As a result if the velocity profile exhibits this characteristic the velocity could be considered as terminal velocity. If the profile is still showing a decreasing trend the rise velocity at that a given point is sometimes called "apparent terminal velocity" in order to compare with literature data.

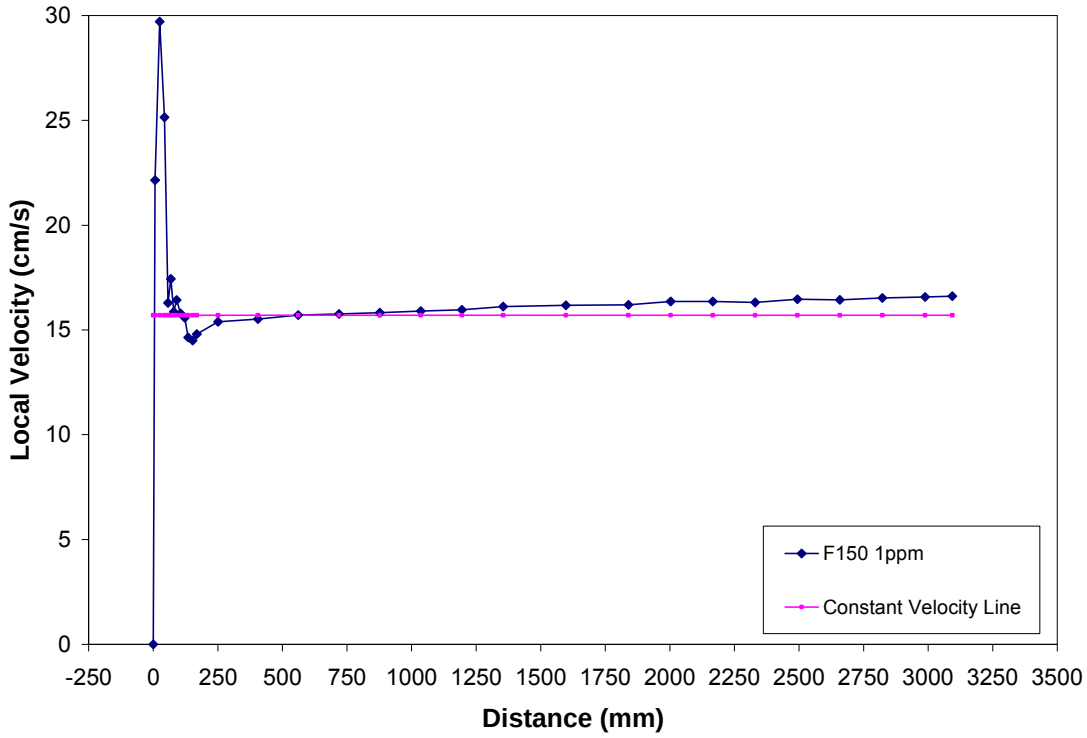

Figure 4.4: An example of velocity profile where bubble reaches terminal velocity in F150 1ppm for ca. 1.45mm bubble.

In each experiment the profiles of at least three bubbles were recorded. An estimate of measurement error is given in Figure 4.5. The term H(mm) in the table in Figure 4.5 refers to the mid height over the last 1.6 ms. The size of bubble corresponding to that height was calculated from the measured value at zero height by knowing the hydrostatic pressure.

If there was no obvious difference among measured rise velocities, the average velocity along the profile was taken. If the data did not check, the experiment was repeated.

Terminal Velocity Calculation				
	Ave(cm/s)	STD	CV(%)	H(mm)
Bubble1	25.91	0.48	1.84	2933.11
Bubble2	25.86	0.29	1.13	2949.78
Bubble3	25.85	0.24	0.92	2933.11
Average	25.88	0.03	0.13	2938.67

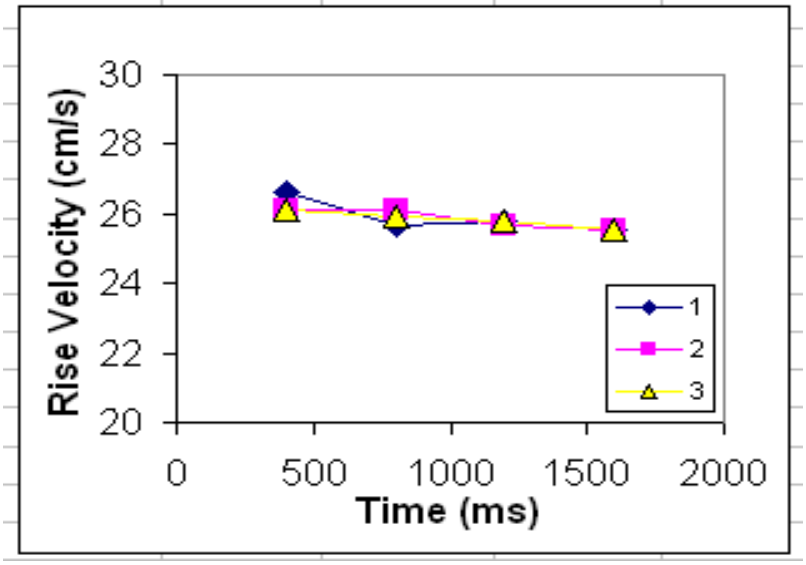

Figure 4.5: An example of measuring terminal rise velocity and reliability.

4.1.3. Bubble size

To record bubble size the camera was put at “front” and “side” positions relative to the column (Figure 3.5). By combining the measured bubble size in two positions an estimate of error could be obtained by comparing the two measurements in the Z-direction.

Table 4.2 is an example of the size measurement calculations. Results of six images were taken to give the size of bubble with acceptable precision. The bubble size was measured essentially at the capillary tip; to give bubble size at the top of the column the ideal gas law was applied, knowing the pressure (water depth). As there are slight differences between bubble sizes for a given orifice as frother type is changed reference is made to, for example, ca. 1.5mm diameter. Where the range is typically less than ±0.05mm.

Table 4.2: An example of measuring bubble size and calculating measurement error.

Direct Measurement of Bubble Size				
Front View-Pixels				
#	X	Z	Scale	Code
1	23	22	97	1
2	23	22	97	1
3	23	22	98	1
4	22	21	98	1
Average	22.75	21.75		4
SD	0.50	0.50		
Error(%)	2.20	2.30		
Side View-Pixels				
#	Y	Z	Scale	Code
1	31	31	131	1
2	31	30	130	1
3	32	31	131	1
4				0
Average	31.33	30.67		3
SD	0.58	0.58		
Error(%)	1.84	1.88		
Bubble Size After Scaling (mm)				
#	X	Z	Y	Z
1	0.71	0.68	0.71	0.71
2	0.71	0.68	0.72	0.69
3	0.70	0.67	0.73	0.71
4	0.67	0.64	0.00	0.00
Average	0.70	0.67	0.72	0.70
SD	0.02	0.02	0.01	0.01

4.2. Velocity profile analysis

4.2.1. Examples

In this section some velocity profiles obtained in this work are compared with the typical profiles described in Figure 1.1. Figure 4.6 shows the velocity profile for four concentrations of F150. The profiles exhibit the typical features and trends. Figure 4.7 expands the first 500mm of the profiles magnify the first and second stages.

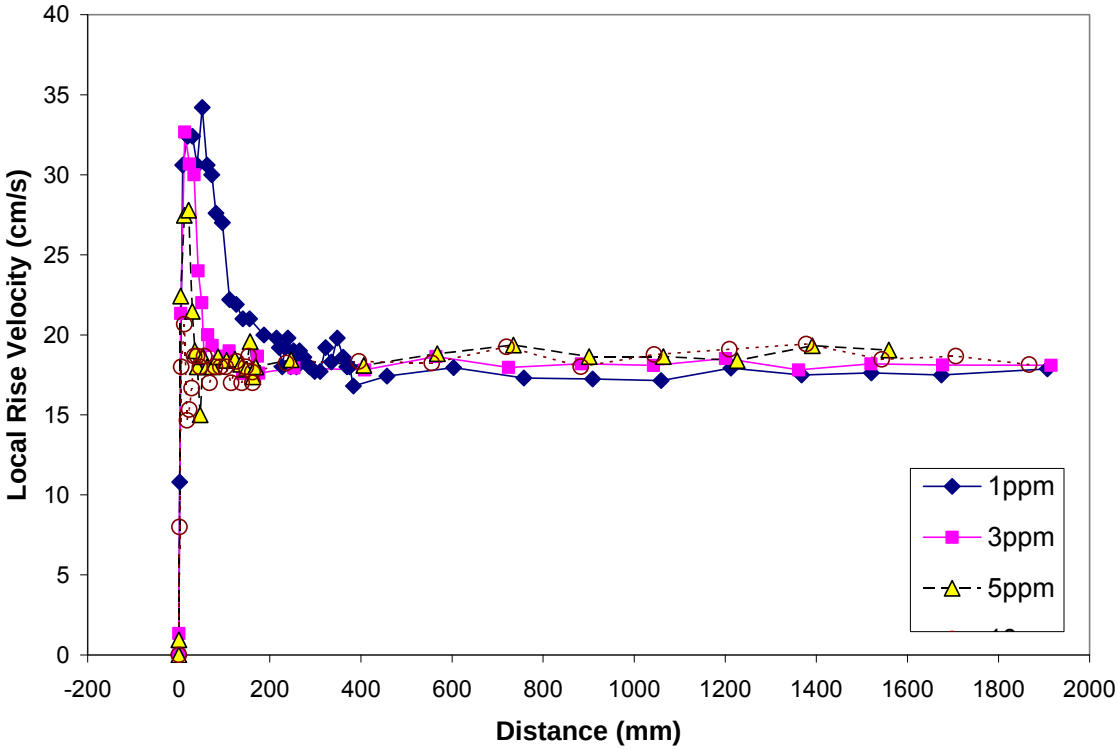

Figure 4.6: Velocity profiles in F150 (ca 1.5mm).

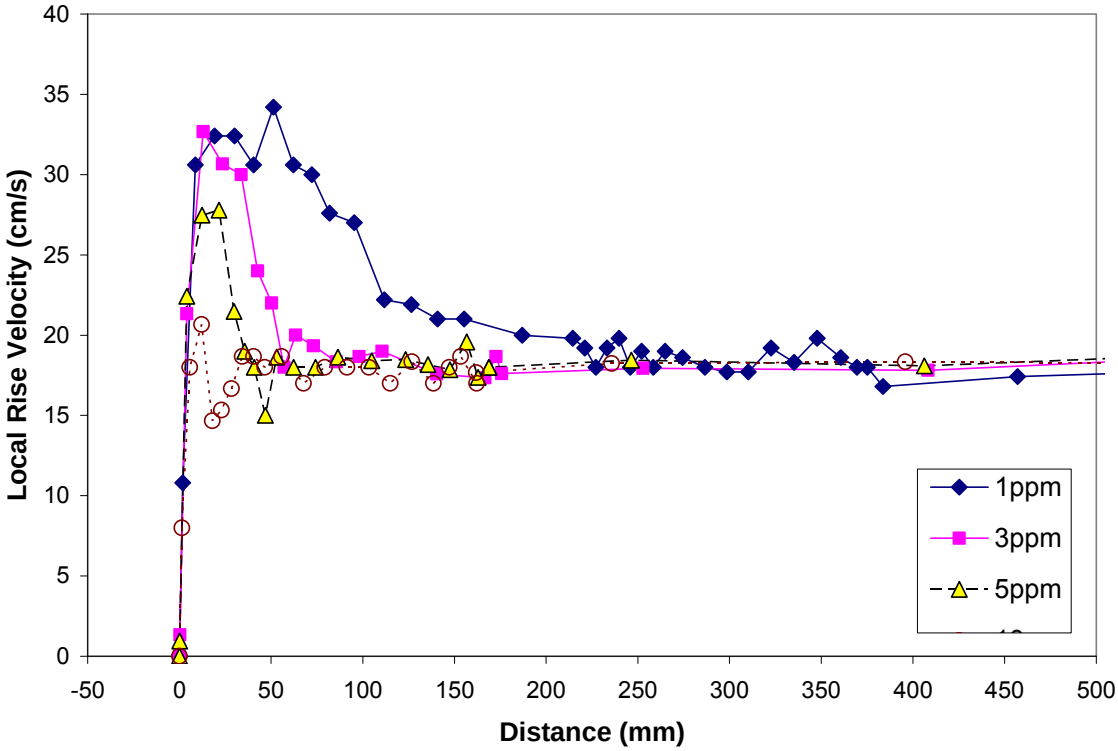

Figure 4.7. Velocity profiles in F150 (ca 1.5mm) over the first 3 seconds for conditions in Figure 4.6.

According to Figure 4.7, as concentration is increased the bubble reaches terminal velocity faster, which is in agreement with observations of Sam et al. (1996) and Zhang and Finch (2000).

4.2.2. Maximum velocity

It has been reported that the higher the concentration of reagent the lower the maximum velocity attained on the profile, suggestive of faster mass transfer of reagent molecules to the bubble surface (Sam et al., 1996). Figure 4.8 presents the influence of concentration on maximum velocity in the presence of MIBC, NaCl and F150. According to Figure 4.8 the higher concentration of MIBC and F150 strongly reduced the maximum velocity. However, addition of NaCl concentration did not change the maximum velocity as significantly.

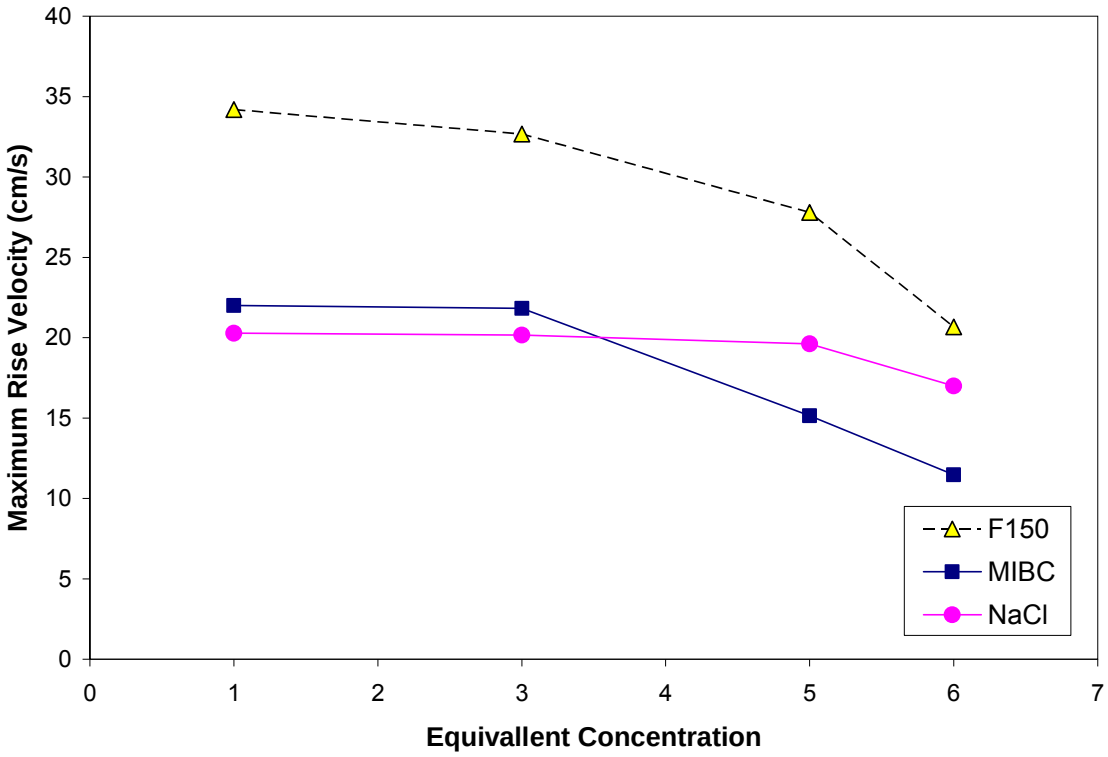

Figure 4.8: The influence of reagent concentration on maximum velocity in the presence of MIBC, NaCl and F150.

4.3. Reagent type: pentanol vs. F150

Azgomi et al. (2007) reported that for the same gas holdup and gas rate, bubble size nevertheless depended on frother type, the extreme case being between

1-pentanol and F150 (Figure 2.12). This observation gave rise to the hypothesis that frother type can affect the bubble rise velocity of same size bubbles. While hinted at in the prior works of Zhou et al. (1992), Sam (1995) and Zhang (2000) the differences were small and could have been ascribed to experimental error.

To test the hypothesis Acuna and Finch (2008) compared 1-pentanol and F150 by measuring the rise velocity of individual bubbles in a multi-bubble system (Figure 2.13). The results established that F150 significantly reduced the rise velocity compared to 1-pentanol. Indeed 1-pentanol acted very similar to pure water.

Azgomi et al. speculated that bubble charging may be a factor, a sedimentation potential effect controlling rise velocity. Elmahdy et al. (2008) measured the zeta potential of air bubbles in the presence of F150 and 1-pentanol showing only minor differences and concluded bubble changing was not a factor. This leaves unknown bubble interactions to explain the results of Azgomi et al. and Acuna and Finch or a difference in single bubble velocity.

In this work the rise velocity of single bubbles was measured in the presence of F150 and 1-pentanol for a bubble size range of 0.8 to 2mm.

4.3.1. Velocity profile

Figure 4.9 presents the velocity profiles (velocity vs. distance) for ca. 1.45mm bubbles in F150, pentanol and tap water, including some full repeats that confirm the reliability. Figure 4.9 clearly reveals that the reagent type affected the velocity in the concentration range tested (which is of interest in flotation). In the presence of F150 the bubble rapidly reached terminal velocity while in 1-pentanol, the bubble velocity was much higher, similar to water and apparently still decreasing to approach terminal.

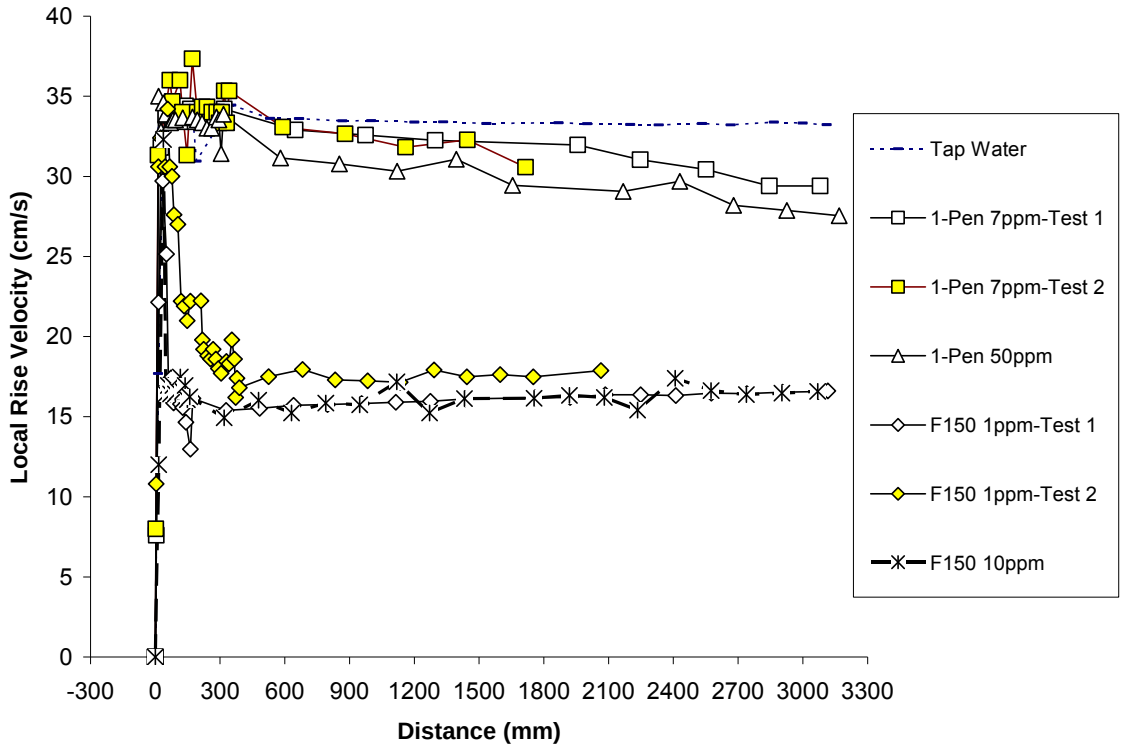

Figure 4.9: Velocity profiles in F150, 1-pentanol and tap water (ca 1.45mm).

4.3.2. Comparison of terminal/apparent terminal velocities

In the case of F150, Figure 4.9 shows terminal velocity is reached – the characteristic increasing "constant" velocity stage is evident. In the case of 1-pentanol, however, Figure 4.9 shows the velocity is only the apparent terminal.

Figure 4.10 presents terminal / apparent terminal rise velocity vs. bubble diameter in the presence of F150, 1-pentanol and tap water, compared with results of Acuna and Finch (2008) and the results for clean and contaminated water given by Clift et al. (1978). As Acuna and Finch (2008) measured the rise velocity at 500mm, the apparent terminal velocities at this distance were determined to make comparison with their work. The presence of F150 shows a significantly lower terminal velocity compared to either tap water or 1-pentanol. In both swarms and single bubble systems, the presence of 1-pentanol hardly influences the rise velocity relative to clean water, while the results of F150 approach contaminated water.

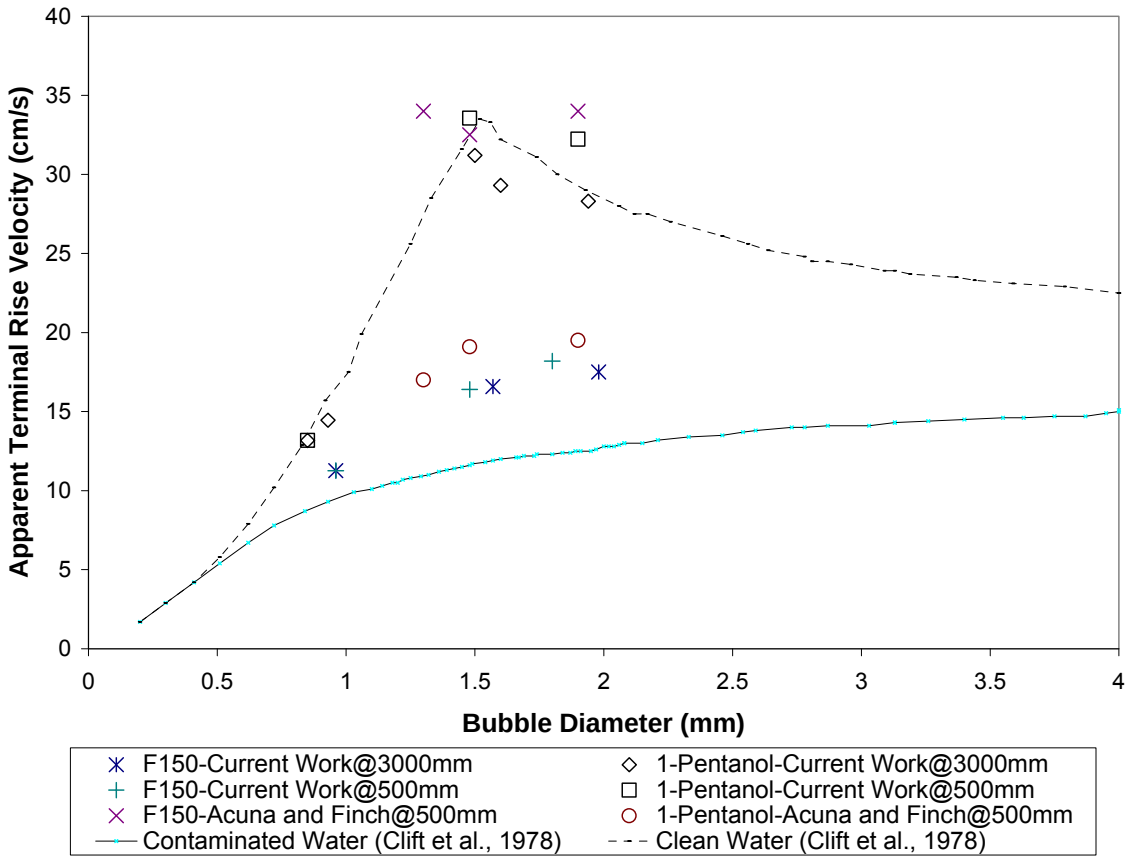

Figure 4.10: The terminal/apparent terminal rise velocity vs. bubble diameter at 500 and 3000mm distance in the presence of F150 and 1-Pentanol compared to swarms results (Acuna and Finch, 2008) and results for single bubble in clean and contaminated water given by Clift et al. (1978).

Regarding Figure 4.9 and Figure 4.10 there is a clear difference between rise velocity in F150 and 1-pentanol. As a consequence, the observation of Azgomi et al. has its origin in the velocity of single bubbles.

4.4. Aliphatic alcohols

As a start to understand the surfactant structure / bubble velocity relationship a homologous series of five aliphatic n-alcohols (C_4-C_8) was used to investigate the influence of chain length.

Figure 4.11 and Figure 4.12 show the terminal/apparent terminal rise velocity vs. bubble diameter at 3000mm for equivalent concentrations 1 and 5, of 1-pentanol, 1-hexanol and 1-heptanol (Figure 4.11); and 1-butanol, 1-hexanol and 1-octanol (Figure 4.12). The Figures indicate that the lower concentration of 1-hexanol (equivalent concentration 1=5.25ppm) acted like 1-butanol and 1-pentanol, and the higher concentration (equivalent concentration 2 =37.5ppm) acted like 1-heptanol and 1-octanol. For 1-butanol, 1-pentanol, 1-heptanol and 1-octanol, the change in concentration did not influence rise velocity practically.

To check if the terminal velocity was achieved, the velocity profiles were examined. Figure 4.13 compares the profiles in 5.25ppm and 37.5ppm 1-hexanol. The 5.25ppm velocity profile has probably not reached terminal velocity because there is a discernable decreasing trend, while the profile at 37.5 ppm has reached terminal velocity.

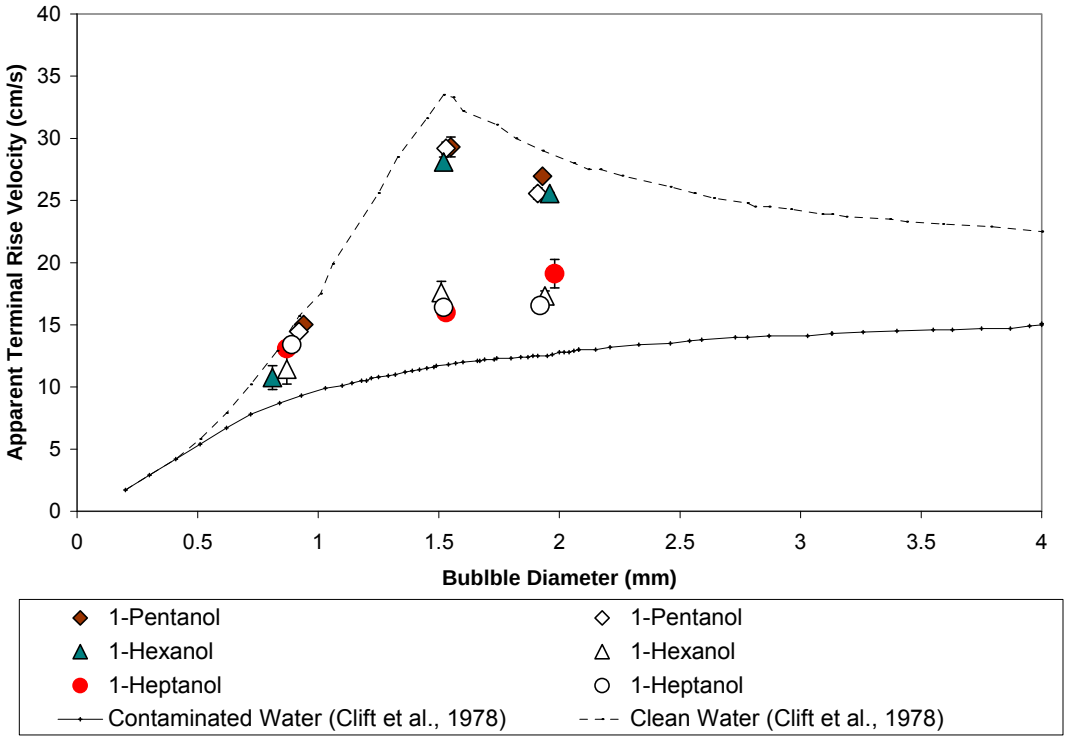

Figure 4.11: The terminal/apparent terminal rise velocity vs. bubble diameter at 3000mm in the presence of low (1) and high (5) concentrations of 1-pentanol, 1-hexanol and 1-heptanol.

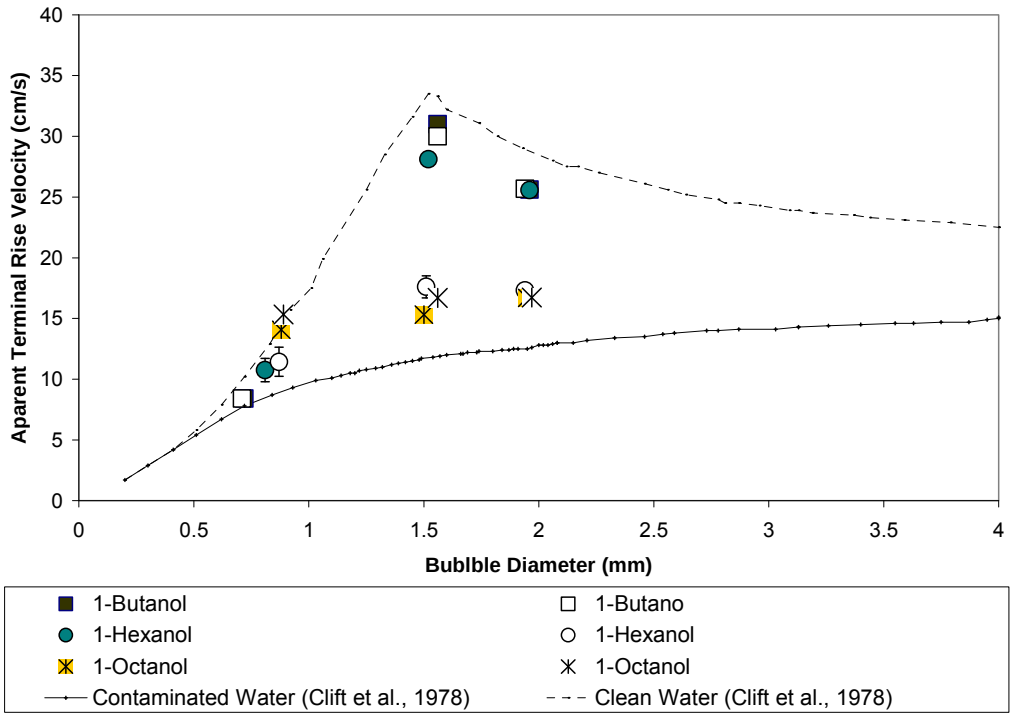

Figure 4.12: The terminal/apparent terminal rise velocity vs. bubble diameter at 3000mm in the presence of low (1) and high (5) concentrations of 1-butanol, 1-hexanol and 1-octanol.

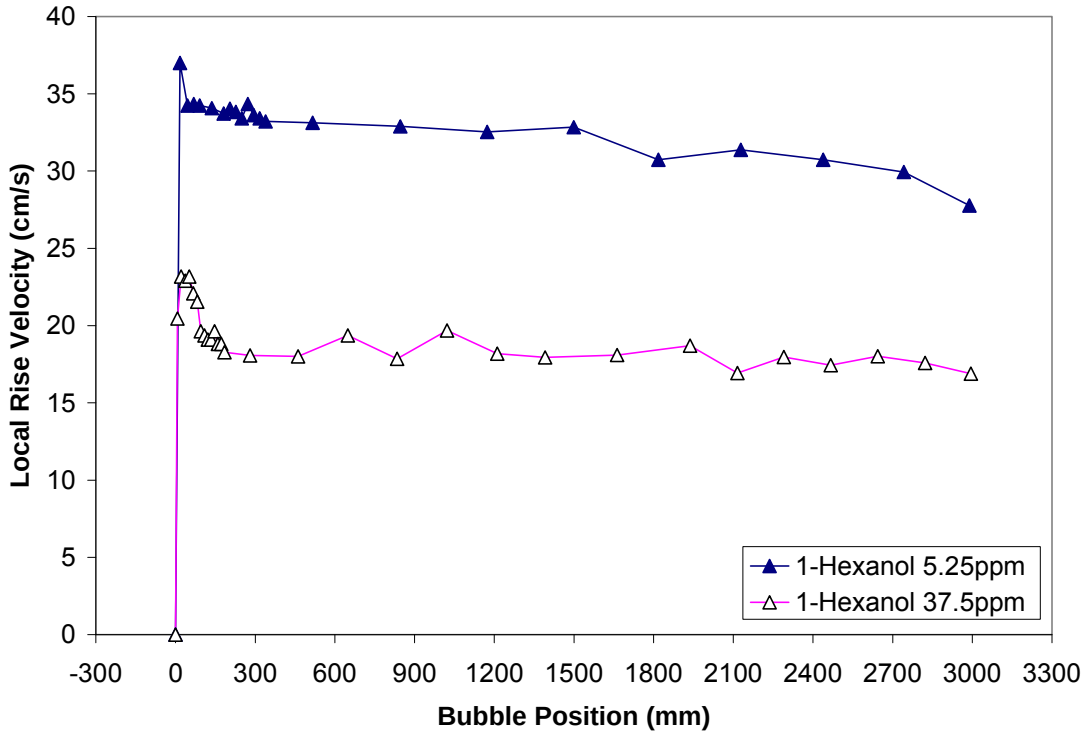

Figure 4.13: Velocity profiles in 1-hexanol (ca 1.5mm).

4.4.1. Concentration effect

Figure 4.11 and 4.12 indicate that 1-pentanol and 1-butanol have not reached terminal velocity even at the highest concentration tested (5) while, the 1-heptanol and 1-octanol have. 1-Hexanol is in between: at high concentration (5) it acts like 1-heptanol and at low concentration (1) it acts like 1-pentanol. The implication is that if we go to higher concentrations of 1-pentanol than tested thus far it too will start to look like 1-heptanol; conversely, 1-heptanol at lower concentrations than tested will take on the character of 1-pentanol. The jump in apparent terminal velocity from 1-pentanol to 1-heptanol is then a ”concentration effect”.

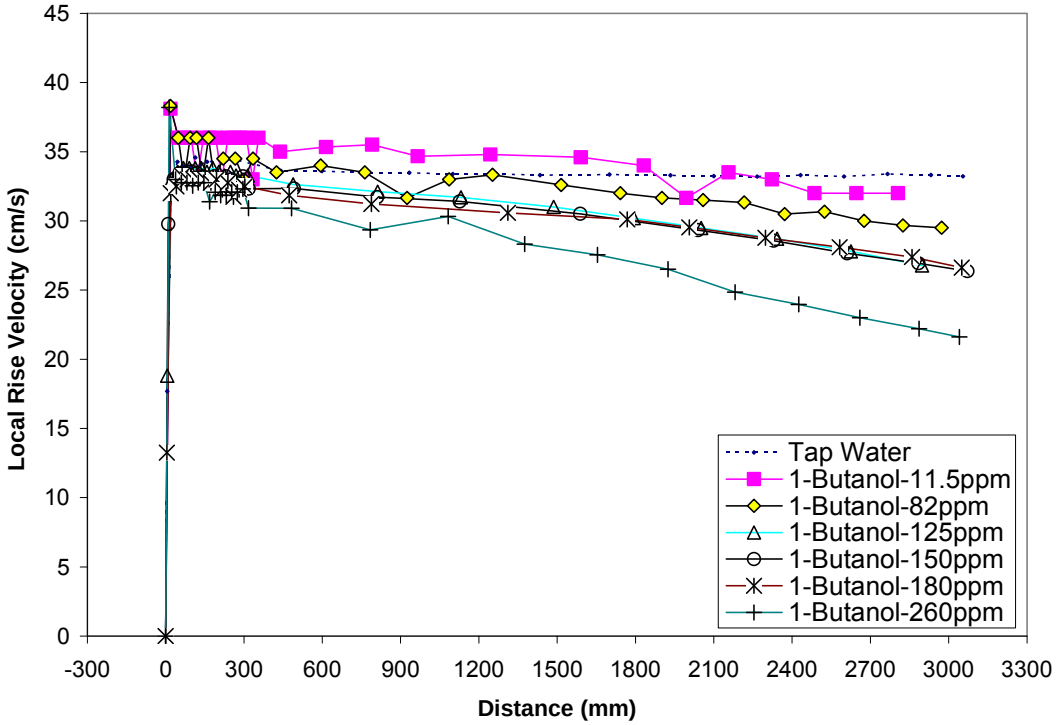

Figure 4.14: Velocity profiles in 1-butanol (ca 1.45mm).

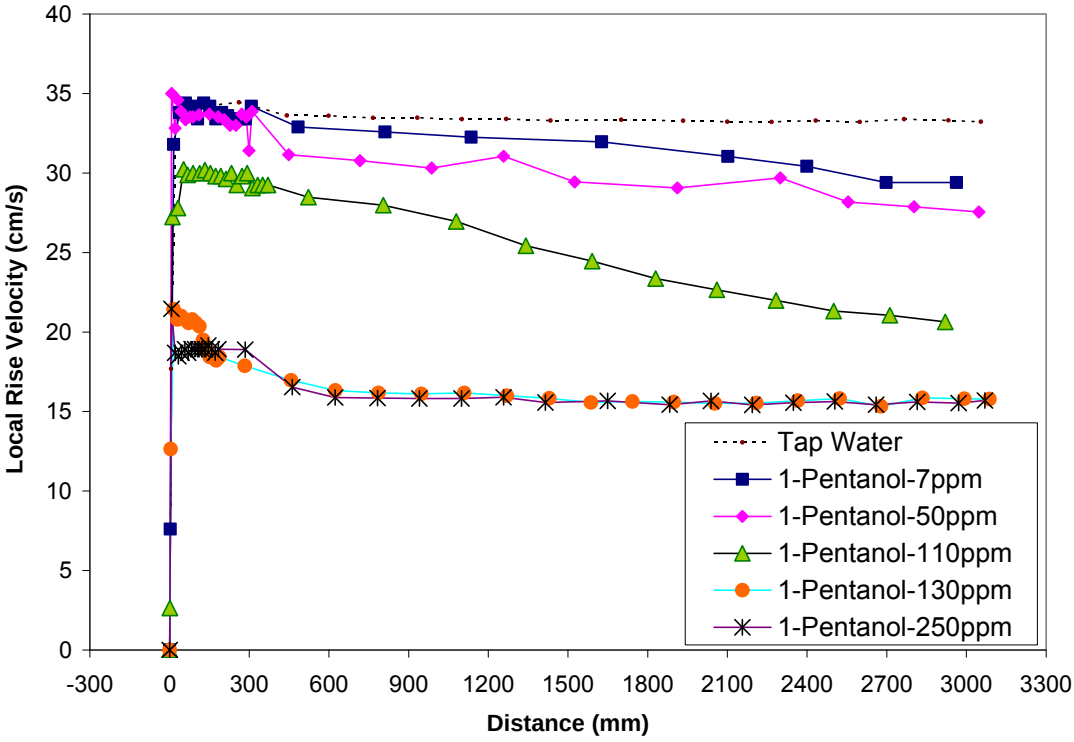

Figure 4.15: Velocity profiles in 1-pentanol (ca 1.45mm).

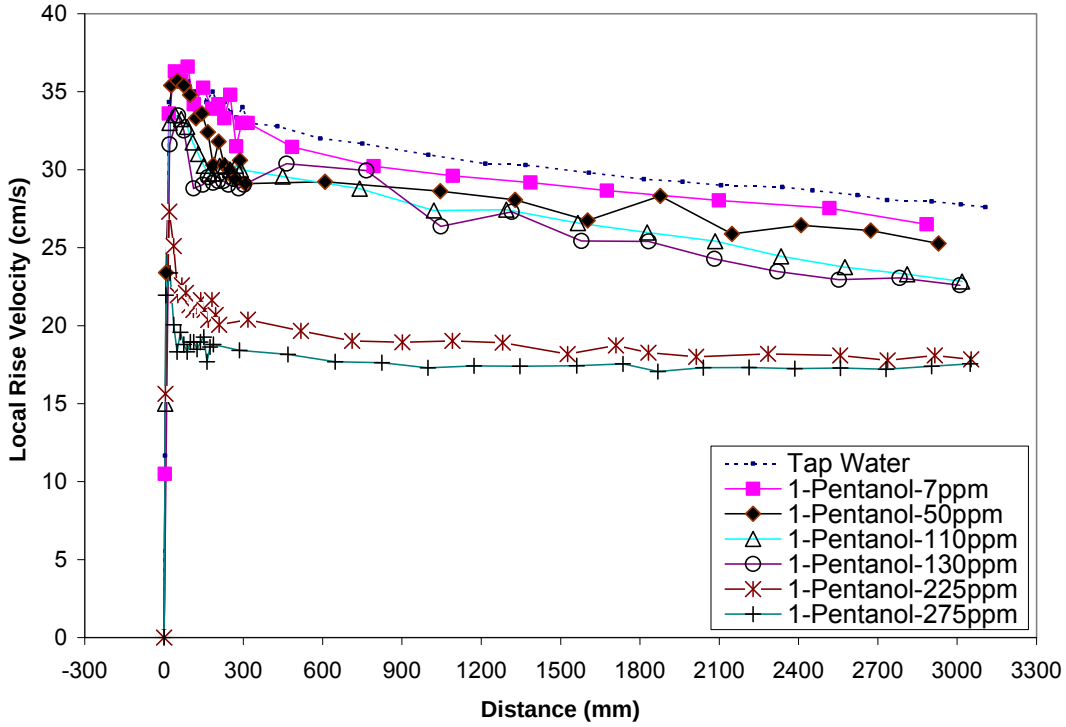

Figure 4.16: Velocity profiles in 1-pentanol (ca 1.85mm).

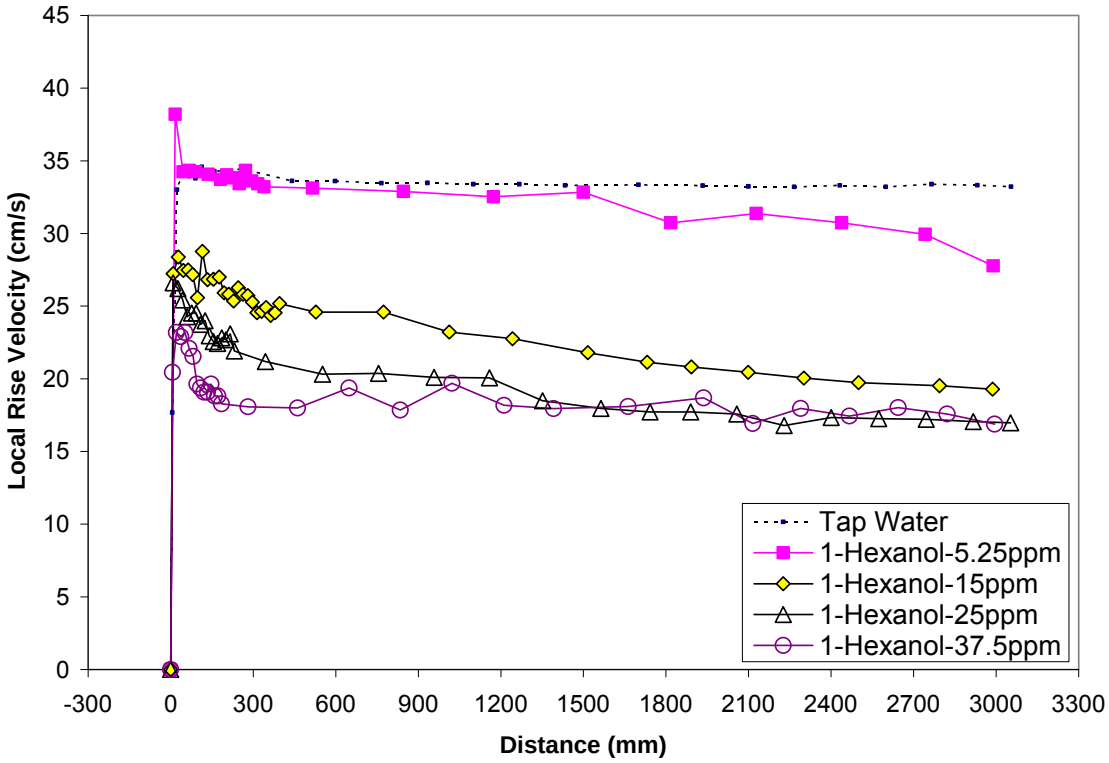

Figure 4.17: Velocity profiles in 1-hexanol (ca 1.45mm).

This concentration effect was explored up. Figure 4.14 show the case of 1-butanol; Figure 4.15 and Figure 4.16 show the velocity profile in 1-pentanol for 1.45mm and 1.85mm bubble sizes, respectively; and Figure 4.17 and Figure 4.18 indicates the velocity profile in 1-hexanol for 1.45mm and 1.85mm bubbles, respectively. According to the velocity profiles for these three n-alcohols, as the concentration increased, the rise velocity reduced to a value close to the contaminated water result, except in the case of 1-butanol even at 260ppm.

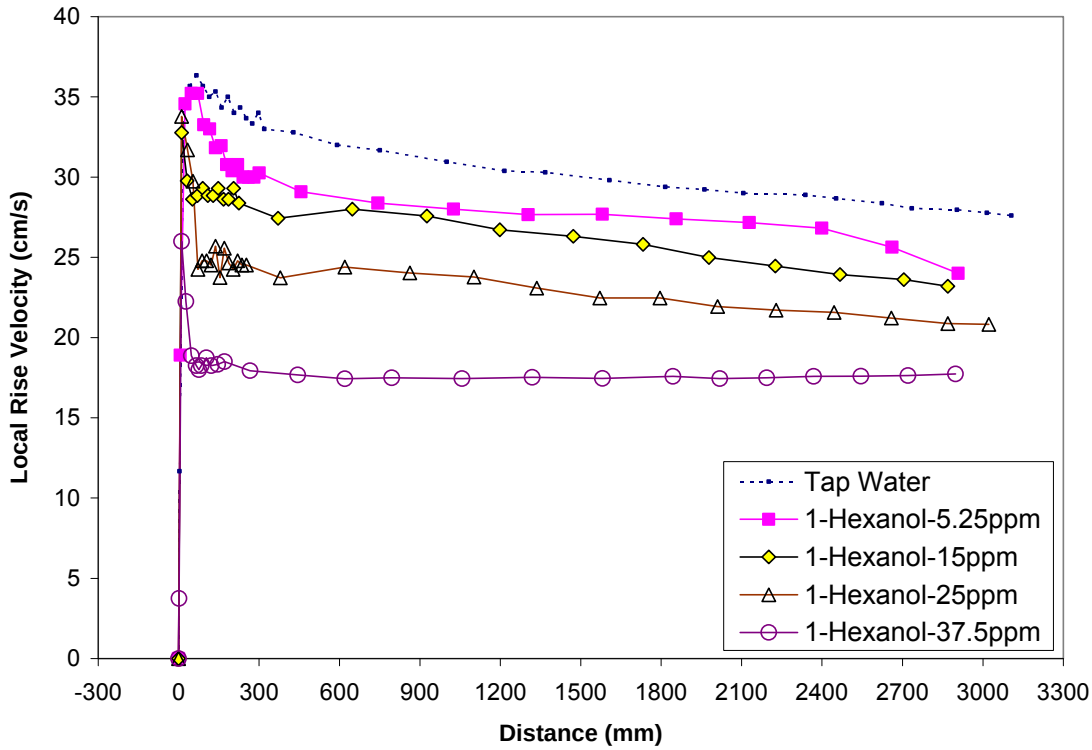

Figure 4.18: Velocity profiles in hexanol (ca 1.85mm).

Krzan and co-workers report velocity profiles for 1-butanol and 1-hexanol (Krzan and Malysa, 2002) and 1-pentanol and 1-octanol (Krzan et al., 2007). They obtained the profiles over the more limited distance of 350mm.

Taking results at 350mm as “apparent” terminal velocity in this case, Figure 4.19, Figure 4.20 and Figure 4.21 compare the results with those of Krzan and co-workers. The figures indicate that the results of the current work at 350mm are close to those of Krzan and co-workers.

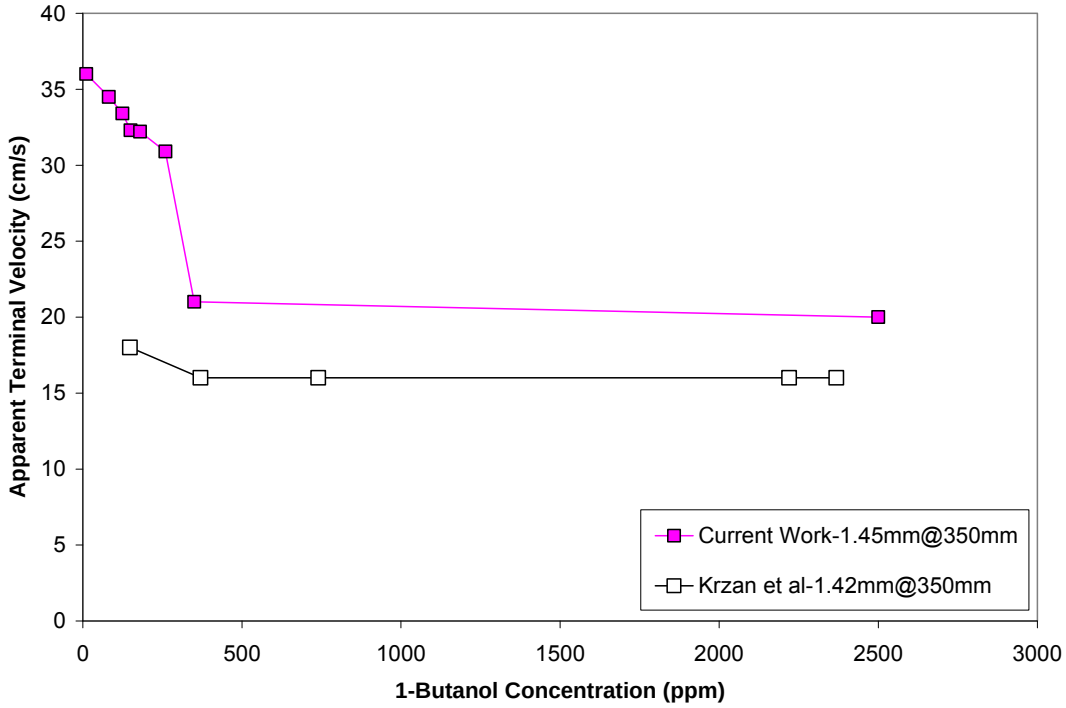

Figure 4.19: Apparent terminal velocity (at 350mm) vs. concentration of single bubbles in 1-butanol.

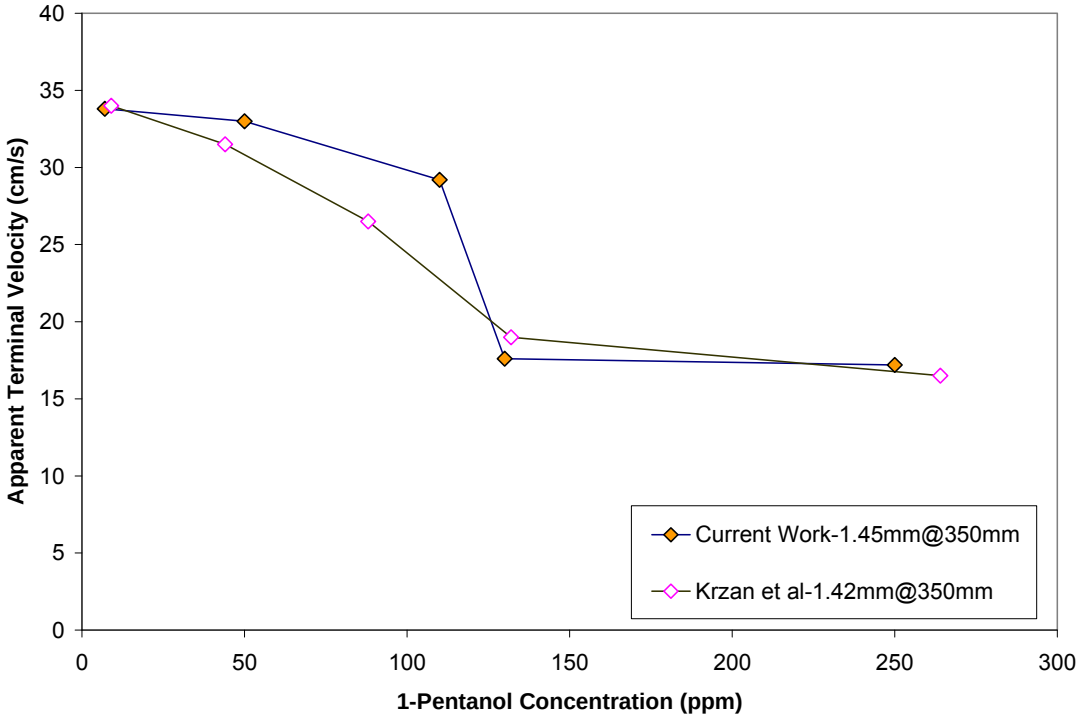

Figure 4.20: Apparent terminal velocity (at 350mm) vs. concentration of single bubbles in 1-pentanol.

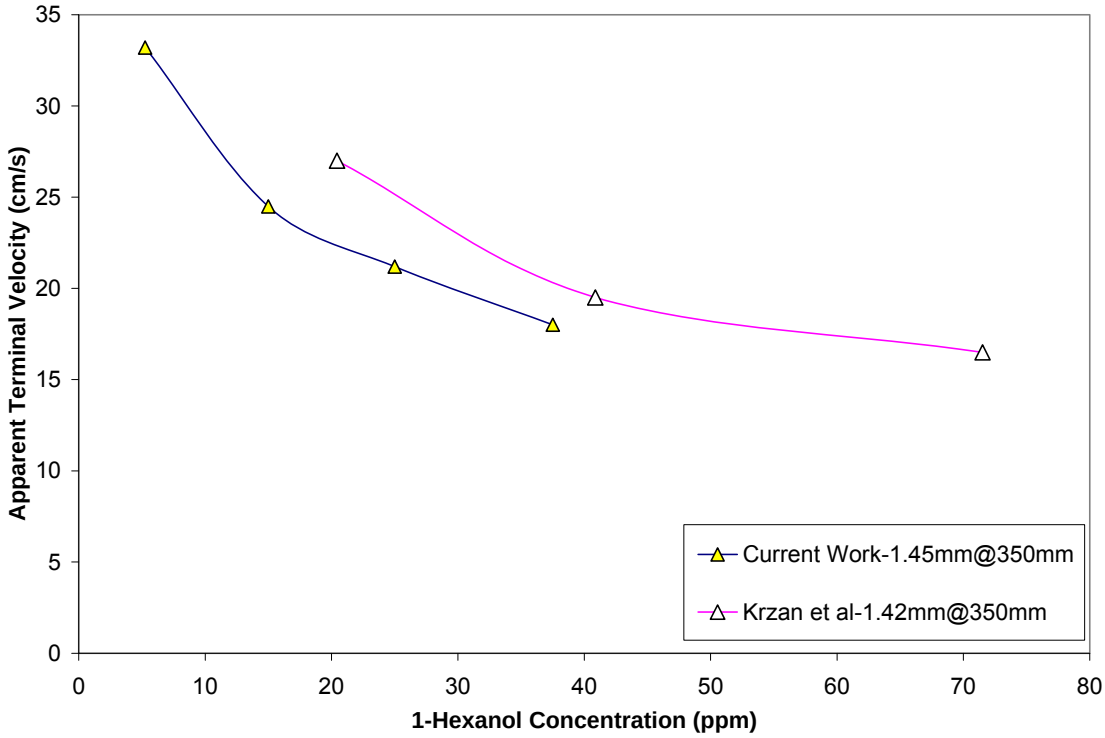

Figure 4.21: Apparent terminal velocity (at 350mm) vs. concentration of single bubbles in 1-hexanol.

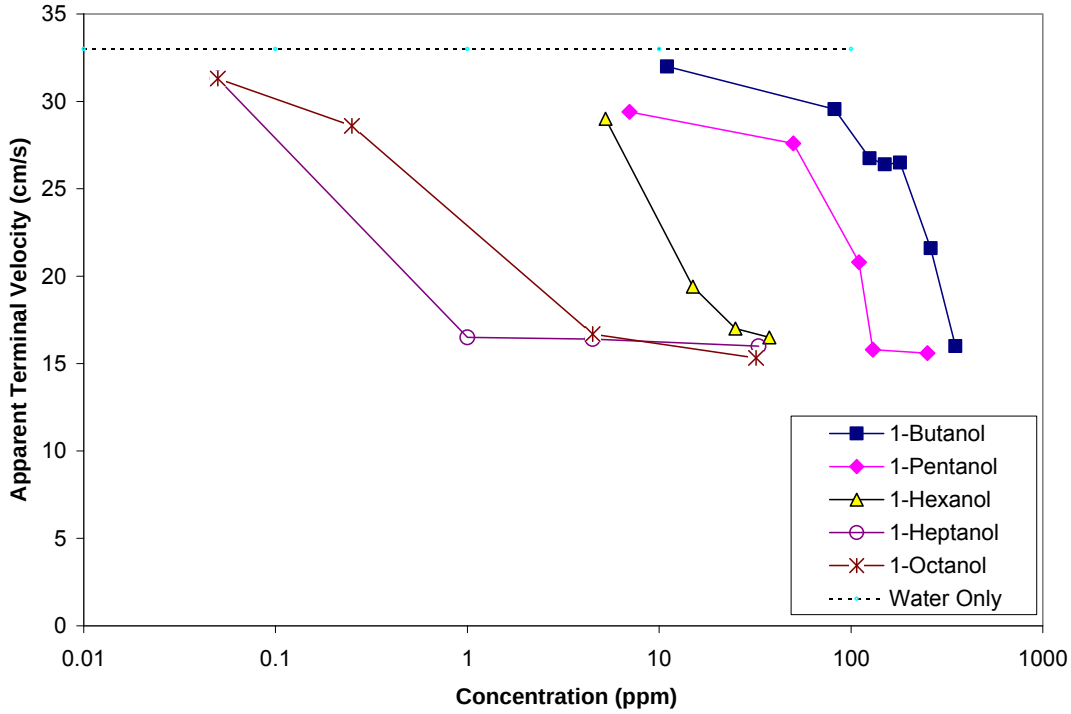

Figure 4.22: Apparent terminal velocity (at 3000mm) vs. concentration (ppm) of single bubbles for series of n-alcohols for ca. 1.45mm bubbles.

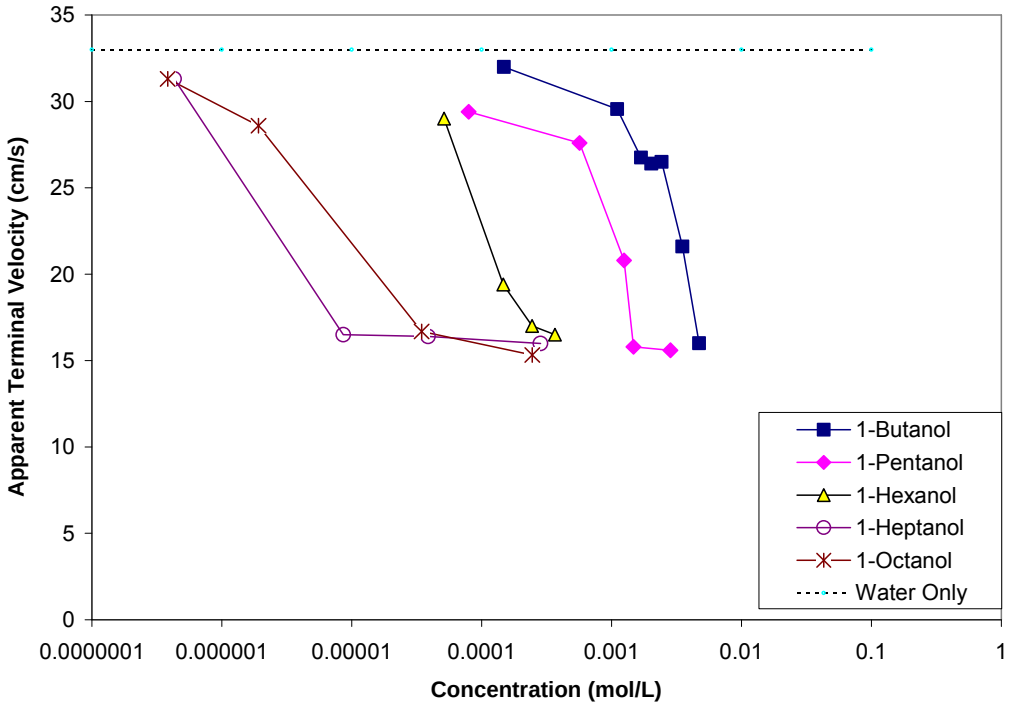

Figure 4.23: Apparent terminal velocity (at 3000mm) vs. concentration (mol/L) of single bubbles for series of n-alcohols for ca. 1.45mm bubbles.

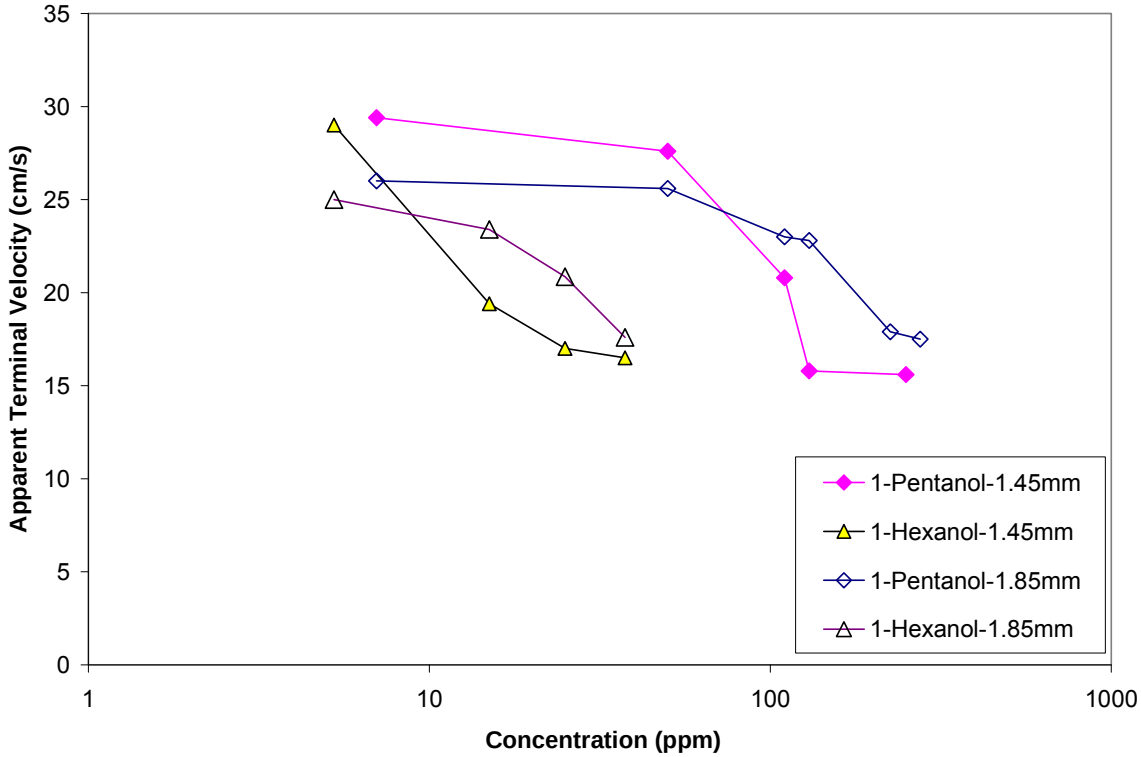

Figure 4.24: Apparent terminal velocity (at 3000mm) vs. concentration (ppm) for ca. 1.45 and 1.85mm single bubbles in 1-pentanol and 1-hexanol.

Figure 4.22 and Figure 4.23 show the apparent terminal velocity at 3000mm vs. concentration based on ppm and mol/L, respectively, for the n-alcohols used in this study. To explore the influence of bubble size on concentration effect, Figure 4.24 presents the apparent terminal velocity at 3000mm vs. concentration for ca. 1.45 and 1.85mm single bubbles in 1-pentanol and 1-hexanol.

There are several observations compared with Figure 4.20- 4.25. First, there is a critical concentration (C_C) to reach terminal velocity that decreases as the chain length increases (Figure 4.23). Second, traveling distance of bubble influences the estimate of terminal velocity. For instance, the apparent terminal velocity at 350mm (Figure 4.20-4.22) is higher than at 3000mm (Figure 4.23), consequently the results of Krzan and co-workers do not represent true terminal velocity, especially for low concentrations. Third, comparison of apparent terminal velocity for 1.45 and 1.85mm bubbles (Figure 4.25) indicates that the larger bubble size requires a higher critical concentration to reach terminal velocity; for instance, in 1-pentanol the critical concentration for 1.45mm bubble is about 130ppm while for 1.85mm it is about 250ppm. Fourth, at concentrations above the critical concentration the terminal rise velocity of all examined alcohols are close i.e., frother type did not influence terminal velocity.

4.4.2. The influence of molecular structure: C-6 alcohols

To expand the observations on 1-hexanol, two isomers, 2-hexanol and MIBC, were included. The difference between the isomers is location of the OH and CH_3 groups. The OH group is bonded with an end CH_2 group in 1-hexanol and with the second to last CH group in 2-hexanol. In MIBC the OH group is also bonded with the CH group but it has three CH_3 groups.

Figure 4.25 presents the terminal/apparent terminal rise velocity vs. bubble diameter in the presence of two concentrations (equivalents 1 and 5) of 1-hexanol, 2-hexanol and MIBC; as with the 1-hexanol a difference between low

and high concentration is observed for 2-hexanol, although the difference is less. For MIBC there is no obvious difference between equivalent concentration 1 and 5.

Figure 4.26 shows the velocity profiles for 5.25 and 37.5ppm of 2-hexanol. Like the 1-hexanol profiles, the bubble did not reach terminal velocity at the low concentration. Figure 4.27 presents the apparent terminal velocity vs. concentration in the presence of 1-hexanol, 2-hexanol and MIBC. Here MIBC reaches terminal velocity at very low concentration compared to the other two isomers; Sam et al. (1996) also found MIBC gave terminal velocity at low dosage (1ppm).

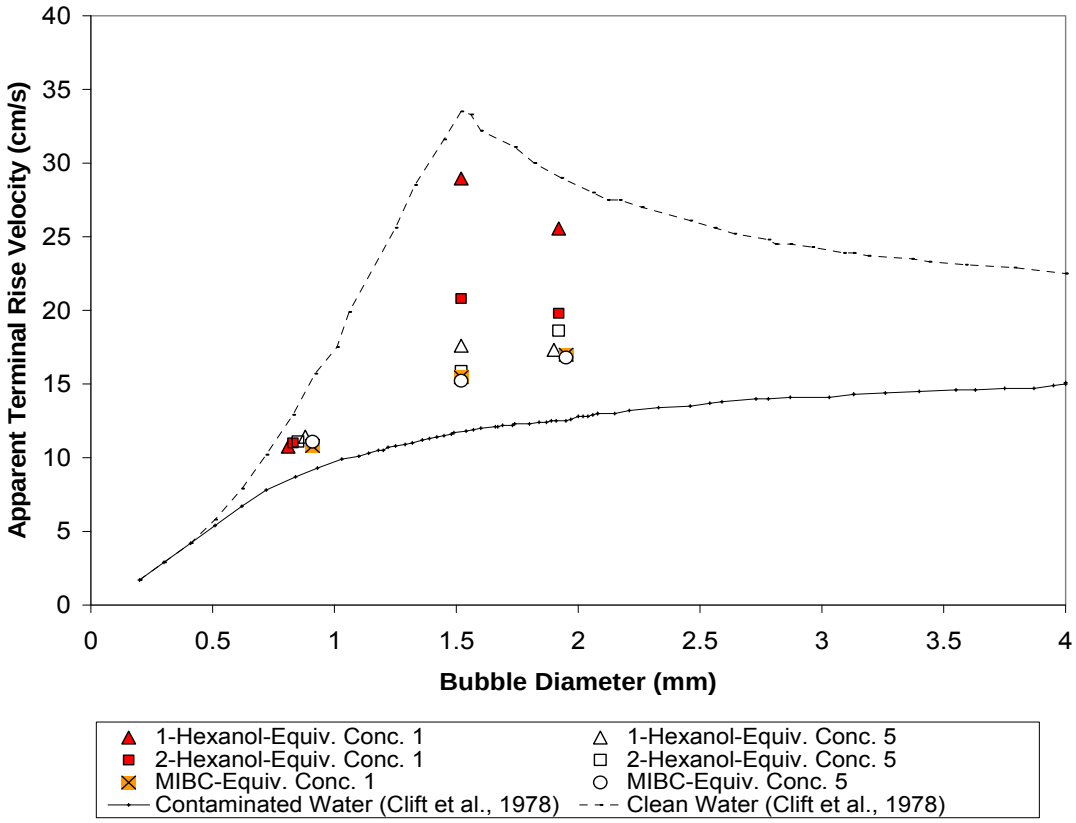

Figure 4.25: The terminal/apparent terminal rise velocity vs. bubble diameter at 3000mm in the presence of MIBC, 1-hexanol and 2-hexanol.

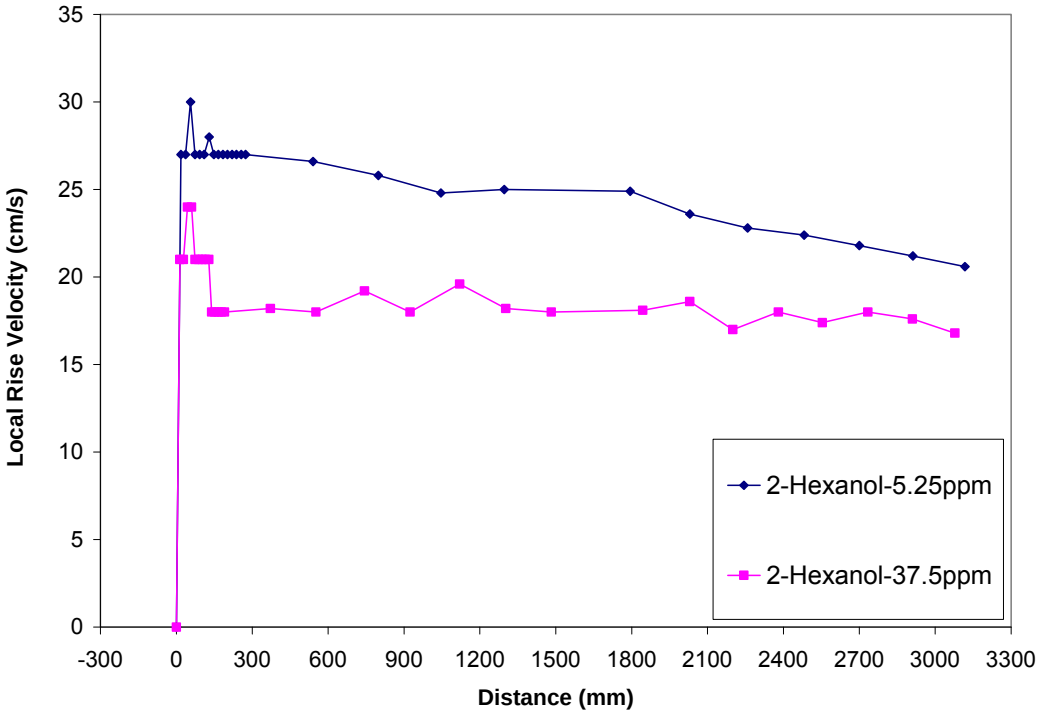

Figure 4.26: Velocity profiles in 2-hexanol (ca 1.5mm).

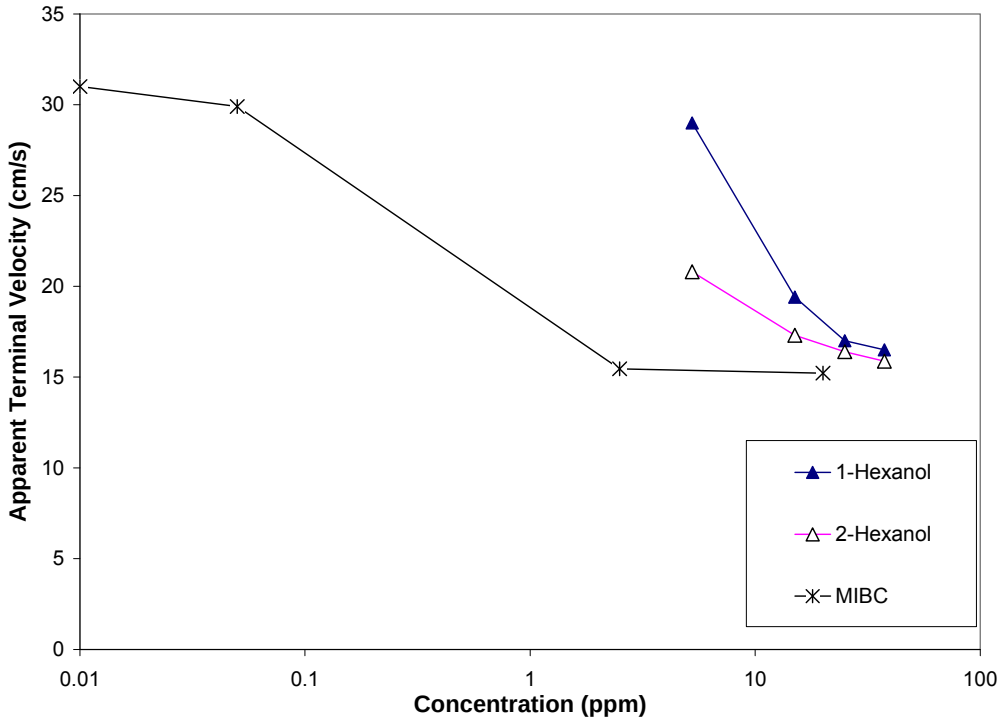

Figure 4.27: Apparent terminal velocity vs. concentration of single bubbles in 1-hexanol, 2-hexanol and MIBC.

According to Figures 4.25-4.27 the chemical structure of the alcohol influences the rise velocity of single bubbles. According to the molecular structure properties of the isomers the order of decreasing hydrophilic character is MIBC>2-hexanol>1-hexanol which corresponds to their order of terminal velocity. The same order was seen in solubility, for instance the solubility of MIBC and 1-hexanol is the maximum and minimum among them that is 17 and 6g/L, respectively.

So the solubility difference between 1-hexanol and MIBC is not enough big (compared to the solubility difference between other alcohols) to support the observed significant difference in bubble rise velocity. The hydrophilicity could be determined using “Hydrophil-Lipophil Balance (HLB)” (Rao, 2004), however the calculated HLB for MIBC and 1-hexanol are 6.1 and 6, respectively, that does not reflects significant difference too.

It seems that the structure affects the orientation of frother molecule on the bubble surface. Perhaps the orientation of MIBC molecules has some advantage compared to 1-hexanol and 2-hexanol, which permits the lower concentration control over bubble surface drag or surface viscosity.

4.4. Comparison of MIBC and NaCl

Quinn et al. (2007) compared the influence on gas holdup and bubble size of some salts with MIBC (as a typical frother). The results indicated that a salt solution with ionic strength of 0.4-0.5, acted similarly to that of 7-10ppm MIBC.

In this work the rise velocity of single bubbles in the presence of MIBC and NaCl was measured to explore this reported similarity. Figure 4.28 presents the velocity profiles in the presence of MIBC and NaCl that shows MIBC reached terminal velocity, while NaCl may be still in the deceleration region.

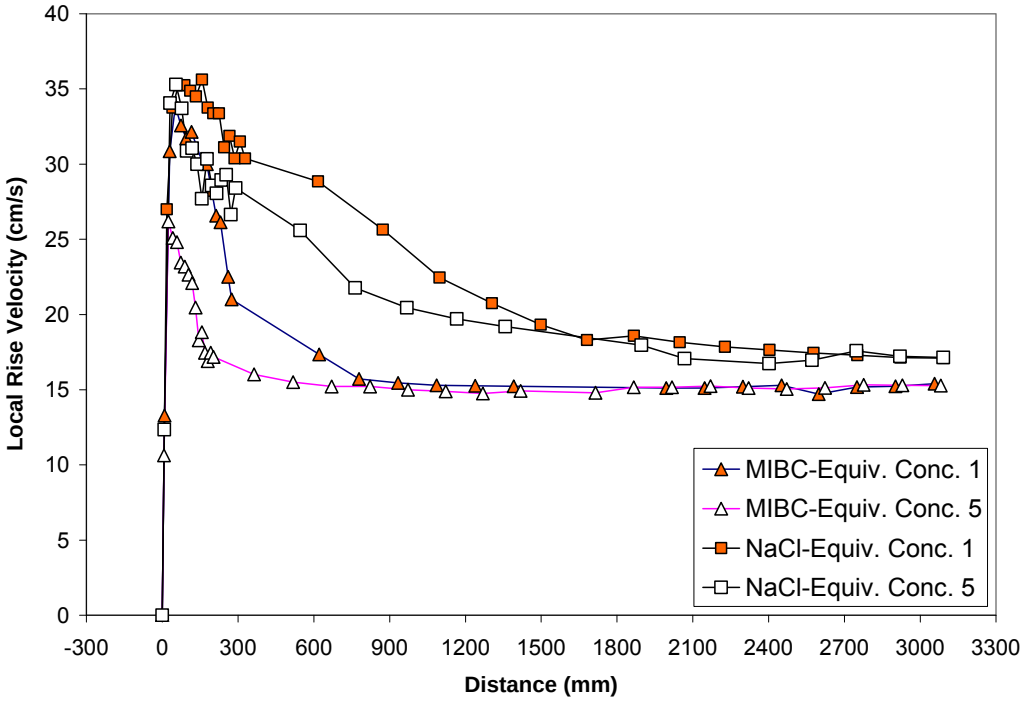

Figure 4.28: Velocity profiles in MIBC (ca. 1.5mm) and NaCl (ca 1.6mm).

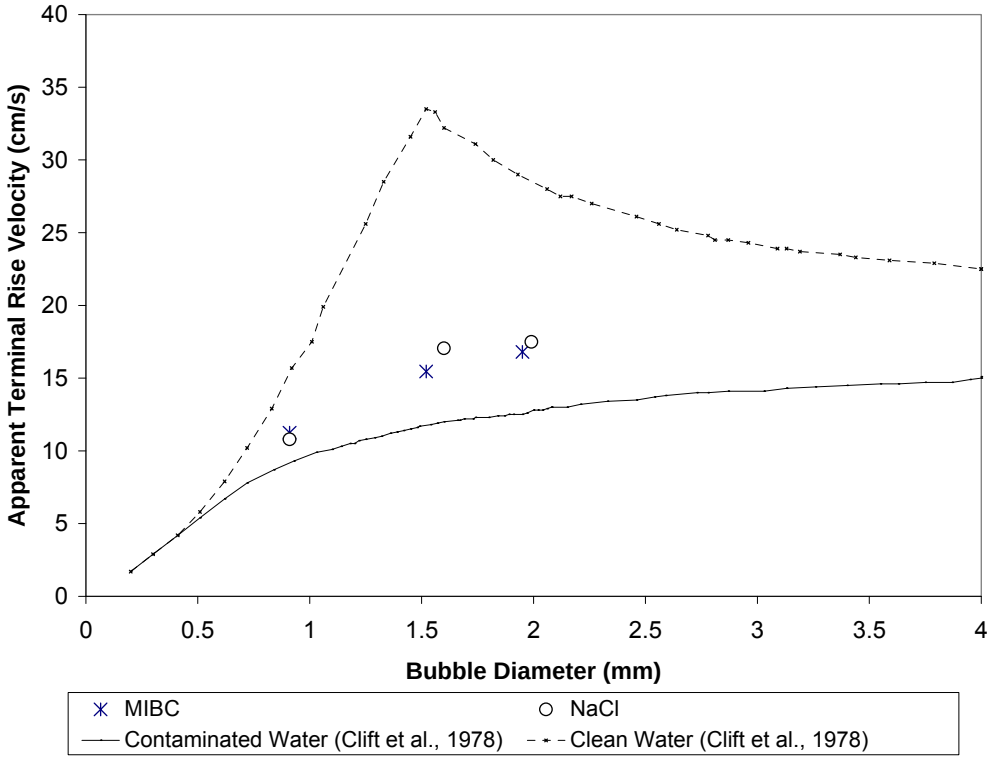

Figure 4.29: The terminal/apparent terminal rise velocity vs. bubble diameter at 3000mm in the presence of MIBC and NaCl.

Figure 4.29 presents apparent terminal rise velocity vs. bubble diameter in the presence of NaCl and MIBC. The Figure shows the velocities are close and both reagents (eventually in the case of NaCl) slow down the bubble rise to that approaching contaminated water. The similarity observed by Quinn et al (2007) is also found for rise velocity of single bubbles.

Henry et al. (2008) measured the terminal rise velocity of very small single bubbles ($40\mu m<d_b<100\mu m$) in the presence of some salts over a similar range of concentration as here. It was reported that addition of NaCl did not reduce the rise velocity compared to pure water. But there is a question, whether their data reflects the terminal velocity as they measured the velocity at a distance of only ca. 1.5mm above the capillary. According to Figure 4.28 the single bubble does not attain terminal velocity at such a short distance, indeed the bubble required 3000mm to be even close to the terminal velocity. However, according to Figure 1.2 the addition of any reagent appears does not reduce the bubble rise velocity for bubbles << 1mm, and therefore a salt effect may not be detectable.

4.6. Comparison of frothers

In this part three industrial frothers were tested: F150, DF250 and MIBC. Figure 4.30 presents the apparent terminal rise velocity vs. bubble diameter in the presence of these frothers. The velocities are close and comparable to contaminated water. Figure 4.31 presents the apparent terminal velocity at 3000mm vs. concentration in F150, DF250 and MIBC. It shows that there is a critical concentration to reach terminal velocity; however their critical concentrations are very low compared to many of the alcohols. DF250 has the lowest critical concentration (in ppm).

Sam et al. (1996) measured the terminal rise velocity of two of the current frothers, DF250 and MIBC. Figure 4.32 presents a comparison between the results. There is good agreement between the DF250 data with slightly lower velocities recorded for MIBC in the current work.

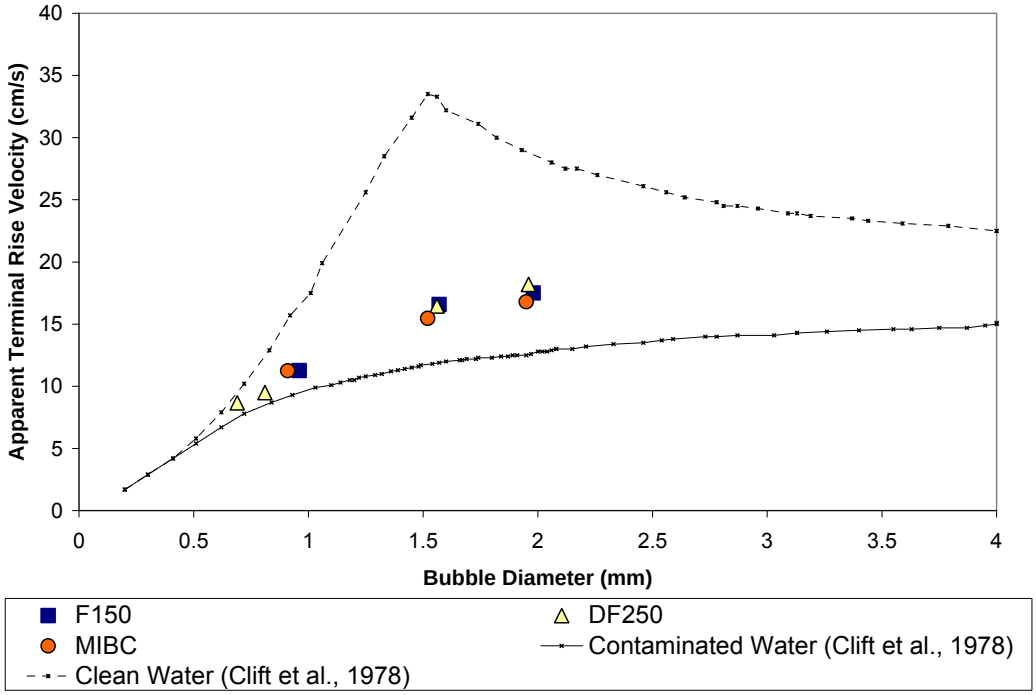

Figure 4.30: The terminal/apparent terminal velocity at 3000mm vs. bubble diameter in the presence of the three commercial frothers.

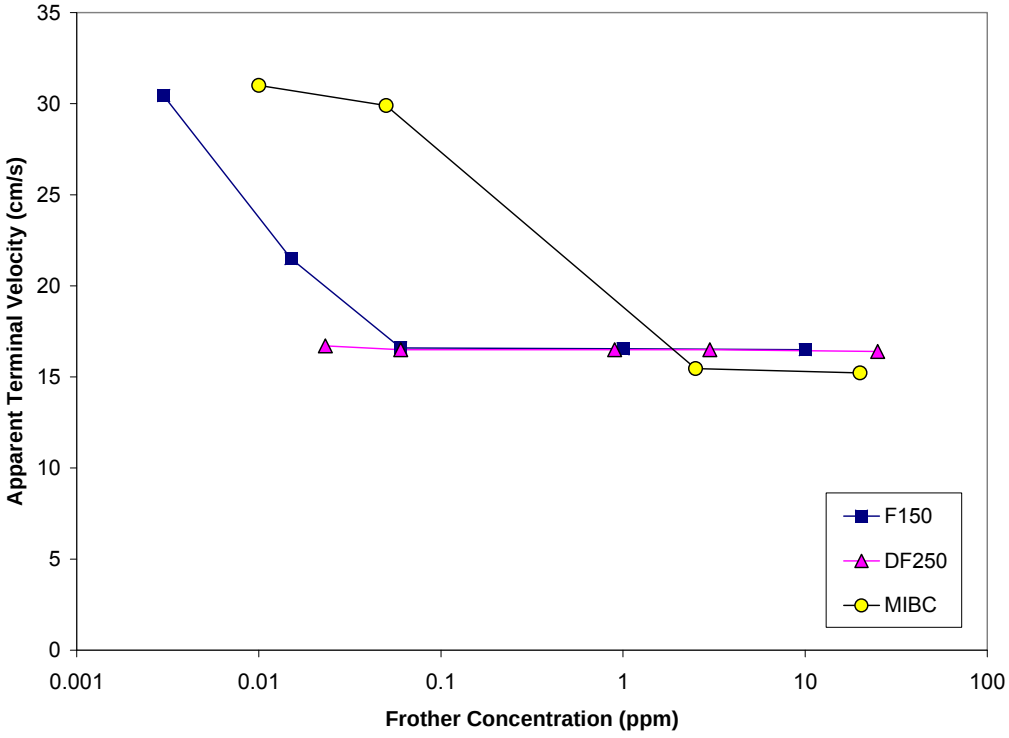

Figure 4.31: Apparent terminal velocity at 3000mm vs. concentration of single bubbles in F150, DF250 and MIBC.

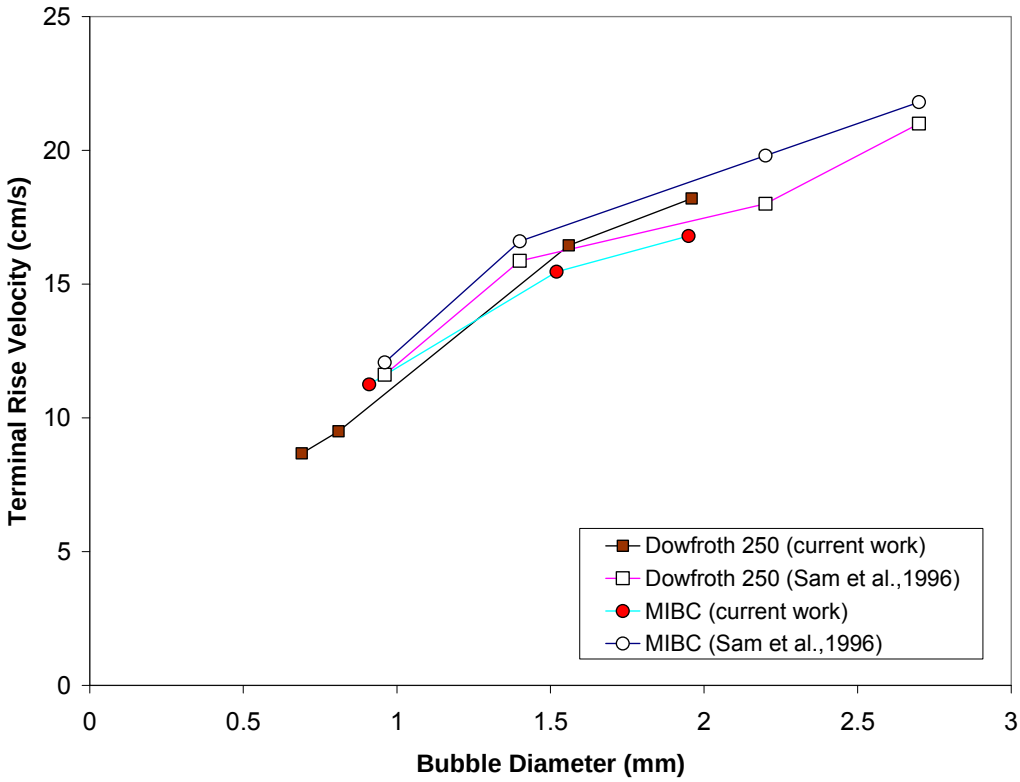

Figure 4.32: The comparison of measured terminal rise velocity of MIBC and Dowfroth 250 between the Sam et al. (1996) and the recent work.

4.7. The dependency of terminal velocity on frother properties

Sam et al. (1996) reported that terminal rise velocity is independent of frother concentration, simply the time taken to reach terminal velocity is increased as concentration is decreased. In practice however, since time is finite (height of flotation cell) there are two effective concentration regimes:

i) At lower than critical concentration the frother concentration affects bubble rise velocity.

ii) At higher than critical concentration the rise velocity is independent of concentration and is reduced to the contaminated water value.

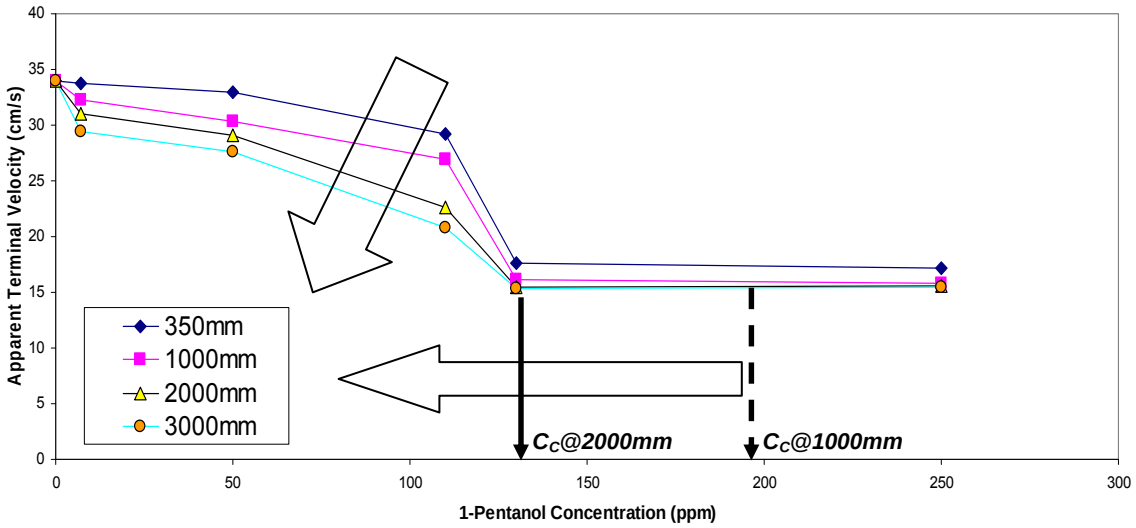

Figure 4.33: The influence of travel distance of bubble on critical concentration and apparent terminal velocity in 1-pentanol for ca. 1.45mm single bubbles.

Accordingly, the interpretation of terminal rise velocity first requires determining the velocity profile.

Regarding the several velocity profiles presented in the current work that exhibited decreasing trend at the end of profile, it could be concluded that if the experiment was repeated in a taller column (longer travel distance) the bubble would reach terminal velocity. The increase in bubble traveling distance gives enough time to reach sufficient surfactant adsorption to terminal velocity. As a result in an infinitely tall column the single bubble would reach terminal velocity in any concentration, in agreement with the conclusion of Sam et al. (1996). The increase in bubble travel distance shifts the critical concentration to lower concentrations.

Sam et al. (1996) did note that frother type affected the profile and possibly the terminal velocity. Figure 4.33 presents the terminal velocity vs. concentration for the frothers used in this study for ca. 1.45mm bubble size. Figure 4.33 indicates that above the critical concentration the frother type did not influence terminal velocity and the terminal velocity approaches that in contaminated water.

Figure 4.34 compares the average terminal velocity of the frothers studied at different bubble size with the clean and contaminated water lines by Clift et al. (1978). Figure 4.35 indicates that the trend of current work is similar to the trend of contaminated water line; however, the current work exhibits a consistently higher terminal velocity.

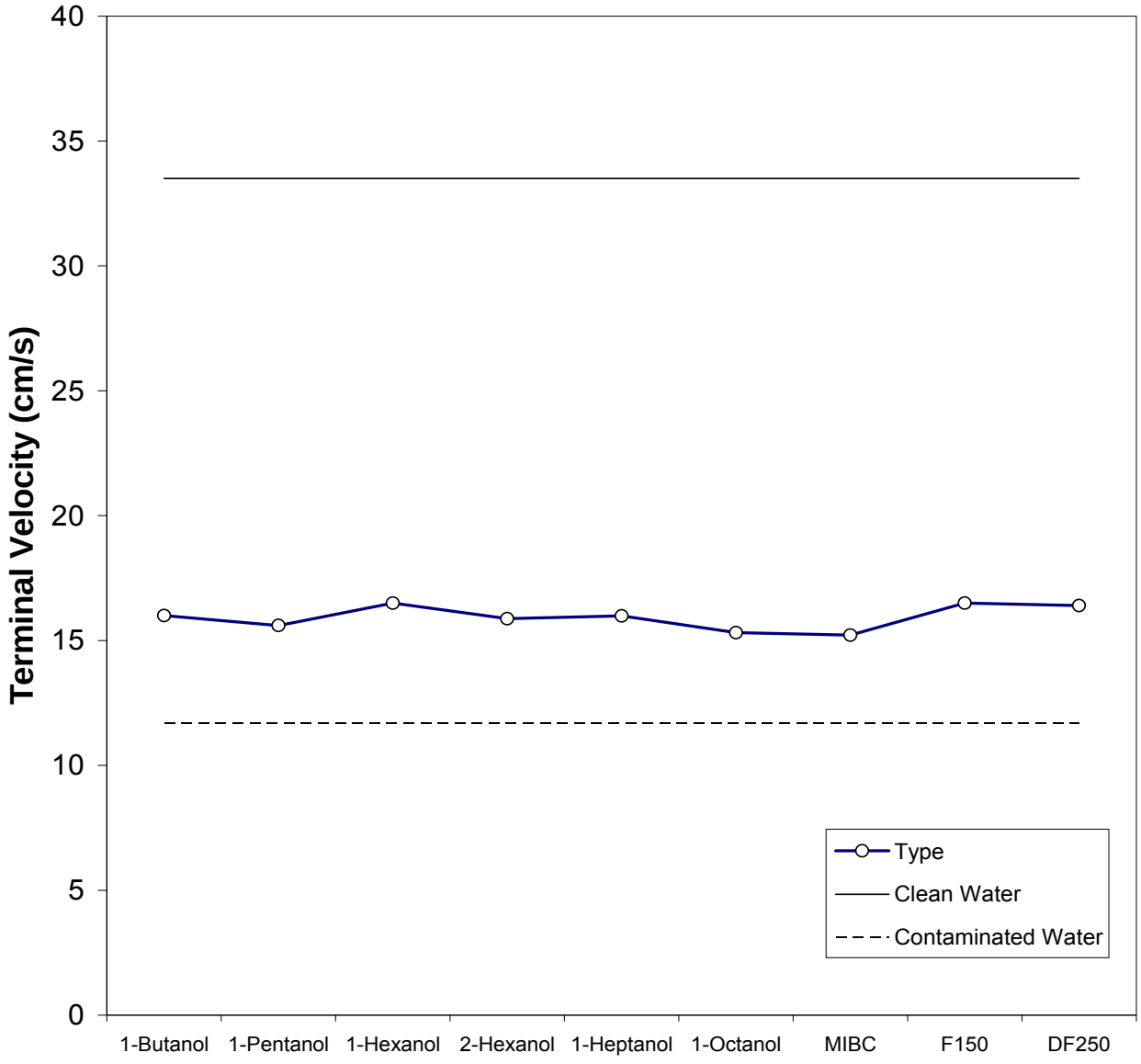

Figure 4.34: Comparison of terminal velocity of the used frother with clean and contaminated water lines by Clift et al. (1978) (ca. 1.5mm).

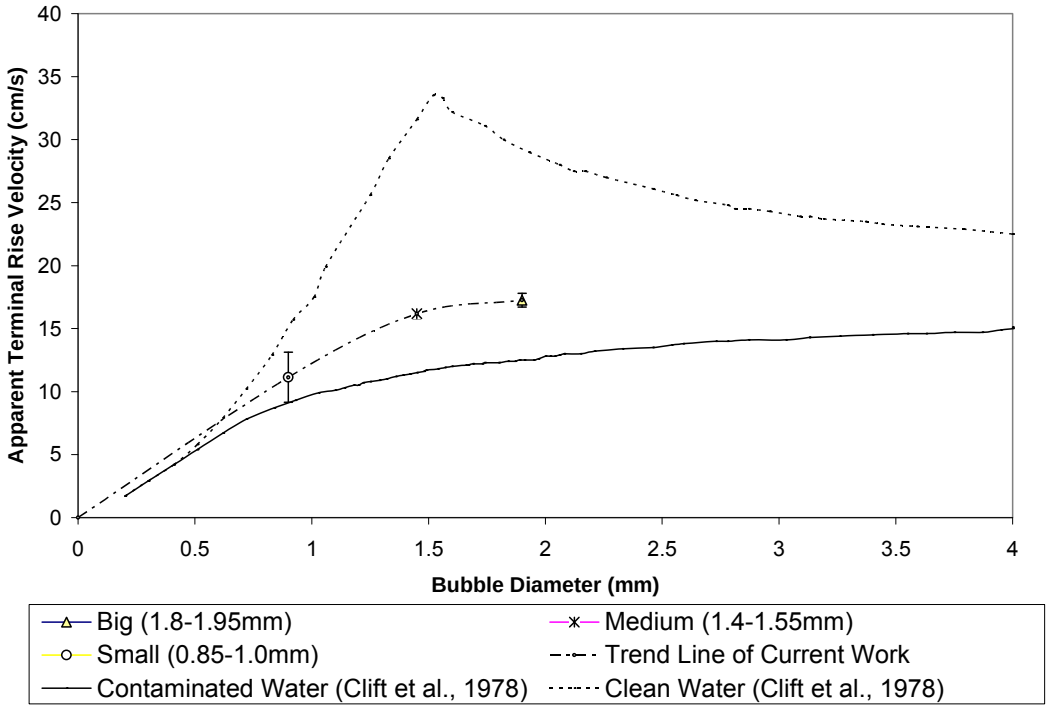

Figure 4.35: Comparison of the trend line of current work with clean and contaminated water lines by Clift et al. (1978).

CHAPTER FIVE: CONCLUSIONS AND RECOMMENDATIONS

Single bubbles in the size (diameter) range 0.8-2.0 mm were generated under a low frequency regime (<80 bubbles/min), and the bubble size and rise velocity over ca. 3500mm were measured using image processing techniques. This chapter summarizes the conclusions and ends with recommendations for future work.

5.1. Conclusions

5.1.1. Bubble generation

- The size of bubbles generated at a capillary at low frequency was not materially influenced by the concentration and type of reagents.

5.1.2. Velocity profile analysis

- The velocity profile was obtained by using a mobile video camera to track and record individual bubbles.
- The observed velocity profiles showed the typical properties, as first reported by Sam et al. (1996).
- Determination of true terminal rise velocity requires analysis of the profile to establish when velocity is constant.
- The “apparent terminal velocity” is introduced that gives the possibility of comparing with the rise velocity of the bubbles reported in the literature when distance is known.

5.1.3. Hypothesis based on observation of Azgomi et al. (2007)

- The results of this work confirmed that reagent type can affect the rise velocity profile of same size bubbles over the concentration range of interest in flotation, which is in agreement with the previous observations of Azgomi et al. (2007) and Acuna and Finch (2008).
- The significant difference between rise velocity of F150 and 1-pentanol shown to be because in the latter bubbles do not reach terminal velocity. This explains the observation of Azgomi et al. (2007).

5.1.4. Aliphatic alcohols

- Over the concentration range used in flotation, 1-butanol and 1-pentanol approximated the trend of pure water (Clift et al., 1978); i.e., their presence did not significantly reduce the bubble rise velocity. 1-heptanol and 1-octanol approached the contaminated water trend.
- On the concentration range of interest in flotation, 1-hexanol proved the exception: the lowest concentration of hexanol acted like 1-butanol and 1-pentanol and the higher concentrations exhibited the trend in 1-heptanol and 1-octanol. Velocity profile analysis showed that the bubble did not reach terminal rise velocity at the lowest concentration of 1-hexanol.
- Comparison of 1-hexanol, 2-hexanol and MIBC confirmed that not only the frother concentration could affect the apparent terminal velocity but also differences in molecular structure. The former impact could be called a "concentration effect" and the latter "molecular structure effect" that makes a link between the mechanism of single bubble rise velocity and the chemistry of surfactant.
- To explore the concentration effect a wider concentration range was examined and it was observed that there is critical concentration, C_C, for each alcohol to reach terminal velocity by a given distance. Below the C_C surfactant concentration affects the apparent terminal rise velocity, while over the critical concentration (when the bubble reaches terminal velocity) the rise velocity is independent of concentration.
- There was agreement with the results of Krzan and Malysa (2002) in the case of 1-butanol, 1-pentanol and 1-hexanol. However, they considered the rise velocity at 350mm (35cm) as the terminal velocity where the results here indicate the bubble does not necessarily reach the terminal velocity at this distance location.

5.1.5. The comparison of MIBC and NaCl

- Both MIBC and NaCl had similar influence on bubble rise velocity, which agrees with the gas holdup data reported by Quinn et al. (2007).

5.1.6. Commercial frothers

- Three commercial frothers, F150, DF250 and MIBC, were tested and were found to reach terminal at low critical concentration (<1ppm) and approximate the contaminated water trend.
- Comparing to results of Sam et al. (1996) the terminal rise velocity in MIBC and DF250 exhibited good agreement.

5.1.7. Dependency of terminal velocity on frother properties

- The traveling distance of bubble affects the apparent terminal velocity. The increase in travel distance results in having lower critical concentration (C_C) as more time available for the rising bubble for reaching terminal velocity. Thus with an infinite travel distance (i.e., very tall column) the single bubble would reach terminal velocity in any concentration, which is in agreement with Sam et al. (1996). As the bubble size increases, the higher critical concentration is required.
- Comparing terminal velocity indicates that the frother type does not affect terminal rise velocity, practically. As a result when the frother concentration is sufficient to reach terminal velocity, the terminal velocity is independent of frother type that is not in agreement with the conclusion of Sam et al. (1996).
- The influence of reagent on terminal rise velocity is strongly dependent on bubble size. For bubble size <1mm there was no obvious difference in rise velocity between any reagents. For the bubble sizes between 1 to 1.5mm the difference increased to a maximum; above 1.5mm the difference started to decline once more.

5.2. Recommendations for future works

- Most of studies on bubble rise velocity consider physical aspects (bubble size, method of generation). The results of this work showed that chemical properties of surfactants of interest in flotation play an important role, which should be understood.

- Study of the influence on bubble rise velocity as a function of structure of the reagent should be expanded. It seems that the adsorption and orientation of frother molecules on the bubble surface depends on the molecular structure, and could influence the number of required molecules for controlling surface mobility.
- Velocity profile analysis is the only confident method to identify the true terminal rise velocity. Any future work must include velocity profile analysis to avoid misinterpretation.
- According to the results of current work it was observed that the applied concentration equivalency (that was based on equivalent bubble size production) did not reflect the real impact of frother concentration on bubble rise velocity. So the suggestions that critical concentration (C_C) concept introduced here can be considered as the basis for comparing frothers.

Refferences

Abou-el-hassan, M.E., 1983. A generalized bubble rise velocity correlation. Chem. Eng. Commun,2, pp. 243.

Abou-el-hassan, M.E., 1983. Correlations for bubble rise in gasliquid systems. Encyclopaedia of Fluid Mechanics, Vol. 3, pp.110.

Acharya, A., 1978. Ulbrecht, J.J. Note on Influence of Viscoelasticity on Coalescence Rate of Bubbles and Drops. AIChE J, 24(2), pp.348.

Acharya, A., Mashelkar, R.A., 1977. Ulbricht, J. Mechanics of bubble motion and deformation in non-Newtonian media. Chem. Eng. Sci., 32, pp.863.

Acuna, C., 2008. Measurement techniques to characterize bubble motion in swarms., Ph.D. Thesis, McGill University, Montreal, Canada.

Acuna, C., Finch, J.A., 2008. Motion of Individual Bubbles Rising in a Swarms., Proceedings XXIV International Mineral Processing Congress, Beijing, Sept 24-18, Vol.1, 891-901.

Agrawal, S.K., and Wasan, D.T., 1979. The effect of interfacial viscosities on the motion of drops and bubbles. Chem. Eng. J., 18, 215-223.

Alves, S.S., Orvalho, S.P., Vasconcelos, J.M.T., 2005. Effect of bubble contamination on rise velocity and mass transfer. Chemical Engineering Science, 60, pp.1-9.

Astarita, G., 1966. Spherical gas bubble motion through Maxwell liquids. Ind. Eng. Chem. Fund.,5(4), 548.

Astarita, G., Apuzzo, G., 1965. Motion of gas bubbles in non Newtonian liquids. AIChE,J., 11(5), 815.

Auton, T.R., 1987. The lift force on a spherical body in a rotational flow. J. Fluid Mech., 183, 199.

Azgomi, F., 2006. Characterizing frothers by their bubble size control properties., M.Sc. Thesis, McGill University, Montreal Canada.

Azgomi, F., Gomez, C.O., Finch, J.A., 2007. Correspondence of Gas Holdup and Bubble Size in Presence of Different Frothers., International Journal of Mineral Processing, Volume 83, Issues 1-2, 2007, 1-11.

Barnett, S.M., Humphrey, A.E., Litt, M., 1966. Bubble motion and mass transfer in non-Newtonian fluid. AIChE J.,12(2), 253.

Bashforth, F., Adams, J.C., 1883. An attempt to test the theories of capillary action. Cambrige University Press: Cambrige.

Beitel, A., and Heideger, W., 1971. Surfactant effects on mass transfer from drops subject to interfacial instability. Chem. Eng. Sci., 26, 711-717.

Bergman, T.L., Webb, B.W., 1990. Simulation of pure metal melting with buoyancy and surface tension forces in the liquid phase. Int. J. Mass Transfer, 33, 1, 139-149.

Bhaga, D., 1976. Bubbles in viscous liquids: shapes, wakes and velocities. Ph.D. Thesis, McGill University, Montreal, Canada.

Bhaga, D., and Weber, M.E., 1980. In-line interaction of a pair of bubbles in a viscous liquid. Chem. Eng. Sci., 35, 2467-2474.

Bhaga, D., Weber, M.E., 1981. Bubbles in viscous liquids: shapes, wakes and velocities. J. Fluid Mech., 105, 61-85.

Binder, R.C., 1973. Fluid mechanics. Prentice-Hall, Englewood Cliffs, N.J.

Blanco, A., 1995. Quelques aspects de 1 e'coulement autour d une bulle de'formable: une approche par simulation directe. Ph.D. Thesis, Inst. Nat. Polytech. Toulouse, Toulouse, France

Bleys, G. and Joos, P., 1985. Adsorption kinetics of bolaform surfactants at the air/water interface. J. Phys. Chern., 89(6), 1027-1032.

Boussinesq, J., 1913. Vitesse de la chute lente, devenue uniforme, d'une goutte liquide spherique. dans un fluid visqueux de poids specifique moindre, C.R. Acad. Sci., 156, 1124-1130.

Bozzano, G., Dente, M., 2001. Shape and terminal velocity of single bubble motion: a novel approach. Computers and Chemical Engineering, 25, pp.571-576.

Bulatovic, S.M., 2007. Handbook of flotation reagents, Vol. 1, Elsevier Publications.

Carreau, P.J., Devic, M., Kapellas, M., 1974. Dynamique des bulles en milieu viscoelastique. Rheol. Acta, 13, 477.

Chhabra, R, 1993. Bubbles, Drops and Particles in Non-Newtonian Fluids: CRC Press: Boca Raton. Fla.

Clift, R., Grace, J.R., and Weber, M.E., 1978. Bubbles, drops and particles. Academic Press.

Craig, V.S.J., Ninham, B.W., Pashley, R.M., 1993. The effect of electrolytes on bubble coalescence in water. J. Phys. Chem., 97 (39), 10192-10197.

Crozier, R.D., 1992. Flotation: theory, reagents and ore testing. Pergamon Press, pp. 95-100.

Cuenot, B., Magnaudet, J., and Spennato, B., 1997. Effects of slightly soluble surfactants on the flow around a spherical bubble. J. FluidMech., 339,25-53.

Davidson, J.F., Harrison, D., 1971. Fluidization., academic Press, London and New York.

Davidson, J.F., Schuler, O.G., 1960. Bubble formation at an orifice in a viscous liquid., Trans. Instn. Chem. Engr., 38, 144-154.

Davidson, J.F., Schuler, O.G., 1960. Bubble formation at an orifice in an invicid liquid., Trans. Instn. Chem. Engr., 38, 335-342.

Davis, R.E., 1966. Acrivos, A. The Influence of Surfactants on the Creeping Motion of Bubbles. Chem. Eng. Sci.,21, 68l.

De Kee, D., Carreau, P.J., Modarski, J., 1986. Bubble velocity and coalescence in viscoelastic liquids. Chem. Eng. Sci.,41, 2273.

De Kee, D., Chhabra, R.P., Dajan, A. 1990. Motion and coalescence of gas-bubbles in non-Newtonian polymer solutions. J. Non Newtonian Fluid Mech., 37(1), 1-18.

De Vries, A.W.G. 2002. Biesheuvel, A, Wijngaarden, L. van, Notes on path and wake of a gas bubble rising in pure water. Int. J. Multiphase Flow, 28, 1823.

De vries, A.W.G., 2001. Path and wake of a rising bubble. Ph.D. Thesis, Twente University, Holland.

Detsch, R., Harris, I., 1989. Dissolution and rise velocity of small air bubbles in water and salt water. Oceans 89, pp.286-291.

Dewsbury, K., Karamanev, D., Margaritis, A., 1991. Hydrodynamic characteristics of free rise of light solid particles and gas bubbles in on-Newtonian liquids. Chem. Eng. Sci., 54, 4825-4830.

Dukhin, S. S., Kretzschmar, G., and Miller, R., 1995. Dynamics of adsorption at liquid interfaces: theory, experiment, application. Elsevier, Amsterdam.

Eames, I., Hunt, J. C. R., 1997. Inviscid flow around bodies moving in a weak density gradient in the absence of buoyancy effects. J. Fluid Mech., 353.

Elzinga, E., and Banchero, 1., 1961. Some observations on the mechanics of drops in liquid-liquid systems. AIChE J., 7, 394-399.

Eskinazi, S., 1968. Principles of fluid mechanics. Allyn and Bacon, Boston.

Fainerman, V.B., Zholob, S.A., Miller, R., and Joos, P., 1998. Non-diffusional adsorption dynamics of surfactants at the air/water interface: adsorption barrier or non-equilibrium surface layer. Colloids and Surfaces, A: Physicochemical and Engineering Aspects 143, 243-249.

Fainerman, V.B., 1985. Kinetics of formation of adsorption layers at a solution-air interface. VNIPIChermetenergoochistka, Donetsk, USSR. Usp. Khim., 54(10),1613-1631.

Fan, L.S., and Tsuchiya, K., 1990. Bubble wake dynamics in liquids and liquid-solid suspensions. Butterworth-Heinemann, 17-66.

Fdhila, R.B., Duineveld, P.C., 1996. The effect of surfactant on the rise of a spherical bubble at high Reynolds and Plecet numbers. Phys. Fluids, 8(2), 310-321.

Finch, J.A., and Smith, G.W., 1972. Dynamic surface tension of alkaline dodecylamine acetate solutions in oxide flotation. Trans IMM, 81, C213-218.

Finch, J.A., 1971. Interfacial phenomena in cationic magnetite flotation. Master Thesis, McGill University, Montreal, Canada.

Finch, J.A., 1973. The liquid-vapor interface and adhesion in flotation. Ph. D. Thesis, McGill University, Montreal, Canada.

Finch, J.A., Nesset, J.E., Acuna, C., 2008. Role of frother on bubble production and behaviour in flotation. Minerals Engineering, 21, 949-957.

Frumkin, A., 1925. Phys. Chem., 116,466.

Frumkin, A., Levich, V.G., 1947. On the surfactants and interfacial motion. Z. Fizicheskoi Khirnii,21,1183-1204.

Fuerstenau, D.W., and Wayman, C.H., 1958. Effect of chemical reagents on the motion of single air bubbles in water. TransactionAIME, June, Mining Engineering, 694-699.

Garner, F.H., and Skelland, A.H.P., 1955. Some factors affecting droplet behaviour in liquid -liquid systems. Chem. Eng. Sci., 4, 149-158.

Garner, F.H., and Hammerton, D., 1954. Circulation inside gas bubbles. Chem. Eng. Sci., 3, I, 1-11.

Gaskell, D.R., 1992. An Introduction to transport phenomena in mineral processing. MacmUlan Publishing Company, New York.

Gonzaleztello, P., Camacho, F., Jurado, E., Bailon, R , 1992. Influence of surfactant concentration on the final rising rate of droplets. Can. J. Chem. Eng., 70(3), 426.

Grace, J.R., Wairegl, T., and Nguyen, T.H., 1976. Shapes and velocities of single drops and bubbles moving freely through immiscible liquids. Trans. Instn Chem. Engrs,54, 167-173.

Griffith, R.M., 1962. The effect of surfactant on the terminal velocity of drops and bubbles. Chem. Eng. Sci., V 17, pp.1057-1070.

Gummalam, S., 1987. Chhabra, R P. Rising velocity of a swarm of spherical bubbles in a power law non-Newtonian liquid. Can. J. Chem. Eng., 65, 1004.

Haberman, W.L, and Morton, R.K., 1953. An experimental investigation of the drag and shape of air bubbles rising in various liquids. Navy Department, The David W. Taylor Model Basin, Report 802.

Hadamard, J., 1911. Mouvement permanent lent d'une sphere liquide et visqueuse dans une liquide visqueux. C. R. Acad. Sci, 152, 1735-1738.

Haque, M.W., Nigam, K.D.P., Viswanathan, K., Joshi, J.B., 1988. Studies on bubble rise velocity in bubble columns employing non-Newtonian solutions. Chem. Eng. Commun., 73, 31.

Haque, M.W., Nigam, K.D.P., Viswanathan, K., Joshi, .J.B., 1987. Studies on gas holdup and bubble parameters in bubblecolumns with (carboxymethyl) cellulose solutions. Ind. Eng. Chem. Res.,26 (1), 86.

Harper, J.F., 1972. The motion of bubbles and drops through liquids. Advance Applied Mechanics, 12,59-129.

Harper, J.F., 1974. On spherical bubbles rising steadily in dilute surfactant solutions. Q.J. Mech. Appl. Math., V XXVII, pp.87-100.

Harper, J.F., 1988. The rear stagnation region of a bubble rising steadily in a dilute surfactant solution. Q. J. Mech. Appl. Math., V 41, pp.203-213.

He, Z., Maldarelli, C., and Dagan, Z., 1991. The size of stagnant caps of bulk soluble surfactant on the interfaces of translating fluid droplets. J. Colloid Interface Sci., 146(2), 442-451.

Henry, C.L., Parkinson, L., Ralston, J.R., Craig, V.S.J., 2008. A mobile gas/water interface in electrolyte solutions. J. Phys. Chem. C, 112 (39), 15094-15097.

Horton, Y.J., Fritsch, I.R., and Kintner, R., 1965. Experimental determination of circulation velocities inside drops. Can. J. Chem. Eng., 43, 143-146.

Huang, W., and Kintner, R.C., 1969. Effects of surfactants on mass transfer inside drops. AlChE J., 15, 735-744.

Jameson, G. J., 1993. Bubbles in motion, Trans. Inst. Chem. Eng., 71(A), 587.

Jamialahmadi, M., Muller-Steinhagen, H., 1992. Effect of alcohol, organic acid and potassium chloride concentration on bubble size rise velocity and gas hold-up in bubble columns. The Chemical Engineering Journal, 50, pp.47-56.

Karamanev, d.G., nikolov, L.N., 1992. Free rising spheres do not obey Newton's law for free settling. AIChE J., 38(11), 1843-1846.

Karamanev, D.G., 1994. Rise of gas bubbles in quiescent liquids. AIChE J., 40(8), 1418-1421.

Khurana A.K, Kumar R ,1969. Studies in bubble formation III. Chem. Eng. Sci., 24, 1711.

King, R.P., 1982. Principles of flotation, South African. Institute of Mining and Metallurgy, Johannesburg.

Kopfsill, A.R, Homsy, G.M., 1988. Bubble motion in a Hele Shaw cell. Phys. Fluids,31(1), 18-26.

Kreischer, B.E., Moritomi, H., and Fan, L.S., 1990. Wake solids holdup characteristics behind a single bubble in a three-dimensional liquid-solid fluidized bed. Int. J. Multiphase Flow, 16, 2, 187200.

Krzan, M., Lunkenheimer, K., Malysa, K., 2004. On the influence of the surfactant's polar group on the local and terminal velocities of bubbles. Colloids and Surfaces a, 250, pp.431-441.

Krzan, M., Malysa, K., 2002. Profiles of local velocities of bubbles in n-butanol, n-hexanol and n-nonanol solutions. Colloid and Surfaces A, 207, pp.279-291.

Krzan, M., Zawala, J., Malysa, K., 2007. Development of Steady State Adsorption Distribution Over Interface of a Bubble Rising in Solutions of n-Alkanols (C_5, C_8) and n-Alkyltrimethylammonium Bromides (C_8, C_{12}, C_{16})., Colloids and Surfaces A, 298, 42-51

Kugou, N., Ishida, K., Yoshida, A., 2003. Experimental study on motion of air bubbles in seawater. Marine Technology, V 3, pp.145-158.

Kulkarani, A..A., Joshi, J.B., 2005. Bubble formation and bubble rise velocity in gas-liquid systems: a review. Ind Eng. Chem. Res., 44, pp.5873-5931.

Lamb, H., 1945. Hydrodynamics, 6th ed., Dover Publications. Co.: New York, pp. 600.

Lan, C.W., and Kou, S., 1992. Heat transfer and fluid flow in flotation-zone crystal growth with a mostly covered melt surface. Int. Heat Mass Transfer, 35, 2, 433-442.

Leal, L.G., Skoog, J., Acrivos, A., 1971. On the motion of gas bubbles in a viscoelastic liquid. Can. J. Chem. Eng., 49, 569.

Lee, J.C., Hodgson, T.D., 1968. Film flow and coalescence-I Basic relations, film shape and criteria for interface mobility. Chem. Eng. Sci., 23,1375-1397.

Letzel, M., 1998. Hydrodynamics and mass transfer in bubble columns at elevated pressures, Ph.D. Thesis, Delft University.

Levich, V.G., 1962. Physicochemical hydrodynamics. Englewood Clifts, Prentice-Hall.

Liao, Y., Mclaughlin, J.B., 2000. Bubble motion in aqueous surfactant solutions. Journal of Colloid and Interface Science, 224, pp.297-310.

Liao, Y., Mclaughlin, J.B., 2000. Dissolution of a freely rising bubble in aqueous surfactant solutions. Chemical Engineering Sciences , 55, pp.5831-5850.

Liao, Y., Wang, J., Nunge, R.J., Mclaughlin, J.B., 2004. Comments on "Bubble motion in aqueous surfactant solution". Journal of Colloid and Interface Science, 272, pp.498-501.

Linton, M., and Sutherland, K.L., 1957. Dynamic surface forces, drop circulation and liquid-liquid mass transfer. Second international congress on surface activity, Butterworth, London, 1, 494-501.

Lochiel, A.C., 1965. The influence of surfactants on mass transfer around spheres. Can. J. Chem. Eng., 43,40-44.

Lunde, K, Perkins, R,1997. Observations on wakes behind spheroidal bubbles and particles. Proc. ASME Fluids Eng. Div. Summer Meeting, Vancouver, 97, 3530.

Luo, X., Zhang, J., Tsuchiya, K, Fan, L. S., 1997. On the rise velocity of bubbles in liquid-solid suspensions at elevated pressure and temperature. Chem. Eng. Sci., 52(21-22), 3693.

Magnaudet, J., Eames, I., 2000. Motion of high Reynolds number bubbles in turbulent flows. Annu. Rev. Fluid Mech., 32,659.

Malysa, K, Masliyah, J.H., Neale, G., and van de Ven, T.G.M., 1988. Settling velocity of a polymer coated particle. Model experiments and theory, Materials Science Forum, 25-26, 401404.

Malysa, K., Krasowska, M., Krzan, M., 2005. Influence of surface active substances on bubble motion and collision with various interfaces. Advanced in Colloid and Interface science, 114-115, 205-225.

Margaritis, A., Te Bokkel, D.W., Karamanev, D., 1999. Bubble rise velocities and drag coefficients in non-Newtonian polysaccharide solutions. Biotech. Bioeng., 64(3), 259.

Massey, B.S., 1983. Mechanics of fluids. Wokingham, Berkshire, England: Van Nostrand Reinhold (UK).

McLaughlin, J.B., 1996. Numerical simulation of bubble motion in water. Journal of Colloid and Interface Science, 184, pp.614-625.

Mei, R, Klausner, J. F., 1992. Unsteady force on a spherical bubble at finite Re with small fucntions in the free stream velocity. Phys. Fluids A, 4, 63.

Miyahara, T., Tsuchiya, K., and Fan, L.S., 1988. Wake properties of a single gas bubble in a three-dimensional liquid-solid fluidized bed. Int. J. Multiphase Flow, 14, 6, 749-763.

Miyahara, T., Yamanaka, S., 1993. Mechanics of motion and deformation of a single bubble rising through quiescent highly viscous Newtonian and non-Newtonian media. J. Chem. Eng. Jpn.,26,297.

Narayanan, S., Gossens, L.H.J., Kossen, N.W.F., 1974. Coalescence of Two Bubbles Rising in Line at Low Reynolds Numbers", Chem. Eng. Sci., 29, 2071-2082.

Newman, J., 1967. Retardation of falling drops. Chem. Eng. Sci., 22, 83-85.

Nguyen, A. V., 1998. Prediction of bubble terminal velocities in contaminated water. AIChE J., 44(1), 226-230.

Oguz, H.N., and Sadhal, S.S., 1988. Effects of soluble and insoluble surfactants on the motion of drops. J. Fluid Mech., 194, 563-579.

Okano, Y., Itoh, M., and Hirata, A., 1989. Natural and Marangoni convections in a two dimensional rectangular open boat. J. Chemical Engineering of Japan, 22, 3, 275-281.

Okazaki, S., 1964. The velocity of ascending air bubbles in aqueous solutions of a surface active substance and the life of the bubble on the same solution. Bull. Chem. Soc. Japan., 37, 144-150.

Parkinson, L., Sedev, R., Fornasiero, D., Ralston, J., 2008. The terminal rise velocity of 10-100 μm diameter bubbles in water. Journal of Colloid and Interface Science, 322, 168-172.

Quinn, J.J., Kracht, W., Gomez, C.O., Gagnon, C., Finch, J.A., 2007. Comparing the effect of salts and frother (MIBC) on gas dispersion and froth properties. Mineral Engineering, 20, 1296-1302.

Quinn, J., 2006. Exploring the effect of salts on gas dispersion and froth properties in flotation system. M.Sc. Thesis, McGill University, Montreal, Canada.

Rabiger, N., Vogelpohl, A., 1986. Bubble formation and its movement in Newtonian and Non-Newtonian liquids. Encyclopaedia of Fluid Mechanics: Gulf Publishing: Houston, , 59.

Ramkrishnan, S., Kumar, R, Kuloor, N.R, 1969. Studies in bubble formation - I, Bubble formation under constant flow conditions. Chem. Eng. Sci. 1,24, 731.

Rao, S. R., 2004, Surface chemistry of froth flotation. Kluwer Academic/ Plenum Publishers Press, New York.

Ribeiro, C.P., Mewes, D., 2007,. The effect of electrolytes on the critical velocity for bubble coalescence. Chemical Engineering Journal, 126, 23-33.

Rodrigue, D., 2001. Generalized correlation for bubble motion. AIChE J., 47, 39.

Rodrigue, D., 2002. A simple oscillation for gas bubbles rising in power-law fluids. Can. J. Chem. Eng., 80(2), 289.

Rodrigue, D., 2004. A general correlation for the rise velocity of single gas bubbles. Can. J. Chern. Eng., 82 (2), 382-386.

Rodrigue, D., De Kee, D., Chan Man Fong, C.F., 1998. Bubble velocities: further developments on the jump discontinuity. ,J. Non-Newt. Fluid Mech, 79(1), 45.

Rodrigue, D., De Kee, D., Chan Man Fong, C.F., 1996. An experimental study of the effect of surfactants on the free rise velocity of gas bubbles. J. Non-Newtonian Fluid Mech., 66,pp.213-232.

Rodrigue, D., de Kee, D., Chan Man Fong, C.F., 1999. The slow motion of a single bubble in a non-Newtonian fluid containing surfactant. J. Non-Newtonian Fluid Mech., 86,pp.211-227.

Sam, A., 1995.Single bubble behavior study in a flotation column. Ph.D. Thesis, McGill University, Montreal, Canada.

Sam, a., Gomez, C.O., Finch, J.A., 1996. Axial velocity profiles of single bubbles in water/frother solutions. International Journal of Mineral Processing, 47, 177-196.

Satyanarayana, A., Kumar, R, Kuloor N.R , 1969. Studies in bubble formation - II, Bubble formation under constant pressure conditions. Chern. Eng. Sd.,24, 731.

Savic, P., 1953. Circulation and distortion of liquid drops falling through a viscous medium. Nat. Res. Counc. Can. Div. Mech. Eng. Report MT -22.

Schechter, R. S., and Fairley, R. W., 1963. Interfacial tension gradients and droplet behaviour. Can. J. Chem. Eng., 41, 103-107.

Scriven, L.E., 1960. Dynamics of a fluid interface. Chem. Eng. Sci., 12, 98-108.

Stone, H.A., and Leal, L.G., 1990. The effect of surfactant on drop deformation and breakup, J. Fluid Mech., 220, 161-186.

Takagi, S., Matsumoto, Y., 1995. Three-dimensional calculation of a rising bubble. Proc. Int. Conf. Multiphase Flow, 2nd, Kyoto, Japan, pp. PD2.9 16.

Takemura, F., 2005. Adsorption of surfactant onto the surface of a spherical rising bubble and its effect on the terminal velocity of bubble. Physics of Fluids, 17, 048104.

Tate, T., 1864. On the magnitude of a drop ofliquid formed under different circumstances. Philosophical Magazine,27, 176.

Tomiyama, A. 2004. Drag, lift and virtual mass forces acting on a Single Bubble, 3rd International Symposium on T\vo-Phase Flow Modelling and Experimentation Pisa, 22-24.

Tomiyama, A., 2002. Reconsideration of Three Fundamental Problems in Modeling Bubbly Flows, Proc. JSME- KSME Fluid Eng. Conf. Pre-Symp., pp 47-53.

Tomiyama, A., Yoshida, S., Hosokawa, S., 2001. Surface Tension Force Dominant Regime of Single Bubbles rising through Stagnant Liquids, on CD-ROM of 4th UK-Japan Seminar on Multiphase Flow, pp 1-6.

Tsuchiya, K., and Fan, L.S., 1988. Near wake structure of a single gas bubble in a two dimensional liquid-solid fluidized bed: Vortex shedding and wake size variation. Chem. Eng. Sci., 43, 1167-1181.

Tsuchiya, K., Miyahara, T., and Fan, L.-S., 1989. Visualization of bubbles-wake interactions for a stream of bubbles in a two-dimensional liquid-solid fluidized bed. Int. J. Multiphase Flow, 15, 1, 35-49.

Tsuge, H., 1986. Hydrodynamics of bubble formation from submerged orifices. In. Encyclopaedia of Fluid Mechanics, Gulf Publishing Company: New York, Vol. 3, 191.

Tsuge, H., and Hibino, S.I., 1977. The onset conditions of oscillatory motion of single gas bubbles rising in various liquids. J. Chem. Eng. Japan, 10, 66-68.

Tsujii, K., 1997. Surface Activity, principles, phenomena, and applications. Academic Press.

Tzounakos, A., Karamanev, D.G., Margaritis, A., Bergougnou, M.A., 2004. Effect of the Surfactant Concentration on the Rise of Gas Bubbles in Power-Law Non-Newtonian Liquids. Ind. Eng. Chem. Res., 43(18), 5790-5795.

Urry, D.W., 1995. Elastic biomolecular machines. Scientific American, Jan. 95.

Vennard, J.K., and Street, R.L., 1975. Fluid flow about immersed objects. John Wiley and Sons Inc, 645-671.

Wu, M., Gharib, M., 2002. Experimental studies on the shape and path of small air bubbles rising in clean water. Phys. Fluids, 14, L49.

Yamamoto, T., and Ishii, T., 1987. Effect of surface active materials on the drag coefficient and shape of single large gas bubbles. Chem. Eng. Sci., 42(6), 1297-1303.

Ybert, C., Di Meglio, J. M., 1998. Ascending air bubbles in protein solutions. Eur. Phys. J. B,4, 313.

Yoshida, S., Manasseh, R, 1997. Trajectories of rising bubbles, The 16th Japanese Multiphase Flow Symposium, Touya, Hokkaido.

Zana, E., Leal, L.G., 1978. Dynamics and dissolution of gas bubbles in a viscoelastic fluid. Int. J. Multiphase Flow, 4(3), 237-262.

Zhang, Y., 2000. Single bubble velocity profile: experimental and numerical simulation. Ph.D. Thesis, McGill University, Montreal, Canada.
Zhang, Y., Finch, J.A., 2000. A note on single bubble motion in surfactant solutions. Journal of Fluid Mechanics, V 429, pp.63-66.

Zhang, Y., McLaughlin, J.B., Finch, J.A., 2001, Chemical Engineering Sciences, 56, pp.6605-6616.

Zhang, Y., Sam, A., Finch, J.A., 2003. Temperature effect on single bubble velocity profile in water and surfactant solution. Colloids and Surfaces Eng., 223, pp.45-54.

Zhou, Z.A., Egiebor, N.O., Plitt, L.R., 1991. On Bubble Size Determination in a Flotation Column., Proceedings of International Conference on Column Flotation, Vol. 1, 249-262.

Zhou, Z.A., Egiebor, N.O., Plitt, L.R., 1992. Frother effects on single bubble motion in a water column., Canadian Metallurgical quarterly, 31, 1, 11-16.

Zhou, Z.A., Egiebor, N.O., Plitt, L.R., 1991. Effect of frothers on bubble rise velocity in a flotation column – 1. Single bubble system, Column 91, 1, 249-261.

Appendix

Figure 4.1: Variation of single bubble size vs. bubble frequency for reagents using 25μm capillary.

Type	Frequency (bubbles/min)	Bubble Size (mm)
1-Butanol	37	0.725
	23	0.774
	35	0.713
1-Pentanol	19.3	0.858
	16.7	0.940
	16.8	0.904
	18.1	0.923
1-Hexanol	18.3	0.843
	28.1	0.817
	22.72	0.785
	26.3	0.807
	17.65	0.877
1-Heptanol	28.2	0.785
	17.6	0.867
	19	0.876
	17.6	0.888
1-Hexanol	18.3	0.843
	28.1	0.817
	22.72	0.785
	26.3	0.807
	17.65	0.877
1-Octanol	17.8	0.891
	18.5	0.883
	18.18	0.868
	18.18	0.877
MIBC	21.27	0.878
	17.6	0.947
	18	0.877
	20	0.926
DF250	37	0.700
	22	0.827
	28	0.792
	35	0.714
F150	34	0.667
	14.5	0.976
	18	0.991
	20.9	0.914
	17.6	0.873
NaCl	18.5	0.927
	20.52	0.750
	16.5	0.941
	19.25	0.846
	17.03	0.935
	19.1	0.861

Figure 4.2: The variation of single bubble size vs. bubble frequency for the three applied capillaries.

Capillary 25μm		Capillary 51μm		Capillary 75μm	
Frequency (bubbles/min)	Bubble Size (mm)	Frequency (bubbles/min)	Bubble Size (mm)	Frequency (bubbles/min)	Bubble Size (mm)
37	0.725	50	1.568	70.58	1.961
23	0.774	50	1.568	75	1.943
35	0.713	51.7	1.563	79.2	1.953
37	0.700	51.8	1.563	79.2	1.975
22	0.827	35.86	1.832	70.58	1.967
28	0.792	51.9	1.571	76.33	1.980
35	0.714	52.88	1.532	80	1.968
34	0.667	55.09	1.527	72.87	1.978
14.5	0.976	53.84	1.524	75.3	1.963
18	0.991	53.78	1.515	77.12	1.943
20.9	0.914	53.88	1.509	70.1	1.919
17.6	0.873	54.07	1.548	75.47	1.959
28.2	0.785	24.23	1.901	73.96	1.978
17.6	0.867	27.9	1.830	84	1.936
19	0.876	51.67	1.562	79.5	1.957
17.6	0.888	52.98	1.493	78.84	1.971
18.3	0.843	56.44	1.571	77.02	1.937
28.1	0.817	53.66	1.519	91	1.914
22.72	0.785	47.39	1.526	65.25	1.969
26.3	0.807			78.5	1.919
17.65	0.877				
21.27	0.878				
17.6	0.947				
18	0.877				
20	0.926				
18.5	0.927				
20.52	0.750				
16.5	0.941				
16.9	0.956				
19.25	0.846				
17.03	0.935				
19.1	0.861				
19.68	0.830				
17.8	0.891				
18.5	0.883				
18.18	0.868				
18.18	0.877				
19.3	0.858				
16.7	0.940				
16.8	0.904				
18.1	0.923				

Figure 4.3: Bubble size as a function of equivalent concentration for 25μm capillary.

Type	Equivalent Concentration			
	1	3	5	6
1-Butanol	0.72		0.71	0.7
1-Heptanol	0.86	0.87	0.89	0.84
MIBC	0.93		0.92	0.92
1-Octanol	0.88	0.86	0.87	0.85
1-Pentanol	0.93	0.91	0.92	0.88

Figure 4.4: An example of velocity profile where bubble reaches terminal velocity in F150 1ppm for ca. 1.45mm bubble.

Distance (mm)	Velocity (cm/s)	Distance (mm)	Velocity (cm/s)
0	0	718.81	15.76
7.38	22.15	876.71	15.82
24.67	29.72	1035.29	15.90
42.95	25.15	1194.57	15.96
56.76	16.29	1354.95	16.12
68.00	17.43	1597.24	16.17
79.10	15.86	1839.95	16.20
89.86	16.43	2002.76	16.36
105.86	15.79	2166.38	16.36
121.57	15.57	2329.76	16.32
134.57	14.64	2493.67	16.47
152.76	14.50	2658.19	16.44
168.52	14.80	2823.00	16.53
250.86	15.39	2988.48	16.57
405.38	15.52	3093.48	16.61
561.48	15.71		

Figure 4.6.a : Velocity profiles in F150 (ca 1.5mm).

1ppm					
Distance (mm)	Velocity (cm/s)	Distance (mm)	Velocity (cm/s)	Distance (mm)	Velocity (cm/s)
0.0	0.0	214.5	19.8	360.6	18.6
1.8	10.8	221.0	19.2	369.5	18.0
8.7	30.6	227.1	18.0	375.1	18.0
19.2	32.4	233.2	19.2	383.6	16.8
30.0	32.4	239.7	19.8	457.0	17.4
40.5	30.6	245.8	18.0	603.3	17.9
51.3	34.2	252.0	19.0	757.5	17.3
62.1	30.6	258.4	18.0	908.6	17.2
72.2	30.0	264.8	19.0	1059.0	17.1
81.8	27.6	274.4	18.6	1212.4	17.9
95.4	27.0	286.6	18.0	1367.3	17.5
111.8	22.2	298.5	17.7	1520.9	17.6
126.5	21.9	310.3	17.7	1674.5	17.5
140.8	21.0	322.6	19.2	1907.4	17.9
155.2	21.0	335.1	18.3		
186.9	20.0	347.8	19.8		

Figure 4.6.b : Velocity profiles in F150 (ca 1.5mm).

3ppm				5ppm			
Distance (mm)	Velocity (cm/s)	Distance (mm)	Velocity (cm/s)	Distance (mm)	Velocity (cm/s)	Distance (mm)	Velocity (cm/s)
0.0	0.0	172.7	18.7	0.0	0.0	147.5	17.8
0.2	1.3	175.8	17.6	0.2	0.9	156.7	19.6
4.0	21.3	252.8	17.9	4.1	22.4	162.9	17.4
13.0	32.7	408.2	17.8	12.4	27.5	168.8	18.0
23.6	30.7	564.6	18.6	21.6	27.8	168.8	18.0
33.7	30.0	724.0	18.0	29.8	21.5	246.5	18.4
42.7	24.0	884.1	18.2	35.6	19.0	406.3	18.1
50.3	22.0	1042.2	18.1	40.8	18.0	567.7	18.8
57.0	18.0	1200.9	18.5	46.9	15.0	734.7	19.4
63.3	20.0	1361.0	17.8	53.1	18.6	900.9	18.6
73.1	19.3	1519.9	18.2	62.2	18.0	1064.0	18.6
85.7	18.3	1677.3	18.1	74.2	18.0	1226.1	18.4
98.0	18.7	1915.3	18.1	86.4	18.6	1391.1	19.3
110.6	19.0			104.9	18.4	1558.9	19.0
140.3	17.6			123.3	18.5		
166.7	17.3			135.5	18.2		

Figure 4.6.c : Velocity profiles in F150 (ca 1.5mm).

10ppm			
Distance (mm)	Velocity (cm/s)	Distance (mm)	Velocity (cm/s)
0.0	0.0	138.6	17.0
1.3	8.0	147.2	18.0
5.7	18.0	153.3	18.7
12.1	20.7	162.1	17.0
18.0	14.7	161.9	17.7
23.0	15.3	235.8	18.2
28.3	16.7	395.8	18.3
34.2	18.7	555.8	18.2
40.4	18.7	719.8	19.3
46.6	18.0	882.8	18.0
55.8	18.7	1043.7	18.8
67.7	17.0	1209.3	19.1
79.3	18.0	1377.9	19.4
91.3	18.0	1543.7	18.5
103.3	18.0	1706.1	18.7
115.0	17.0	1867.1	18.1

Figure 4.7.a: Velocity profiles in F150 (ca 1.5mm) over the first 3 seconds.

1ppm				3ppm			
Distance (mm)	Velocity (cm/s)	Distance (mm)	Velocity (cm/s)	Distance (mm)	Velocity (cm/s)	Distance (mm)	Velocity (cm/s)
0.0	0.0	214.5	19.8	0.0	0.0	172.7	18.7
1.8	10.8	221.0	19.2	0.2	1.3	175.8	17.6
8.7	30.6	227.1	18.0	4.0	21.3	252.8	17.9
19.2	32.4	233.2	19.2	13.0	32.7	408.2	17.8
30.0	32.4	239.7	19.8	23.6	30.7	564.6	18.6
40.5	30.6	245.8	18.0	33.7	30.0		
51.3	34.2	252.0	19.0	42.7	24.0		
62.1	30.6	258.4	18.0	50.3	22.0		
72.2	30.0	264.8	19.0	57.0	18.0		
81.8	27.6	274.4	18.6	63.3	20.0		
95.4	27.0	286.6	18.0	73.1	19.3		
111.8	22.2	298.5	17.7	85.7	18.3		
126.5	21.9	310.3	17.7	98.0	18.7		
140.8	21.0	322.6	19.2	110.6	19.0		
155.2	21.0	335.1	18.3	140.3	17.6		
186.9	20.0	347.8	19.8	166.7	17.3		

Figure 4.7.b: Velocity profiles in F150 (ca 1.5mm) over the first 3 seconds.

5ppm				10ppm			
Distance (mm)	Velocity (cm/s)	Distance (mm)	Velocity (cm/s)	Distance (mm)	Velocity (cm/s)	Distance (mm)	Velocity (cm/s)
0.0	0.0	147.5	17.8	0.0	0.0	126.8	18.3
0.2	0.9	156.7	19.6	1.3	8.0	138.6	17.0
4.1	22.4	162.9	17.4	5.7	18.0	147.2	18.0
12.4	27.5	168.8	18.0	12.1	20.7	153.3	18.7
21.6	27.8	168.8	18.0	18.0	14.7	162.1	17.0
29.8	21.5	246.5	18.4	23.0	15.3	161.9	17.7
35.6	19.0	406.3	18.1	28.3	16.7	235.8	18.2
40.8	18.0	567.7	18.8	34.2	18.7	395.8	18.3
46.9	15.0			40.4	18.7	555.8	18.2
53.1	18.6			46.6	18.0		
62.2	18.0			55.8	18.7		
74.2	18.0			67.7	17.0		
86.4	18.6			79.3	18.0		
104.9	18.4			91.3	18.0		
123.3	18.5			103.3	18.0		
135.5	18.2			115.0	17.0		

Figure 4.8: The influence of reagent concentration on maximum velocity in the presence of MIBC, NaCl and F150.

	1	3	5	6
MIBC	22	21.82	15.14	11.47
NaCl	20.28	20.16	19.62	17
F150	34.2	32.67	27.79	20.67

Figure 4.9: Velocity profiles in F150, pentanol and tap water (ca 1.5mm).

Tap Water		1-Pen 7ppm-Test 1		1-Pen 7ppm-Test 2		1-Pen 50ppm	
Distance (mm)	Velocity (cm/s)	Distance (mm)	Velocity (cm/s)	Distance (mm)	Velocity (cm/s)	Distance (mm)	Velocity (cm/s)
0.0	0.0	0.0	0.0	0.0	0.0	0.0	0.0
11.8	17.7	5.1	7.6	2.7	8.0	14.9	35.0
33.8	33.0	26.3	31.8	13.1	31.3	25.9	32.8
56.6	34.3	48.8	33.8	67.8	36.0	37.4	34.6
79.3	34.0	71.7	34.4	79.3	34.7	48.7	33.9
101.8	33.8	94.5	34.2	114.4	36.0	70.9	33.4
124.8	34.6	116.8	33.4	125.8	34.0	82.1	33.5
147.6	34.1	139.7	34.4	146.7	31.3	93.3	33.5
170.4	34.3	162.5	34.2	171.6	37.3	126.9	33.7
191.1	31.0	184.8	33.4	194.2	34.0	171.9	33.7
351.8	34.4	207.3	33.8	217.1	34.3	194.2	33.5
531.1	33.6	229.7	33.6	240.0	34.3	216.5	33.4
665.5	33.6	252.0	33.4	262.7	34.0	238.5	33.0
866.2	33.5	274.3	33.4	285.3	34.0	260.5	33.0
1000.1	33.5	296.5	33.4	296.4	33.3	282.9	33.7
1200.4	33.4	319.3	34.2	307.8	34.0	294.1	33.5
1334.0	33.4	648.3	32.9	319.6	35.3	304.6	31.4
1533.8	33.3	974.0	32.6	330.7	33.3	315.9	33.9
1867.3	33.4	1296.5	32.3	342.4	35.3	580.7	31.2
2000.4	33.3	1957.1	32.0	590.4	33.1	852.6	30.8
2199.8	33.2	2246.8	31.0	878.9	32.7	1120.4	30.3
2332.6	33.2	2551.1	30.4	1160.0	31.8	1394.7	31.1
2532.4	33.3	2845.1	29.4	1445.1	32.3	1654.7	29.4
2665.3	33.2	3080.3	29.4	1715.1	30.6	2168.0	29.1
2865.6	33.4			1445.1	32.3	2430.2	29.7
2998.8	33.3			1715.1	30.6	2679.2	28.2
3109.6	33.2					2925.4	27.9
						3168.7	27.5

Figure 4.10: Terminal rise velocity vs. bubble diameter in the presence of F150 and Pentanol compared to swarms results (Acuna and Finch, 2008) and results for single bubble in clean and contaminated water given by Clift et al. (1978).

Type	Size (mm)	Velocity (cm/s)
F150	0.96	11.27
	1.57	16.58
	1.98	17.5
1-Pentanol	0.85	13.17
	0.93	14.46
	1.5	31.2
	1.6	29.31
	1.94	28.3

Figure 4.11: Terminal rise velocity vs. bubble diameter in the presence of low (1) and high (5) concentrations of pentanol, hexanol and heptanol.

1-Pentanol- low	Bubble size (mm)	0.94	1.55	1.93
	Apparent terminal Velocity (cm/s)	15.02	29.31	26.95
	Standard Deviation (mm)	0.001	0.8	0.08
1-Pentanol- high	Bubble size (mm)	0.92	1.53	1.91
	Apparent terminal Velocity (cm/s)	14.46	29.2	25.56
	Standard Deviation (mm)	0.06	0.5	0.46
1-Hexanol- low	Bubble size (mm)	0.81	1.52	1.96
	Apparent terminal Velocity (cm/s)	10.75	28.1	25.56
	Standard Deviation (mm)	0.96	0.4	0.1
1-Hexanol-high	Bubble size (mm)	0.87	1.51	1.94
	Apparent terminal Velocity (cm/s)	11.43	17.6	17.32
	Standard Deviation (mm)	1.2	0.9	0.4
1-Heptanol- low	Bubble size (mm)	0.87	1.53	1.98
	Apparent terminal Velocity (cm/s)	13.09	15.99	19.12
	Standard Deviation (mm)	0.55	0.1	1.15
1-Heptanol- high	Bubble size (mm)	0.89	1.52	1.92
	Apparent terminal Velocity (cm/s)	13.4	16.4	16.55
	Standard Deviation (mm)	0.04	0.2	0.2

Figure 4.12: The terminal rise velocity vs. bubble diameter in the presence of low (1) and high (5) concentrations of butanol, hexanol and octanol.

1-Butanol- Equiv. Conc. 1	Bubble size (mm)	0.72	1.56	1.96
	Apparent terminal Velocity (cm/s)	8.41	31	25.62
	Standard Deviation (mm)	0.09	0.2	0.08
1-Butanol- Equiv. Conc. 5	Bubble size (mm)	0.71	1.56	1.94
	Apparent terminal Velocity (cm/s)	8.41	30	25.67
	Standard Deviation (mm)	0.02	0.2	0.45
1-Hexanol- Equiv. conc. 1	Bubble size (mm)	0.81	1.52	1.96
	Apparent terminal Velocity (cm/s)	10.75	28.1	25.56
	Standard Deviation (mm)	0.96	0.4	0.1
1-Hexanol- Equiv. conc. 5	Bubble size (mm)	0.87	1.51	1.94
	Apparent terminal Velocity (cm/s)	11.43	17.6	17.32
	Standard Deviation (mm)	1.2	0.9	0.4
1-Octanol – Equiv. Conc. 1	Bubble size (mm)	0.88	1.5	1.95
	Apparent terminal Velocity (cm/s)	14.07	15.32	16.69
	Standard Deviation (mm)	0.48	0.08	0.24
1-Octanol- Equiv. Conc. 5	Bubble size (mm)	0.89	1.56	1.97
	Apparent terminal Velocity (cm/s)	15.33	16.69	16.72
	Standard Deviation (mm)	0.02	0.44	0.21

Figure 4.13: Velocity profiles in 1-hexanol (ca 1.5mm).

1-Hexanol 5.25ppm		1-Hexanol 37.5ppm			
Distance (mm)	Velocity (cm/s)	Distance (mm)	Velocity (cm/s)	Distance (mm)	Velocity (cm/s)
0.0	0.0	0.0	0.0	1937.3	18.7
16.9	50.6	6.8	20.5	2115.4	16.9
45.1	34.2	21.4	23.2	2289.8	18.0
68.0	34.3	36.7	22.9	2466.8	17.4
90.9	34.2	52.1	23.2	2644.1	18.0
136.3	34.1	67.2	22.1	2822.1	17.6
181.7	33.7	81.7	21.5	2994.5	16.9
204.2	34.0	95.5	19.6	3103.7	13.3
226.9	33.8	108.5	19.4		
249.3	33.4	121.3	19.1		
271.9	34.3	134.0	19.1		
294.5	33.6	146.9	19.6		
316.9	33.4	159.7	18.8		
339.1	33.2	172.3	18.8		
515.7	33.1	184.6	18.3		
845.8	32.9	281.1	18.1		
1172.9	32.5	461.5	18.0		
1499.8	32.8	648.3	19.4		
1817.7	30.7	834.4	17.9		
2128.2	31.4	1022.1	19.7		
2438.7	30.7	1211.5	18.2		
2742.1	29.9	1392.1	17.9		
2989.1	27.8	1662.8	18.1		

Figure 4.14: The terminal rise velocity vs. bubble diameter in the presence of 1-hexanol and 2-hexanol.

1-Hexanol- Equiv. conc. 1	Bubble size (mm)	0.81	1.52	1.92
	Apparent terminal Velocity (cm/s)	10.75	28.95	25.56
	Standard Deviation (mm)	0.96	0.49	0.1
1-Hexanol- Equiv. conc. 5	Bubble size (mm)	0.88	1.52	1.9
	Apparent terminal Velocity (cm/s)	11.43	17.6	17.32
	Standard Deviation (mm)	1.21	0.9	0.4
2-Hexanol- Equiv. conc. 1	Bubble size (mm)	0.83	1.52	1.92
	Apparent terminal Velocity (cm/s)	11	20.8	19.8
	Standard Deviation (mm)	0.8	0.24	0.21
2-Hexanol- Equiv. conc. 5	Bubble size (mm)	0.85	1.52	1.92
	Apparent terminal Velocity (cm/s)	11.1	15.87	18.63
	Standard Deviation (mm)	0.8	0.19	0.27

Figure 4.15.a: Velocity profiles in butanol (ca 1.45mm).

Tap Water		1-Butanol-11.5ppm		1-Butanol-82ppm		1-Butanol-125ppm	
Distance (mm)	Velocity (cm/s)	Distance (mm)	Velocity (cm/s)	Distance (mm)	Velocity (cm/s)	Distance (mm)	Velocity (cm/s)
0.0	0.0	0.0	0.0	0.0	0.0	0.0	0.0
5.9	17.7	19.0	38.1	18.0	38.3	6.3	18.8
22.8	33.0	50.0	36.0	48.0	36.0	23.5	33.0
45.2	34.3	74.0	36.0	71.0	33.0	45.7	33.5
67.9	34.0	98.0	36.0	94.0	36.0	68.2	33.8
90.5	33.8	121.0	33.0	118.0	36.0	90.7	33.8
113.3	34.6	144.0	36.0	141.0	33.0	113.3	33.8
136.2	34.1	168.0	36.0	164.0	36.0	135.8	33.8
159.0	34.3	192.0	36.0	187.0	33.0	158.3	33.5
261.1	34.4	215.0	33.0	221.0	34.5	180.7	33.8
441.4	33.6	238.0	36.0	267.0	34.5	203.2	33.5
598.3	33.6	262.0	36.0	301.0	33.0	225.5	33.3
765.8	33.5	286.0	36.0	335.0	34.5	247.7	33.5
933.2	33.5	310.0	36.0	425.0	33.5	270.0	33.3
1100.3	33.4	333.0	33.0	594.0	34.0	292.1	33.0
1267.2	33.4	356.0	36.0	763.0	33.5	314.2	33.3
1433.9	33.3	438.0	35.0	925.0	31.7	488.5	32.6
1700.5	33.4	614.0	35.3	1086.0	33.0	812.2	32.1
1933.8	33.3	791.0	35.5	1252.0	33.3	1131.3	31.7
2100.1	33.2	966.0	34.7	1515.0	32.6	1486.2	31.0
2266.2	33.2	1244.0	34.8	1742.0	32.0	1793.3	30.2
2432.5	33.3	1591.0	34.6	1901.0	31.7	2051.5	29.5
2598.8	33.2	1832.0	34.0	2059.0	31.5	2342.5	28.7
2765.4	33.4	1995.0	31.7	2216.0	31.3	2625.0	27.8
2932.2	33.3	2157.0	33.5	2371.0	30.5	2897.9	26.8
3054.2	33.2	2323.0	33.0	2524.0	30.7		
		2486.0	32.0	2676.0	30.0		
		2646	32.00	2825	29.66		
		2806	32.00	2973	29.50		

Figure 4.15.b: Velocity profiles in butanol (ca 1.45mm).

1-Butanol-150ppm		1-Butanol-180ppm		1-Butanol-260ppm	
Distance (mm)	Velocity (cm/s)	Distance (mm)	Velocity (cm/s)	Distance (mm)	Velocity (cm/s)
0.0	0.0	0.0	0.0	0.0	0.0
9.9	29.8	4.4	13.3	13.3	38.2
30.9	33.0	19.5	32.0	37.8	33.0
53.0	33.4	41.0	32.5	59.7	32.8
75.3	33.4	62.9	33.3	81.5	32.8
97.6	33.6	85.0	33.0	103.3	32.5
120.0	33.4	107.0	33.0	125.1	32.8
142.2	33.2	129.0	33.0	146.9	32.8
164.3	33.0	151.0	33.0	168.3	31.4
186.3	33.2	172.9	32.8	189.4	32.1
208.4	33.0	194.8	33.0	210.8	31.8
230.5	33.2	216.6	32.3	232.0	31.8
252.6	33.0	238.3	32.8	253.3	32.1
274.5	32.8	259.8	31.8	274.7	32.1
296.5	33.2	281.1	32.3	296.1	32.3
318.3	32.3	302.7	32.5	317.2	30.9
490.9	32.3	472.8	31.9	482.1	30.9
811.1	31.7	788.1	31.2	783.4	29.4
1126.7	31.4	1311.1	30.6	1081.8	30.3
1588.8	30.5	1768.3	30.1	1375.0	28.3
2040.5	29.3	2006.3	29.5	1654.3	27.5
2330.0	28.6	2297.9	28.8	1924.5	26.5
2611.1	27.7	2582.3	28.1	2181.3	24.8
2884.1	26.9	2859.8	27.4	2425.4	24.0
3071.6	26.4	3049.9	26.6	2660.2	23.0
				2886.3	22.2
				3040.6	21.6

Figure 4.16.a: Velocity profiles in pentanol (ca 1.45mm).

Tap Water		1-Pentanol-7ppm		1-Pentanol-50ppm		1-Pentanol-110ppm	
Distance (mm)	Velocity (cm/s)	Distance (mm)	Velocity (cm/s)	Distance (mm)	Velocity (cm/s)	Distance (mm)	Velocity (cm/s)
0.0	0.0	0.0	0.0	0.0	0.0	0.0	0.0
5.9	17.7	2.5	7.6	7.5	35.0	0.9	2.6
22.8	33.0	15.7	31.8	20.4	32.8	10.8	27.2
45.2	34.3	37.5	33.8	31.6	34.6	31.0	27.8
67.9	34.0	60.3	34.4	43.1	33.9	52.2	30.2
90.5	33.8	83.1	34.2	59.8	33.4	67.5	29.9
113.3	34.6	105.7	33.4	76.5	33.5	87.9	30.0
136.2	34.1	128.3	34.4	87.7	33.5	113.2	30.0
159.0	34.3	151.1	34.2	110.1	33.7	133.2	30.2
261.1	34.4	173.7	33.4	149.4	33.7	153.3	30.0
441.4	33.6	196.1	33.8	183.1	33.5	173.2	29.8
598.3	33.6	218.5	33.6	205.4	33.4	193.1	29.8
765.8	33.5	240.9	33.4	227.5	33.0	212.9	29.6
933.2	33.5	263.1	33.4	249.5	33.0	232.8	30.0
1100.3	33.4	285.4	33.4	271.7	33.7	252.6	29.3
1267.2	33.4	307.9	34.2	288.5	33.5	272.2	29.8
1433.9	33.3	483.8	32.9	299.4	31.4	292.2	30.0
1700.5	33.4	811.1	32.6	310.2	33.9	311.9	29.1
1933.8	33.3	1135.3	32.3	448.3	31.2	331.3	29.3
2100.1	33.2	1626.8	32.0	716.6	30.8	350.8	29.3
2266.2	33.2	2101.9	31.0	986.5	30.3	370.3	29.3
2432.5	33.3	2398.9	30.4	1257.5	31.1	522.5	28.5
2598.8	33.2	2698.1	29.4	1524.7	29.4	804.8	28.0
2765.4	33.4	2962.7	29.4	1911.4	29.1	1079.5	27.0
2932.2	33.3			2299.1	29.7	1341.4	25.4
3054.2	33.2			2554.7	28.2	1590.9	24.5
				2802.3	27.9	1830.0	23.4
				3047.1	27.5	2060.1	22.7
						2283.2	22.0
						2499.7	21.3
						2711.6	21.1
						2920.0	20.6

Figure 4.16.b: Velocity profiles in pentanol (ca 1.45mm).

1-Pentanol-130ppm		1-Pentanol-250ppm	
Distance (mm)	Velocity (cm/s)	Distance (mm)	Velocity (cm/s)
0.0	0.0	0.0	0.0
4.2	12.6	7.2	21.5
15.6	21.4	20.5	18.7
29.6	20.8	32.9	18.5
43.6	21.0	45.3	18.7
57.5	20.8	57.8	18.9
71.3	20.6	70.4	18.7
85.1	20.8	82.9	18.9
98.9	20.6	95.5	18.9
112.5	20.4	108.2	18.9
125.8	19.5	120.8	18.9
138.6	18.9	133.4	18.9
151.0	18.4	146.1	19.2
163.3	18.4	158.8	18.9
175.5	18.2	171.3	18.7
187.7	18.4	183.8	18.9
283.2	17.9	284.6	18.9
457.4	17.0	461.8	16.5
623.9	16.3	623.8	15.9
786.4	16.2	782.5	15.8
947.9	16.1	940.8	15.8
1109.3	16.2	1098.9	15.8
1270.1	16.0	1257.5	15.9
1429.3	15.8	1414.8	15.6
1586.3	15.6	1649.2	15.7
1742.3	15.6	1883.0	15.4
1898.4	15.6	2038.5	15.7
2053.8	15.5	2193.8	15.4
2208.9	15.5	2348.7	15.6
2365.0	15.7	2504.6	15.6
2522.5	15.8	2659.9	15.4
2678.2	15.3	2815.1	15.6
2834.1	15.9	2970.7	15.5
2992.4	15.8	3069.2	15.7
3087.2	15.8		

Figure 4.17.a: Velocity profiles in pentanol (ca 1.85mm).

Tap Water		1-Pentanol-7ppm		1-Pentanol-50ppm		1-Pentanol-110ppm	
Distance (mm)	Velocity (cm/s)	Distance (mm)	Velocity (cm/s)	Distance (mm)	Velocity (cm/s)	Distance (mm)	Velocity (cm/s)
0.0	0.0	0.0	0.0	0.0	0.0	0.0	0.0
11.7	3.9	3.5	10.5	7.8	23.4	5.0	15.0
34.3	19.2	18.2	33.6	27.4	35.4	21.0	33.0
35.7	42.6	41.5	36.3	51.1	35.7	43.2	33.5
36.3	66.6	65.5	35.7	74.8	35.4	65.4	33.3
35.7	90.6	89.6	36.6	98.2	34.8	87.4	32.8
35.0	114.1	113.2	34.2	120.9	33.3	108.9	31.8
35.3	137.6	148.1	35.3	143.2	33.6	129.8	31.0
34.3	160.8	182.9	33.9	165.2	32.4	150.3	30.3
35.0	183.9	205.6	34.2	186.1	30.3	170.3	29.8
34.0	206.9	228.1	33.3	206.8	31.8	190.1	29.8
34.3	229.7	250.8	34.8	227.5	30.3	210.1	30.3
33.7	252.3	272.9	31.5	247.6	30.0	230.3	30.3
33.3	274.7	294.4	33.0	267.4	29.4	250.3	30.0
34.0	297.1	316.4	33.0	287.4	30.6	270.4	30.3
33.0	319.4	484.7	31.5	307.3	29.1	290.5	30.0
32.8	428.8	793.1	30.2	609.2	29.2	448.3	29.6
32.0	591.1	1092.2	29.6	1044.5	28.6	740.1	28.8
31.7	750.1	1386.1	29.2	1327.9	28.1	1020.9	27.4
31.0	999.9	1675.3	28.7	1601.9	26.7	1295.0	27.4
30.4	1215.4	2098.9	28.0	1877.2	28.3	1565.1	26.6
30.3	1367.1	2516.9	27.5	2148.2	25.9	1827.8	26.0
29.8	1607.0	2884.3	26.5	2409.8	26.4	2084.8	25.4
29.4	1814.8			2672.5	26.1	2334.1	24.5
29.2	1961.2			2929.3	25.3	2575.1	23.8
29.0	2106.9					2810.3	23.3
28.9	2338.2					3018.2	22.8
28.7	2452.9						
28.4	2623.1						
28.1	2735.3						
28.0	2903.1						
27.8	3014.2						
27.6	3106.2						

Figure 4.17.b: Velocity profiles in pentanol (ca 1.85mm).

1-Pentanol-130ppm		1-Pentanol-225ppm		1-Pentanol-275ppm	
Distance (mm)	Velocity (cm/s)	Distance (mm)	Velocity (cm/s)	Distance (mm)	Velocity (cm/s)
0.0	0.0	0.0	0.0	0.0	0.0
21.1	31.6	5.2	15.6	7.3	21.9
53.3	33.5	19.5	27.3	22.4	23.4
75.3	32.5	37.0	25.1	36.9	20.1
111.5	28.8	52.7	21.9	49.7	18.3
146.5	29.0	67.5	22.6	62.3	19.6
166.0	29.5	82.4	22.1	75.1	18.8
185.6	29.2	96.9	21.3	87.5	18.3
205.0	29.3	111.0	21.0	99.9	18.9
224.6	29.3	125.1	21.3	112.5	18.9
244.0	29.0	139.4	21.6	125.0	18.5
263.5	29.4	153.6	21.0	137.5	18.9
282.9	28.8	167.4	20.4	150.2	19.3
302.2	29.0	181.4	21.6	162.5	17.7
463.8	30.4	195.5	20.7	174.6	18.6
765.4	29.9	209.1	20.1	187.1	18.8
1047.0	26.4	317.7	20.4	285.5	18.4
1315.3	27.3	517.9	19.7	468.4	18.2
1578.9	25.4	711.3	19.0	647.6	17.7
1833.0	25.4	901.1	18.9	824.1	17.6
2081.4	24.3	1090.9	19.0	998.7	17.3
2320.2	23.5	1280.5	18.9	1172.3	17.4
2552.2	22.9	1526.5	18.2	1346.4	17.4
2782.2	23.1	1709.2	18.7	1561.2	17.4
3010.5	22.6	1831.7	18.3	1735.8	17.5
		2013.1	18.0	1867.9	17.1
		2284.9	18.2	2039.7	17.3
		2557.3	18.1	2212.8	17.3
		2736.7	17.8	2385.6	17.2
		2915.0	18.1	2558.2	17.3
		3053.0	17.8	2730.6	17.2
				2903.6	17.4
				3049.1	17.5

Figure 4.18.a: Velocity profiles in hexanol (ca 1.45mm).

Tap Water		1-Hexanol-5.25ppm		1-Hexanol-15ppm	
Distance (mm)	Velocity (cm/s)	Distance (mm)	Velocity (cm/s)	Distance (mm)	Velocity (cm/s)
0.0	0.0	0.0	0.0	0.0	0.0
5.9	17.7	16.9	38.2	9.1	27.2
22.8	33.0	45.1	34.2	27.6	28.4
45.2	34.3	68.0	34.3	46.2	27.5
67.9	34.0	90.9	34.2	63.2	27.5
90.5	33.8	136.3	34.1	80.1	27.2
113.3	34.6	181.7	33.7	97.7	25.6
136.2	34.1	204.2	34.0	115.8	28.8
159.0	34.3	226.9	33.8	134.3	26.8
261.1	34.4	249.3	33.4	155.4	26.8
441.4	33.6	271.9	34.3	176.6	27.0
598.3	33.6	294.5	33.6	194.3	25.9
765.8	33.5	316.9	33.4	211.5	25.8
933.2	33.5	339.1	33.2	228.6	25.4
1100.3	33.4	515.7	33.1	245.8	26.3
1267.2	33.4	845.8	32.9	263.2	25.8
1433.9	33.3	1172.9	32.5	280.3	25.7
1700.5	33.4	1499.8	32.8	297.3	25.3
1933.8	33.3	1817.7	30.7	313.9	24.5
2100.1	33.2	2128.2	31.4	330.3	24.6
2266.2	33.2	2438.7	30.7	346.9	24.9
2432.5	33.3	2742.1	29.9	363.3	24.4
2598.8	33.2	2989.1	27.8	379.6	24.5
2765.4	33.4			396.2	25.2
2932.2	33.3			527.5	24.6
3054.2	33.2			773.4	24.6
				1012.5	23.2
				1242.3	22.8
				1515.9	21.8
				1732.2	21.1
				1892.6	20.8
				2098.9	20.4
				2301.4	20.0
				2500.3	19.7
				2794.2	19.5
				2987.0	19.3

Figure 4.18.b: Velocity profiles in hexanol (ca 1.45mm).

1-Hexanol-25ppm		1-Hexanol-37.5ppm	
Distance (mm)	Velocity (cm/s)	Distance (mm)	Velocity (cm/s)
0.0	0.0	0.0	0.0
8.9	26.6	6.8	20.5
26.5	26.2	21.4	23.2
43.7	25.4	36.7	22.9
60.3	24.3	52.1	23.2
76.5	24.5	67.2	22.1
92.9	24.5	81.7	21.5
109.0	23.7	95.5	19.6
124.9	24.0	108.5	19.4
140.5	23.0	121.3	19.1
155.7	22.6	134.0	19.1
170.7	22.4	146.9	19.6
185.8	22.8	159.7	18.8
201.0	22.7	172.3	18.8
216.2	23.1	184.6	18.3
231.2	21.9	281.1	18.1
344.4	21.2	461.5	18.0
552.0	20.3	648.3	19.4
755.5	20.4	834.4	17.9
957.9	20.1	1022.1	19.7
1158.7	20.1	1211.5	18.2
1351.5	18.5	1392.1	17.9
1563.7	18.0	1662.8	18.1
1742.5	17.7	1937.3	18.7
1890.2	17.7	2115.4	16.9
2057.7	17.6	2289.8	18.0
2229.5	16.8	2466.8	17.4
2400.2	17.3	2644.1	18.0
2573.2	17.3	2822.1	17.6
2745.5	17.2	2994.5	16.9
2916.9	17.1	3103.7	13.3
3053.1	17.0		

Figure 4.19.a: Velocity profiles in 1-hexanol (ca 1.85mm).

Tap Water		1-Hexanol-5.25ppm		1-Hexanol-15ppm	
Distance (mm)	Velocity (cm/s)	Distance (mm)	Velocity (cm/s)	Distance (mm)	Velocity (cm/s)
0.0	0.0	0.0	0.0	0.0	0.0
11.7	3.9	6.3	18.9	10.9	32.8
34.3	19.2	24.1	34.6	31.8	29.8
35.7	42.6	47.4	35.2	51.2	28.6
36.3	66.6	70.9	35.2	70.4	28.8
35.7	90.6	93.7	33.3	89.8	29.3
35.0	114.1	115.8	33.0	109.2	28.8
35.3	137.6	137.4	31.8	128.4	28.8
34.3	160.8	158.7	32.0	147.8	29.3
35.0	183.9	179.6	30.8	167.1	28.6
34.0	206.9	200.0	30.4	186.2	28.6
34.3	229.7	220.3	30.8	205.5	29.3
33.7	252.3	240.6	30.0	224.7	28.4
33.3	274.7	260.6	30.0	371.3	27.4
34.0	297.1	280.6	30.0	648.5	28.0
33.0	319.4	300.7	30.3	926.3	27.6
32.8	428.8	456.2	29.1	1197.8	26.7
32.0	591.1	743.6	28.4	1471.7	26.3
31.7	750.1	1025.5	28.0	1732.5	25.8
31.0	999.9	1303.8	27.7	1977.8	25.0
30.4	1215.4	1580.5	27.7	2225.1	24.5
30.3	1367.1	1856.0	27.4	2467.0	23.9
29.8	1607.0	2128.8	27.2	2704.7	23.6
29.4	1814.8	2398.7	26.8	2869.4	23.2
29.2	1961.2	2661.0	25.6		
29.0	2106.9	2908.0	24.0		
28.9	2338.2				
28.7	2452.9				
28.4	2623.1				
28.1	2735.3				
28.0	2903.1				
27.8	3014.2				
27.6	3106.2				

Figure 4.19.b: Velocity profiles in 1-hexanol (ca 1.85mm).

1-Hexanol-25ppm		1-Hexanol-37.5ppm	
Distance (mm)	Velocity (cm/s)	Distance (mm)	Velocity (cm/s)
0.0	0.0	0.0	0.0
11.3	33.8	1.3	3.8
33.1	31.7	11.2	26.0
53.6	29.7	27.3	22.3
71.6	24.3	47.3	18.9
87.9	24.8	65.9	18.3
104.4	24.8	75.3	18.0
120.9	24.5	84.8	18.3
137.6	25.7	103.3	18.8
154.1	23.7	121.9	18.3
170.5	25.6	146.3	18.3
187.3	24.7	170.8	18.5
203.6	24.3	266.7	17.9
219.9	24.8	444.7	17.7
236.3	24.5	620.2	17.4
252.7	24.5	794.8	17.5
379.5	23.7	1056.8	17.5
620.2	24.4	1318.9	17.5
862.3	24.0	1581.1	17.5
1101.4	23.8	1843.6	17.6
1335.8	23.1	2018.8	17.5
1571.0	22.5	2193.5	17.5
1795.7	22.5	2368.9	17.6
2010.2	21.9	2544.8	17.6
2228.3	21.7	2721.0	17.6
2444.7	21.6	2897.6	17.7
2658.6	21.2		
2869.1	20.9		
3022.1	20.8		

Figure 4.20: Apparent terminal velocity vs. concentration of single bubbles in 1-butanol.

Current Work-1.45mm@350mm	Concentration (ppm)	11	82	125	150	180	260	2500
	Velocity (cm/s)	36	34.5	33.4	32.3	32.2	30.9	20
Krzan et al-1.42mm@350mm	Concentration (ppm)	148	370	740	2220	2368	7400	
	Velocity (cm/s)	18	16	16	16	16	16	

Figure 4.21: Apparent terminal velocity vs. concentration of single bubbles in 1-pentanol.

Current Work-1.45mm@350mm	Concentration (ppm)	7	50	110	130	250	
	Velocity (cm/s)	33.8	33	29.2	17.6	17.2	
Krzan et al-1.42mm@350mm	Concentration (ppm)	8.81	44.07	88.15	132.225	264.45	440.75
	Velocity (cm/s)	34	31.5	26.5	19	16.5	16.5

Figure 4.22: Apparent terminal velocity vs. concentration of single bubbles in 1-hexanol.

Current Work-1.45mm@350mm	Concentration (ppm)	5.25	15	25	37.5
	Velocity (cm/s)	33.2	24.5	21.2	18
Krzan et al-1.42mm@350mm	Concentration (ppm)	20.43	40.87	71.52	510.9
	Velocity (cm/s)	27	19.5	16.5	15.5

Figure 4.23: Apparent terminal velocity (at 3000mm over the capillary) vs. concentration (ppm) of single bubbles for range of n-alcohols for ca. 1.45mm bubbles.

1-Butanol	Concentration (ppm)	11	82	125	150	180	260	2500
	Velocity (cm/s)	32	29.55	26.75	26.4	26.5	21.6	16
1-Pentanol	Concentration (ppm)	7	50	110	130	250		
	Velocity (cm/s)	29.4	27.6	20.8	15.8	15.6		
1-Hexanol	Concentration (ppm)	5.25	15	25	37.5			
	Velocity (cm/s)	29	19.4	17	16.5			
1-Heptanol	Concentration (ppm)	0.05	1	4.5	33			
	Velocity (cm/s)	31.3	16.5	16.4	15.99			
1-Octanol	Concentration (ppm)	0.05	0.25	4.5	32			
	Velocity (cm/s)	31.3	28.6	16.69	15.32			

Figure 4.24: Apparent terminal velocity (at 3000mm over the capillary) vs. concentration (mol/L) of single bubbles for range of n-alcohols for ca. 1.45mm bubbles.

1-Butanol	Concentration (ppm)	0.000149	0.001108	0.001689	0.002027	0.002432	0.003514	0.033784
	Velocity (cm/s)	32	29.55	26.75	26.4	26.5	21.6	16
1-Pentanol	Concentration (ppm)	7.94E-05	0.000567	0.001248	0.001475	0.002836		
	Velocity (cm/s)	29.4	27.6	20.8	15.8	15.6		
1-Hexanol	Concentration (ppm)	5.14E-05	0.000147	0.000245	0.000367			
	Velocity (cm/s)	29	19.4	17	16.5			
1-Heptanol	Concentration (ppm)	4.3E-07	8.61E-06	3.87E-05	0.000284			
	Velocity (cm/s)	31.3	16.5	16.4	15.99			
1-Octanol	Concentration (ppm)	3.84E-07	1.92E-06	3.46E-05	0.000246			
	Velocity (cm/s)	31.3	28.6	16.69	15.32			

Figure 4.25: Apparent terminal velocity (at 3000mm over the capillary) vs. concentration (ppm) for ca. 1.45 and 1.85mm single bubbles in 1-pentanol and 1-hexanol.

1-Pentanol	1.45mm	Concentration (ppm)	7	50	110	130	250	
		Velocity (cm/s)	29.4	27.6	20.8	15.8	15.6	
	1.85mm	Concentration (ppm)	7	50	110	130	225	275
		Velocity (cm/s)	26	25.6	23	22.8	17.9	17.5
1-Hexanol	1.45mm	Concentration (ppm)	5.25	15	25	37.5		
		Velocity (cm/s)	29	19.4	17	16.5		
	1.85mm	Concentration (ppm)	5.25	15	25	37.5		
		Velocity (cm/s)	25	23.4	20.85	17.6		

Figure 4.26: The apparent terminal rise velocity vs. bubble diameter at 3000mm in the presence of MIBC, 1-hexanol and 2-hexanol.

1-Hexanol-Equiv. Conc. 1	Vel	10.75	28.95	25.56
	Size	0.81	1.52	1.92
1-Hexanol-Equiv. Conc. 5	Vel	11.43	17.6	17.32
	Size	0.88	1.52	1.9
2-Hexanol-Equiv. Conc. 1	Vel	11	20.8	19.8
	Size	0.83	1.52	1.92
2-Hexanol-Equiv. Conc. 5	Vel	11.1	15.87	18.63
	Size	0.85	1.52	1.92
MIBC-Equiv. Conc. 1	Vel	10.8	15.46	17
	Size	0.91	1.52	1.95
MIBC-Equiv. Conc. 5	Vel	11.08	15.22	16.8
	Size	0.91	1.52	1.95

Figure 4.27: Velocity profiles in 2-hexanol (ca 1.5mm).

2-Hexanol-5.25ppm		2-Hexanol-37.5ppm	
Distance (mm)	Velocity (cm/s)	Distance (mm)	Velocity (cm/s)
0.0	0.0	0.0	0.0
18.0	27.0	14.0	21.0
36.0	27.0	28.0	21.0
56.0	30.0	44.0	24.0
74.0	27.0	60.0	24.0
92.0	27.0	74.0	21.0
110.0	27.0	88.0	21.0
130.0	28.0	102.0	21.0
148.0	27.0	114.0	21.0
166.0	27.0	128.0	21.0
184.0	27.0	140.0	18.0
202.0	27.0	152.0	18.0
220.0	27.0	166.0	18.0
238.0	27.0	178.0	18.0
256.0	27.0	190.0	18.0
274.0	27.0	372.0	18.2
540.0	26.6	552.0	18.0
798.0	25.8	744.0	19.2
1046.0	24.8	924.0	18.0
1296.0	25.0	1120.0	19.6
1794.0	24.9	1302.0	18.2
2030.0	23.6	1482.0	18.0
2258.0	22.8	1844.0	18.1
2482.0	22.4	2030.0	18.6
2700.0	21.8	2200.0	17.0
2912.0	21.2	2380.0	18.0
3118.0	20.6	2554.0	17.4
		2734.0	18.0
		2910.0	17.6
		3078.0	16.8
		3128.0	13.4

Figure 4.28: Apparent terminal velocity vs. concentration of single bubbles in 1-hexanol, 2-hexanol and MIBC.

1-Hexanol	Concentration (ppm)	5.25	15	25	37.5
	Velocity (cm/s)	29	19.4	17	16.5
2-Hexanol	Concentration (ppm)	5.25	15	25	37.5
	Velocity (cm/s)	20.8	17.3	16.4	15.87
MIBC	Concentration (ppm)	0.01	0.05	2.5	20
	Velocity (cm/s)	31	29.9	15.46	15.22

Figure 4.29: Velocity profiles in MIBC (ca. 1.5mm) and NaCl (ca 1.6mm).

MIBC-Equiv. Conc. 1		MIBC-Equiv. Conc. 5		NaCl-Equiv. Conc. 5		NaCl-Equiv. Conc. 1	
Distance (mm)	Velocity (cm/s)	Distance (mm)	Velocity (cm/s)	Distance (mm)	Velocity (cm/s)	Distance (mm)	Velocity (cm/s)
0.0	0.0	0.0	0.0	0.0	0.0	0.0	0.0
8.9	13.3	7.1	10.6	8.2	12.4	8.2	12.4
29.4	30.9	24.5	26.2	30.9	34.1	30.9	34.1
52.0	33.9	41.3	25.1	54.5	35.3	54.5	35.3
73.7	32.6	57.8	24.8	76.9	33.7	76.9	33.7
94.9	31.7	73.5	23.5	97.5	30.9	97.5	30.9
116.3	32.1	88.9	23.2	118.2	31.1	118.2	31.1
156.6	30.2	104.0	22.6	138.2	30.0	138.2	30.0
176.6	30.0	118.7	22.1	156.7	27.7	156.7	27.7
195.4	28.3	132.4	20.5	176.9	30.4	176.9	30.4
213.1	26.6	144.5	18.3	196.0	28.6	196.0	28.6
230.6	26.1	157.1	18.8	214.7	28.1	214.7	28.1
260.6	22.5	168.7	17.5	234.0	28.9	234.0	28.9
274.6	21.0	180.0	16.9	253.5	29.3	253.5	29.3
621.4	17.3	191.6	17.5	271.3	26.6	271.3	26.6
778.6	15.7	203.1	17.2	290.2	28.4	290.2	28.4
933.1	15.5	363.3	16.0	546.2	25.6	546.2	25.6
1086.0	15.3	518.4	15.5	764.0	21.8	764.0	21.8
1238.6	15.3	670.5	15.2	968.5	20.4	968.5	20.4
1390.9	15.2	822.7	15.2	1165.5	19.7	1165.5	19.7
1995.1	15.1	972.7	15.0	1357.5	19.2	1357.5	19.2
2146.3	15.1	1121.6	14.9	1896.5	18.0	1896.5	18.0
2298.3	15.2	1269.1	14.7	2067.2	17.1	2067.2	17.1
2451.1	15.3	1418.4	14.9	2402.0	16.7	2402.0	16.7
2598.3	14.7	1714.2	14.8	2571.6	17.0	2571.6	17.0
2750.0	15.2	1865.8	15.2	2747.5	17.6	2747.5	17.6
2902.3	15.2	2017.5	15.2	2919.8	17.2	2919.8	17.2
3056.3	15.4	2169.8	15.2	3091.2	17.1	3091.2	17.1
		2320.9	15.1				
		2471.5	15.1				
		2622.7	15.1				
		2776.0	15.3				
		2928.9	15.3				
		3081.6	15.3				

Figure 4.30: The apparent terminal rise velocity vs. bubble diameter at 3000mm in the presence of MIBC and NaCl.

MIBC		NaCl	
Size (mm)	Velocity (cm/s)	Size (mm)	Velocity (cm/s)
0.91	11.25	0.91	10.8
1.52	15.46	1.6	17.05
1.95	16.8	1.99	17.5

Figure 4.31: The apparent terminal rise velocity vs. bubble diameter at 3000mm in the presence of the three commercial frothers.

MIBC		F150		DF250	
Size (mm)	Velocity (cm/s)	Size (mm)	Velocity (cm/s)	Size (mm)	Velocity (cm/s)
0.91	11.25	0.96	11.27	0.69	8.67
1.52	15.46	1.57	16.58	0.81	9.5
1.95	16.8	1.98	17.5	1.56	16.45
				1.96	18.2

Figure 4.32: Apparent terminal velocity vs. concentration of single bubbles in F150, DF250 and MIBC.

MIBC	Concentration (ppm)	0.01	0.05	2.5	20	
	Velocity (cm/s)	31	29.9	15.46	15.22	
F150	Concentration (ppm)	0.003	0.015	0.06	1	10
	Velocity (cm/s)	30.45	21.5	16.6	16.55	16.5
DF250	Concentration (ppm)	0.0232	0.06	0.9	3	25
	Velocity (cm/s)	16.7	16.5	16.5	16.5	16.4

Figure 4.33: The comparison of measured terminal rise velocity of MIBC and Dowfroth 250 between the Sam et al. (1996) results and the recent work.

MIBC (Sam et al.,1996)		Dowfroth 250 (Sam et al.,1996)		Dowfroth 250 (current work)		MIBC (current work)	
Size (mm)	Velocity (cm/s)	Size (mm)	Velocity (cm/s)	Size (mm)	Velocity (cm/s)	Size (mm)	Velocity (cm/s)
0.96	12.07	0.96	11.61	0.69	8.67	0.91	11.25
1.4	16.6	1.4	15.87	0.81	9.5	1.52	15.46
2.2	19.8	2.2	18	1.56	16.45	1.95	16.8
2.7	21.8	2.7	21	1.96	18.2		

Figure 4.34: The influence of travel distance of bubble on critical concentration and rise velocity in 1-pentanol for ca. 1.45mm single bubbles.

350mm	Concentration (ppm)	0	7	50	110	130	250
	Velocity (cm/s)	34	33.8	33	29.2	17.6	17.2
1000mm	Concentration (ppm)	0	7	50	110	130	250
	Velocity (cm/s)	34	32.3	30.3	26.96	16.17	15.8
2000mm	Concentration (ppm)	0	7	50	110	130	250
	Velocity (cm/s)	34	31.04	29.1	22.65	15.5	15.6
3000mm	Concentration (ppm)	0	7	50	110	130	250
	Velocity (cm/s)	34	29.4	27.6	20.8	15.3	15.5

Figure 4.35: Comparison of terminal velocity of the used frother with clean and contaminated water lines by Clift et al. (1978) (ca. 1.5mm).

Type	Terminal Velocity (cm/s)
Clean Water	34.5
Butanol	16
Pentanol	15.6
1-Hexanol	16.5
2-Hexanol	15.87
Heptanol	15.99
Octanol	15.32
MIBC	15.22
F150	16.5
DF250	16.4
Contaminated Water	18.5

Figure 4.36: Comparison of the trend line of current work with clean and contaminated water lines by Clift et al. (1978).

Size	Big (1.8-1.95mm)	Medium (1.4-1.55mm)	Small (0.85-1.0mm)
Data	18.2	16	8.4
	17.5	16.45	8.67
	16.55	16.2	11.27
	17.32	16.5	11.3
	16.8	15.87	11.25
	17.5	15.46	10.8
	16.72	16.5	13.17
	17.5	16.5	14.25
Average	17.26	16.19	11.14
Standard Deviation	0.54	0.38	1.98